Identification of large ribosomal proteins required for the full activation of the protein kinase Gcn2 in *Saccharomyces cerevisiae*

A thesis presented in partial fulfilment of the

requirements for the degree of

Master of Science

in

Biological Sciences

at Massey University, Albany

New Zealand

Reuben Andrew Anderson

2019

Abstract

Protein synthesis is a fundamental biological process that all organisms require for maintaining life, growth and development. The maintenance of amino acid levels, the building blocks of proteins, is essential for maintaining protein synthesis under all biological conditions. Hence, amino acid shortage can be deleterious to the cell. Therefore, cells harbour mechanisms to cope and overcome amino acid starvation. When eukaryotes are subjected to amino acid starvation, the resulting accumulation of uncharged tRNAs activates the protein kinase Gcn2, leading to phosphorylation of eIF2α and activation of the amino acid starvation response. Uncharged tRNAs are the signal of starvation, directly detected by Gcn2. Gcn2 must bind to the effector protein Gcn1 and both must contact ribosomes for Gcn2 activation. The current working model for how the starvation signal is delivered to Gcn2 postulates that these uncharged tRNAs bind in the A-site of the ribosome in a codon specific manner, which are subsequently transferred to Gcn2. Gcn1 is directly involved in this process but its exact involvement is unknown. To test the working model, it is paramount to investigate where Gcn1 and Gcn2 bind on the ribosome. Ribosomes consist of a large and small subunit, each containing multiple ribosomal proteins placed in unique locations. Identification of ribosomal proteins contacting Gcn1 or Gcn2 will allow for deduction of where Gcn1 and Gcn2 bind on the ribosome.

This study aimed to determine Gcn1 and Gcn2 contact points on the large ribosomal subunit, using a genetic approach. The hypothesis was that if an interaction of Gcn1 or Gcn2 with a particular large ribosomal protein (Rpl) is important for Gcn2 activation, then its overexpression would impair Gcn2 function.

Overexpression of several large ribosomal proteins impaired cell growth on a medium triggering amino acid starvation, suggesting Gcn2 activation was impaired. Groups of two or more of these Rpls were found in several regions which contain ribosomal proteins shown or suggested to interact with Gcn1 or Gcn2 previously. This included a region containing the P-stalk proteins (part of the large ribosomal complex) known to contact Gcn2. A region close to the small ribosomal protein Rps10, known to contact Gcn1, was also identified. Another region with Rpls which contacts a protein eEF3, which is suggested to share similar ribosomal contacts as Gcn1, was identified.

It would appear multiple contact points on the large ribosomal subunit are involved in Gcn1 and Gcn2 binding. This is not surprising given the relatively large size of both Gcn1 and Gcn2. These findings can give insight into potential Gcn1 and Gcn2 contacts and can give an indication on what future work can be done to confirm these findings. This will ultimately lead to a better understanding of how Gcn2 is activated under amino acid starvation conditions and the involvement of ribosomal contact.

Acknowledgments

I would like to thank my supervisor Dr. Evelyn Sattlegger for her support, suggestions, ideas and encouragement throughout the course of my studies. I am thankful for the opportunities she has given me to further my knowledge and abilities with respect to scientific research. I have enjoyed the time spent in the lab and learning how to challenge my own capabilities and overcome any obstacles that have come along the way on my journey so far.

Thanks to all those I share a workspace with in our lab and the many new friends I have made including: Siaosi Koloamatang, Susanne Gottfried, Hayley Prescott, Magy Jose, Reagan Dear and Aditi Ghugh. You have all made it an enjoyable experience to work alongside you. Your constant support, ideas and our scientific discussions have made it easier to understand the complexities of our field of research.

A special thanks to my parents who will forever support and encourage me through anything I pursue or come up against no matter how big or how small.

Also, I would like to thank all the current and previous members of the Sattlegger group who contributed to information and conducted experiments that have helped in the formulation of this thesis.

Table of Contents

List of Figures

List of Tables

List of Abbreviations

3AT	3-Amino-1,2,4-triazole
3AT's	3-Amino-1,2,4-triazole sensitivity
ATP	Adenosine triphosphate
ABC	ATP binding cassette
A-site	Acceptor-site
ATF4	Activating Transcription Factor 4
bp	Base pair
EDTA	Ethylene Diamine Tetra Acetic acid
eEF3	eukaryotic Elongation Factor 3
eIF2	eukaryotic Initiation Factor 2
eIF2α-P	eukaryotic Initiation Factor alpha subunit phosphorylated
eIF2B	eukaryotic Initiation Factor 2 B
E-site	Exit-site
Gcn1	General control non-derepressible 1
Gcn2	General control non-derepressible 2
Gcn4	General control non-derepressible 4
Gcn20	General control non-derepressible 20
HA	Human influenza hemagglutinin
kDa	kilo Dalton
LB	Luria-Bertani

Met-tRNA	Methionyl initiator tRNA
NaCl	Sodium Chloride
NaOH	Sodium Hydroxide
ORF	Open Reading Frame
PEG	Poly ethylene glycol
P-site	Peptidyl donor site
RNase	Ribonuclease
Rps	Ribosomal protein small
Rpl	Ribosomal protein large
Rpm	Revolutions per minute
rRNA	ribosomal RNA
SC	Synthetic Complete
SD	Synthetic Defined
SDS	Sodium dodecyl sulphate
SDS PAGE	Sodium dodecyl sulphate polyacrylamide gel electrophoresis
Tris	tris(hydroxymethyl)aminomethane
TAE	Tris Acetate EDTA
tRNA	transfer RNA
Y2H	Yeast 2 Hybrid
YPD	Yeast Peptone Dextrose
YPG	Yeast Peptone Glycerol

Chapter 1 Introduction

1.1 Amino acid starvation and the cellular response

Amino acids are the building blocks of proteins which are required by all organisms to carry out a vast array of biological functions essential for life, growth and development. The levels of amino acids need to be constantly maintained at an adequate level to ensure continuous and efficient protein synthesis can take place. Under normal or replete conditions amino acids will bind to their respective tRNAs, these tRNAs bound to their cognate amino acids are termed charged tRNAs. When cellular levels of any one or more amino acid are reduced below that which is required to maintain efficient protein synthesis, amino acid starvation occurs. This is caused most commonly due to poor diet or nutrient uptake from the environment by an organism, leading to an amino acid imbalance. Amino acid starvation leads to the cellular increase in concentration of uncharged tRNAs (free tRNAs not bound to their respective amino acids). For efficient protein synthesis to be restored, amino acid starvation needs to be sensed and responded to appropriately. This occurs via the amino starvation response.

The uncharged tRNAs which accumulate in the cell during amino acid starvation lead to the activation of the amino acid starvation response (Hinnebusch, 2005). In eukaryotic organisms, increase in the levels of uncharged tRNAs of any of their respective cognate amino acids activates the stress response protein kinase Gcn2 (General control non-derepressable 2) (Hinnebusch, 2005). Activation of Gcn2 allows for it to phosphorylate its substrate eIF2α. eIF2α along with eIF2β and eIF2γ form the heterotrimeric complex of eIF2 (eukaryotic initiation factor 2). Phosphorylation of eIF2α (eIF2α-P) leads to reduced global protein synthesis which allows the cell to conserve vital amino acids while cellular levels are reduced (Baird & Wek, 2012; Chaveroux et al., 2010; Hinnebusch, 2005). Conversely, eIF2α-P also leads to increased translation of a transcription factor that upregulates the transcription of genes required for amino acid biosynthesis and transport. This transcription factor in yeast is Gcn4 and in mammals the equivalent is named ATF4 (Hinnebusch, 1997, 2005). Thus, the increased translation of GCN4 (or ATF4) occurring during amino acid starvation leads to restoration of amino acid homeostasis. How phosphorylation of eIF2α leads to reduced global protein synthesis while also increasing GCN4 translation will be explained in further detail in the following section.

1.2 Initiation of protein synthesis

Initiation of protein synthesis first requires eIF2 bound to GTP to bind to initiator methionyl tRNA (Met-tRNA$_i^{Met}$). This forms a ternary complex, which binds to the 40S small subunit of the ribosome, forming a 43S preinitiation complex (Kimball, 1999). The preinitiation complex binds to the 5' capped structure of an mRNA it will eventually translate. The complex then scans the mRNA for an AUG start codon, which is recognised via the anticodon of the Met-tRNA$_i^{Met}$ of the preinitiation complex. Upon reaching the AUG start codon, the 60S large ribosomal subunit is acquired by the preinitiation complex forming an 80S initiation complex. Formation of an initiator complex coincides with the hydrolysis of the GTP bound eIF2 to GDP. Following this, GDP bound eIF2 is released in a now inactive form. For the next round of translation to be initiated, GDP bound eIF2 needs to be converted back to its GTP bound form by the guanine exchange factor eIF2B (Kimball, 1999). A summary of the process of protein synthesis initiation is represented in Figure 1.1 below.

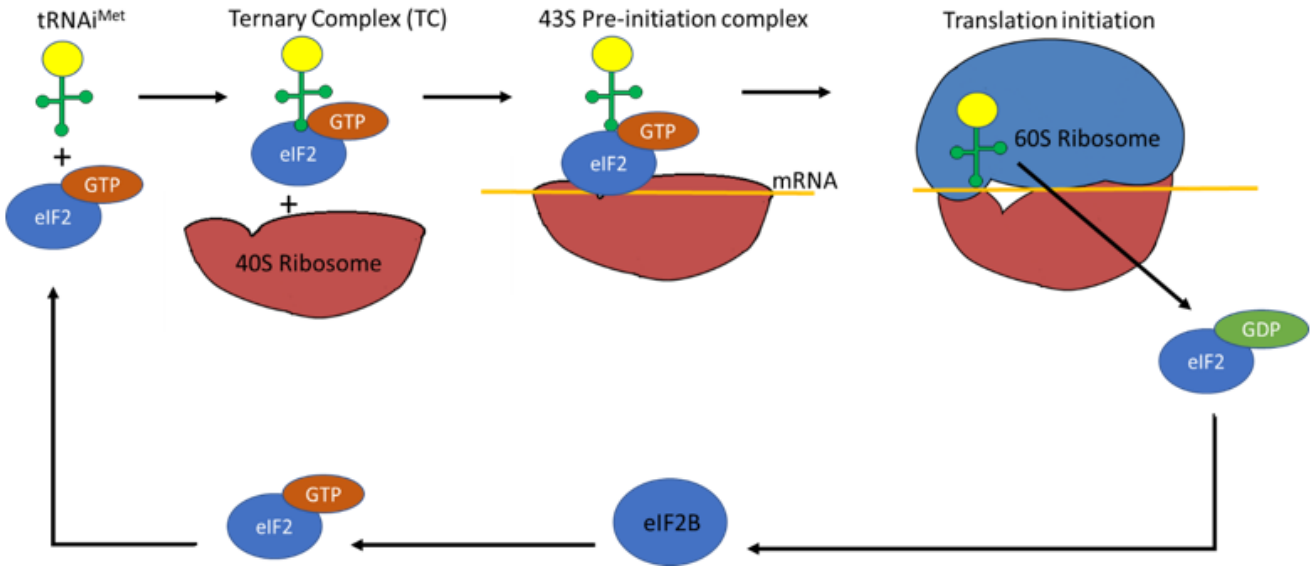

Figure 1.1 *Initiation of protein synthesis*

Met-tRNA$_i^{Met}$ binds to GTP forming a ternary complex. First, a small ribosomal subunit is acquired by the ternary complex forming a pre-initiation complex which associates with mRNA. The mRNA is then scanned by the pre-initiation complex until a start codon is reached. Upon reaching a start codon, the pre-initiation complex acquires a large ribosomal subunit forming the initiation complex and leading to hydrolysis of GTP to GDP. GDP bound eIF2 is released and is recycled back to GTP bound eIF2 by eIF2B, allowing for another round of protein synthesis initiation to occur.

1.3 Protein synthesis initiation under amino acid starvation conditions

The process and rate of protein synthesis initiation is greatly affected following the activation of the amino acid starvation response. Phosphorylation of the α subunit of eIF2 (eIF2α-P) by Gcn2 occurring during amino acid starvation leads to eIF2α-P binding to eIF2B with higher affinity than its non-phosphorylated form, thereby significantly reducing the rate of GTP/GDP exchange on eIF2. Thus eIF2α-P acts as a competitive inhibitor of non-phosphorylated eIF2α (Hinnebusch, 1997). Inhibition of eIF2B activity by bound eIF2α-P prevents the recycling of the inactive GDP bound eIF2 to the active GTP bound form. The phosphorylation of eIF2α resulting from amino acid starvation thus leads to reduced global protein synthesis by the reduction in the turnover of eIF2 (Hinnebusch, 1997). Protein synthesis initiation under amino acid starvation conditions is outlined in Figure 1.2 below.

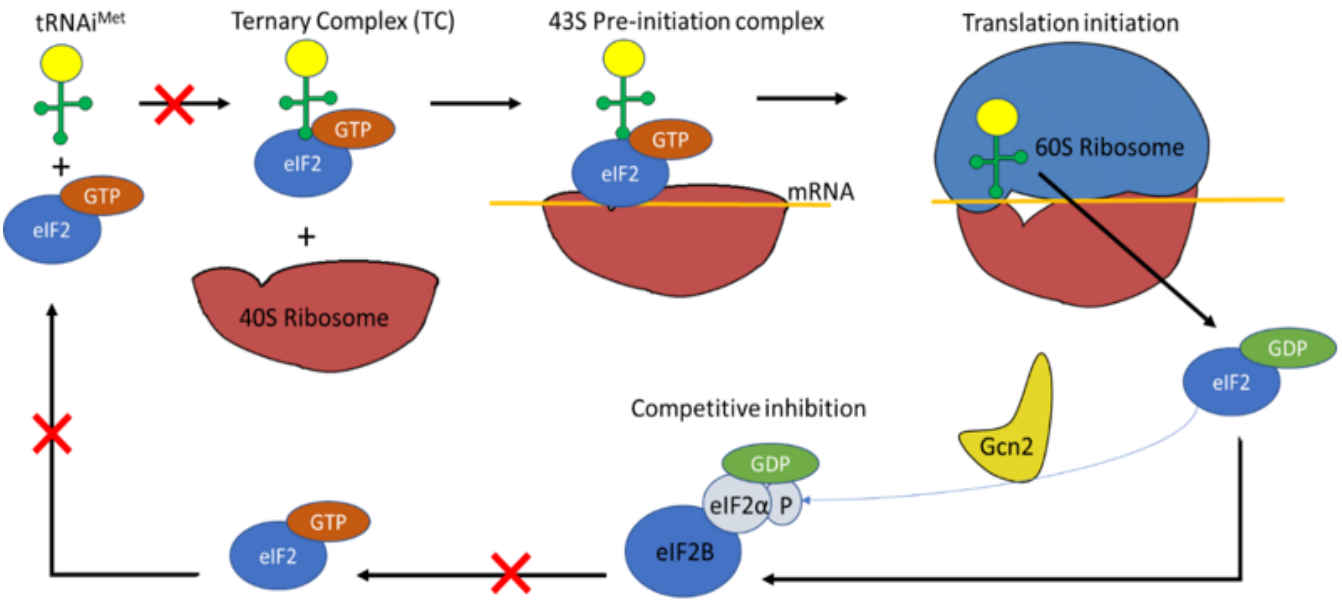

Figure 1.2 *Protein synthesis initiation under amino acid starvation conditions*

Phosphorylation of the α subunit of eIF2 (eIF2α) by Gcn2 occurring during amino acid starvation leads to eIF2α-P binding to eIF2B with higher affinity than its non-phosphorylated eIF2α. eIF2α-P acts as a competitive inhibitor of non-phosphorylated eIF2 (Hinnebusch, 1997). Inhibition of eIF2B activity by bound eIF2α-P prevents the recycling of the inactive GDP bound eIF2 to the active GTP bound form.

In addition to reducing global protein synthesis, eIF2α-P leads indirectly to the increase in translation of specific mRNAs with unique upstream open reading frames (uORF) in the 5' untranslated region. These mRNAs code for specific transcription factors, for example Gcn4 in yeast and the mammalian equivalent ATF4 (Hinnebusch, 1997). The mRNA of Gcn4 contains four of these uORFs, while ATF4 mRNA contains two (Hinnebusch, 1997; Marton, Vazquez de Aldana, Qiu, Chakraburtty, & Hinnebusch, 1997). As the experiments conducted in this present study are not conducted in mammalian cells, expression of ATF4 will not be discussed here. However, fundamentally, the mechanisms involved are much the same as for Gcn4 (Castilho et al., 2014).

When the ternary complex binds to the mRNA of GCN4 it recruits the 40s small ribosomal subunit, forming the 43S preinitiation complex. This complex then scans the mRNA until it reaches the start codon of the first uORF (uORF1), the large ribosomal subunit is acquired, and translation occurs. The unique property of uORF1 is that its stop codon is "weak". In contrast to the action of standard stop codons, the stop codon of uORF1 allows the majority of small ribosomal subunits to remain bound to the mRNA while the other translation machinery dissociates. This allows for the continued scanning of *GCN4* mRNA by these still bound small ribosomal subunits (Hinnebusch, 1997, 2005).

The scanning small ribosomal subunit can continue to uORF2 and while scanning can re-acquire the ternary complex. Thus, the large ribosomal subunit is acquired, and translation initiation occurs as it reaches the uORF2 start codon. In comparison to uORF1, uORF2 has a "strong" stop codon, resulting in the release of most translating ribosomes (both the small and large subunit). Any remaining ribosomal subunits that did not re-acquire a ternary complex while scanning the mRNA before uORF2 remain bound and continue scanning to uORF3. Similarly, to uORF2, the majority of any bound small ribosomal subunits scanning will be removed at uORF3 due to the acquisition of a ternary complex. The very few remaining small ribosomal subunits will be reduced even further by uORF4, again similarly as for uORF2 and uORF3 (Hinnebusch, 1997, 2005).

Therefore, under replete conditions (when ternary complex levels are high) very few small ribosomal subunits will pass uORF4 due to the acquisition of ternary complexes and translation of uORF2, uORF3 or uORF4 which results in release of ribosomes. This results in very low levels of

GCN4 translation and so under replete conditions, *GCN4* translation is said to be repressed. The mechanisms leading to GCN4 repression under replete conditions are shown below in Figure 1.3.

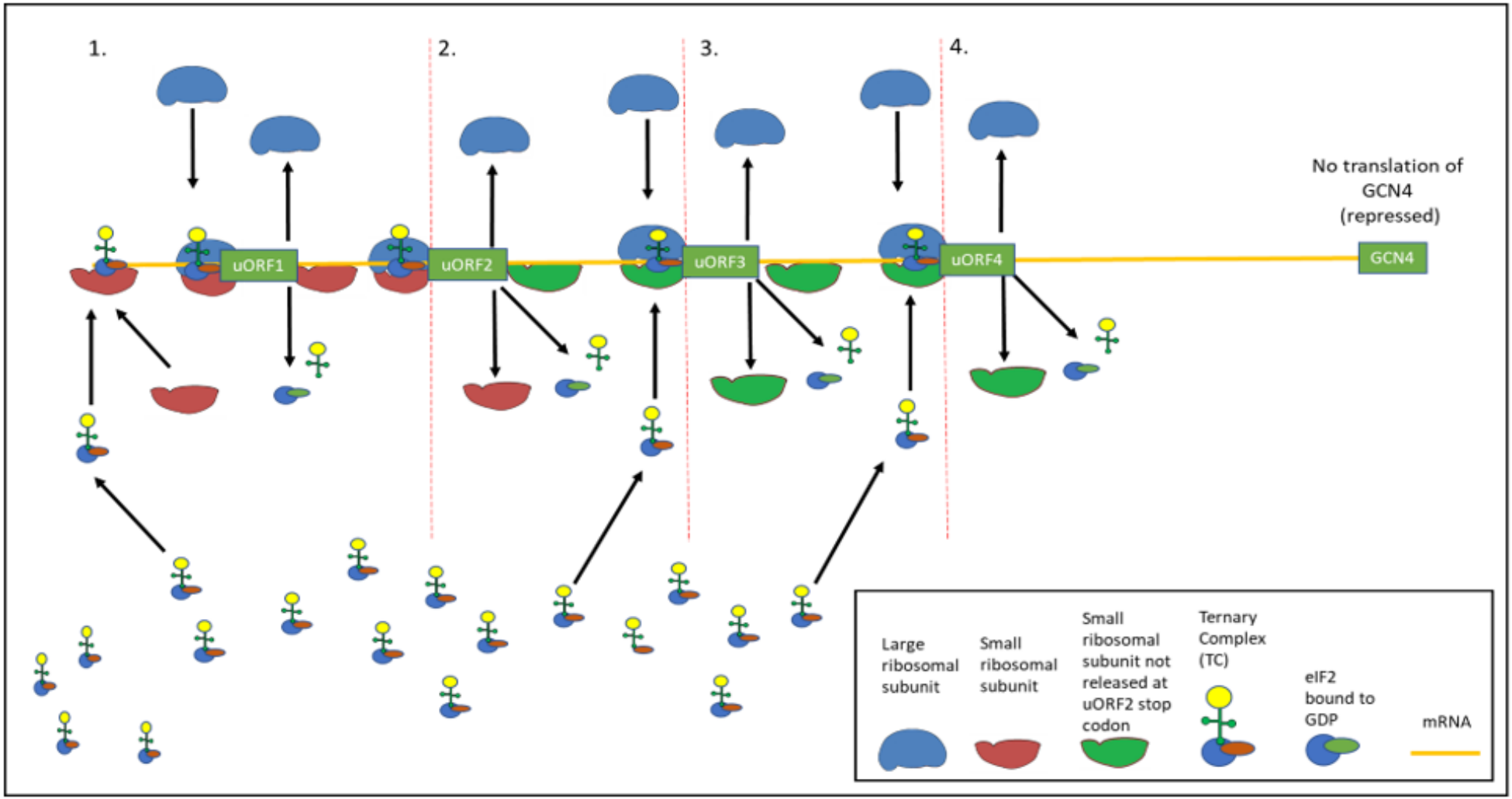

Figure 1.3 *The mechanisms leading to GCN4 repression under non-starvation conditions*

1. Initiation of protein synthesis occurs as is depicted in "Figure 1.1 Initiation of protein synthesis" above, with the exception the stop codon of uORF1 is "weak" allowing continued scanning of the mRNA by small ribosomal subunits. Reformation of the 80S initiation complex can occur due to the high abundance of ternary complexes in the cell. 2. The entirety of the 80S initiation complexes formed in 1 dissociate from the mRNA upon scanning the "strong stop codon of uORF2 leading to no translation of GCN4. The small majority of small ribosomal complexes that did not reform the 80S initiation complex in 1 can again reform the 80S initiation complex, due to high ternary complex levels. 3. and 4. The function of uORF3 and uORF4 are the same as uORF2, the very small majority of small ribosomal subunits not released at uORF2 will mostly be removed at uORF3 and uORF. This leads to very little translation of GCN4 and in this state it is said to be repressed. Figure 1.3 is adapted from (Hinnebusch 2005).

Under amino acid starvation conditions, the ternary complex concentrations in the cell are very low (see section “1.2 Initiation of protein synthesis" and Figure 1.1 above). Very few of the scanning small ribosomal subunits will be dissociated from the mRNA at uORF2, uORF3 and uORF4, as the large ribosomal subunit is not acquired (due to reduced ternary complex levels) and translation of the stop codons does not occur. Bypassing the stop codons of the uORF’s under these conditions means the majority of scanning small ribosomal subunits remain scanning past uORF4. In contrast to the length of the mRNA between the other uORF’s, the mRNA between uORF4 and GCN4 is significantly longer. The much longer length of the mRNA correlates to a greater increase in the time spent by the small ribosomal subunit scanning the mRNA. This increased time allows for a much higher probability of a ternary complex being acquired, even when cellular levels are low. The majority of scanning small ribosomal subunits will acquire a ternary complex before reaching the ORF of *GCN*4, ultimately leading to *GCN*4 translation. The translation of *GCN*4 occurring under these conditions is therefore termed “derepressed”, due to the reversal of the repressed state occurring under replete conditions. The mechanisms leading to *GCN4* being derepressed under amino acid starvation conditions is shown in Figure 1.4 below (Hinnebusch, 1997, 2005).

Thus, it is the concentration of the ternary complex that dictates the rate of translation of *GCN*4, with lower ternary complex concentrations increasing *GCN*4 translation. The phosphorylation of eIF2α occurring during amino acid starvation decreases the concentration of the ternary complex, therefore this stress response increases translation of *GCN*4 (Hinnebusch, 1997, 2005).

The transcription initiation factor Gcn4 regulates the expression of a large set of genes, including the upregulation of genes coding for proteins required for amino acid biosynthesis and transport. Thus increased *GCN*4 translation induced by amino acids starvation leads to restoration of amino acid homeostasis (Hinnebusch, 1997).

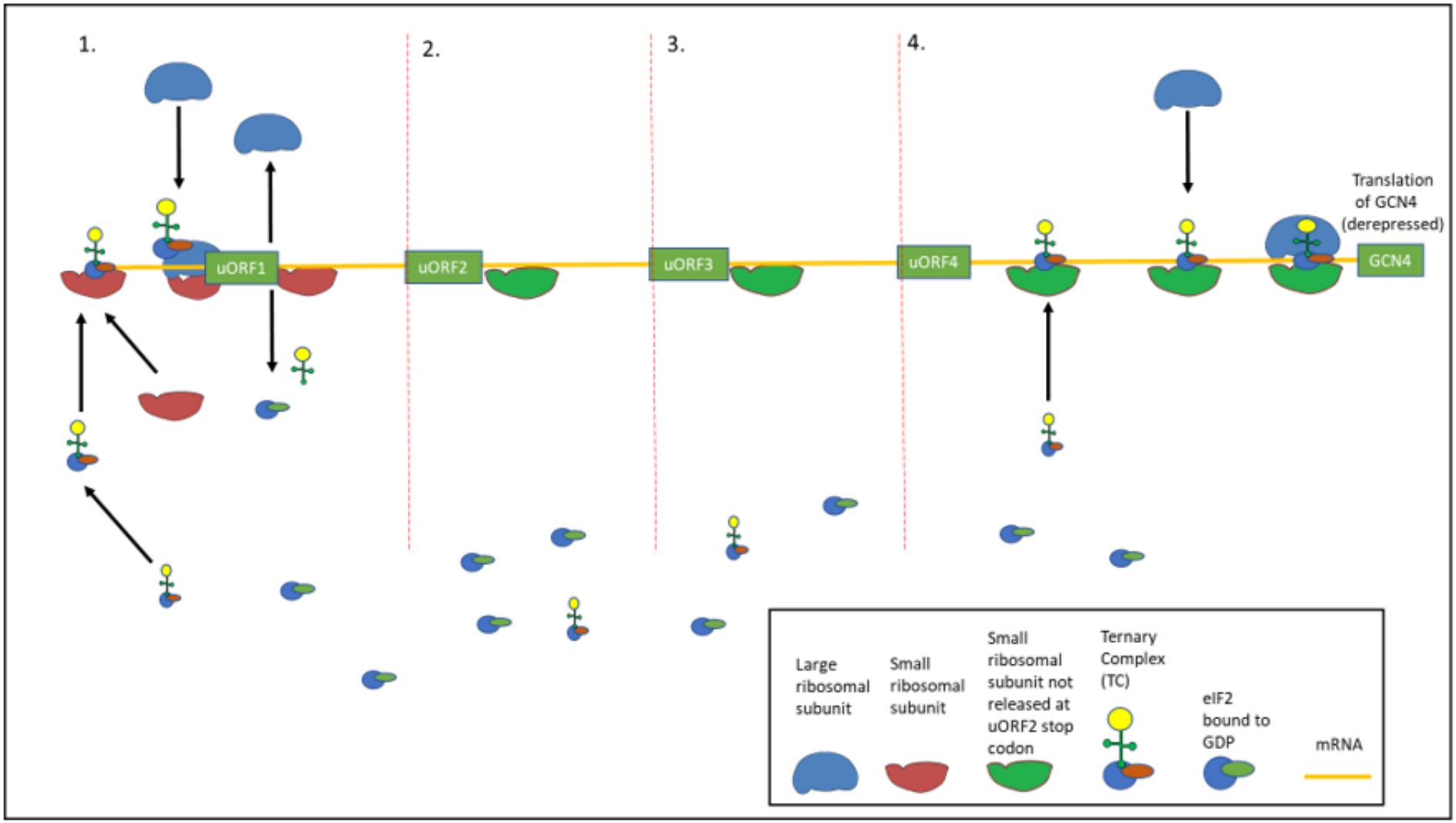

Figure 1.4 *The mechanisms leading to* GCN4 *derepression under starvation conditions*

1. Formation of translation machinery occurs, which is released at uORF1 with the exception of the continued scanning of the small ribosomal subunit. **2, 3 and 4**. Due to the very low abundance of ternary complexes in the cell, the 80S initiation complex is not reformed, allowing the majority of scanning small ribosomal subunits to remain on the mRNA (small ribosomal subunits in green) and bypass their removal at uORF2, uORF3 and uORF4. The length of the mRNA between uORF4 and *GCN*4 is much longer than between the other uORF, leading to the small ribosomal subunits spending a much longer time scanning the mRNA. The increased time allows for the reformation of the 80S initiation complex and the translation of *GCN*4. The translation of *GCN*4 in this state is said to be derepressed. Figure 1.3 is adapted from (Hinnebusch 2005).

1.4 Gcn2: domains and function

The protein kinase Gcn2 (Figure 1.5 below) is a large protein consisting of 1659 amino acids and is present in all studied eukaryotes to date from yeast to humans (Castilho et al., 2014; Qiu, Garcia-Barrio, & Hinnebusch, 1998). Gcn2 is an eIF2α kinase which plays a critical role in the response to the stress condition of amino acid starvation, whereby it is activated by uncharged tRNAs that accumulate during amino acid starvation (see "The amino acid starvation response" above) (Dong, Qiu, Garcia-Barrio, Anderson, & Hinnebusch, 2000; Hinnebusch, 1997; Ramirez, Wek, & Hinnebusch, 1991; Wek, Zhu, & Wek, 1995). Gcn2 is a multi-domain protein and including the HisRS-like domain. The HisRS-like domain is similar in structure to histidyl-tRNA synthetases but this specific domain in Gcn2 is catalytically inactive. Uncharged tRNAs bind directly to the HisRS-like domain, along with the C-terminal dimerization and ribosome binding domain (CTD) of Gcn2 (Dong et al., 2000; Wek et al., 1995). Conformational changes are induced upon tRNA binding to Gcn2, leading to the auto-phosphorylation of the protein kinase (PK) domain of Gcn2. Auto-phosphorylation of the PK domain puts Gcn2 into its fully active state, allowing Gcn2 to then phosphorylate its substrate eIF2α (Dong et al., 2000; Qiu, Hu, Dong, & Hinnebusch, 2002). Adjacent to the PK domain is a pseudo kinase (ΨPK) domain, sharing homology to the PK domain but lacking residues required for the enzymic function.

Under replete conditions and in the absence of uncharged tRNAs, molecular interactions within Gcn2 cause auto-inhibitory effects which place Gcn2 in an inactive state. Uncharged tRNAs are required to bind to the HisRS like domain and the CTD domain to overcome the auto inhibitory effects. Allosteric re-arrangements in Gcn2 occur upon tRNA binding that as a consequence lead to auto-phosphorylation of Gcn2. Auto-phosphorylation of Gcn2 leads to its full activation and is required for the efficient phosphorylation of its substrate eIF2α (Padyana, Qiu, Roll-Mecak, Hinnebusch, & Burley, 2005; Qiu et al., 1998). The ΨPK domain is also said to play a role in placing Gcn2 in an inactive state under non starvation conditions. This is suggested as the ΨPK domain interacts with the kinase domain under non-starvation conditions, which would likely prevent the catalytic activity (Boudeau, Miranda-Saavedra, Barton, & Alessi, 2006; Lageix, Rothenburg, Dever, & Hinnebusch, 2014).

The N-terminal 127 amino acids of Gcn2 consists of the **RWD** domain (found in **R**ING finger proteins, **W**D-repeat containing proteins, and yeast **D**EAD-like helicases), this is the binding

region of the effector protein Gcn1. Amino acids 1-125 of the RWD domain are sufficient for binding to the complex of Gcn1-Gcn20 (Garcia-Barrio, Dong, Ufano, & Hinnebusch, 2000; Kubota, Sakaki, & Ito, 2000). The interaction of Gcn2 with Gcn1 is essential for the *in vivo* activation of Gcn2 (Sattlegger & Hinnebusch, 2000). Gcn1 also complexes with another effector of Gcn20 which is required for the full activation of Gcn2 (Vazquez de Aldana, Marton, & Hinnebusch, 1995). Within the CTD domain of Gcn2, amino acids 1536-1659 are required for ribosomal binding. Other regions in Gcn2 are indicated as being involved in the ribosomal association including sections of the N-terminus and the HisRS-like domain, where deletion of these sections leads to a slight reduction in Gcn2-ribosomal association (Marton et al., 1997; Ramirez et al., 1991; Wek, Ramirez, Jackson, & Hinnebusch, 1990; Zhu & Wek, 1998). The binding of Gcn2 to the ribosome is crucial for the amino acid starvation response (Ramirez et al., 1991; Wek et al., 1990; Zhu & Wek, 1998).

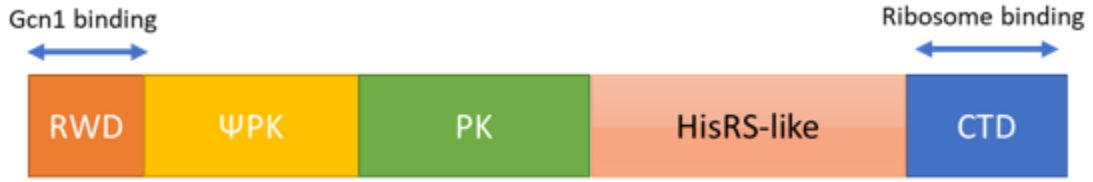

Figure 1.5 *Schematic of domains located in Gcn2*

The RWD domain consisting of the N-terminal 1-125 amino acids of Gcn2 binds to Gcn1. Uncharged tRNAs binds to the HisRS-like and CTD domains. The ΨPK domain inhibits the PK domain under replete conditions. Amino acids 1536-1659 of the CTD are involved in binding to the ribosome. Figure 1.5 is adapted from (Castilho et al., 2014)

Using purified components in an in *vitro assay*, mammalian Gcn2 has been shown to bind to and be activated by mammalian ribosomes. The rate and extent ribosome-activated Gcn2 phosphorylates eIF2α in this *in vitro* system seems to be far greater than that achieved with tRNA activation of Gcn2 (Inglis et al., 2019). The proteins of the ribosome responsible for activation of Gcn2 in this system were shown to be specifically those that make up the pentameric complex of the P-stalk (uL10 $(P1P2)_2$) which includes uL10 and two heterodimers of the protein complex of P1 and P10, which are located in the large ribosomal subunit. The purified components used also

showed that mammalian Gcn2 binds ribosomes specifically with the P-stalk proteins. To achieve maximum ribosomal binding by this system, the pseudokinase domain, the HisRS-like domain and the CTD of Gcn2 are all required. However for the activation of Gcn2, the binding and resulting activation of Gcn2 was shown to only require the HisRS-like domain (Inglis et al., 2019). Binding of Gcn2 and its activation by P-stalk proteins has yet to be shown to occur *in vitro* under amino acid starvation conditions. Also, the interaction and activation of yeast Gcn2 with P-stalk proteins has yet to be confirmed to occur *in vivo* or *in vitro*.

1.5 Gcn1 and Gcn20: domains and function

Gcn1 (Figure 1.6 below) is a 297 kDa protein, making it a very large protein (approximately one tenth the size of the ribosome) (Castilho et al., 2014; Sattlegger & Hinnebusch, 2000). As with Gcn2, Gcn1 is present in all eukaryotes studied to date; this suggests similarly for Gcn2, that its function is conserved. Gcn1 contains a Gcn2 binding domain located within amino acids 2052 to 2438 of the C-terminal domain of Gcn1 (Sattlegger & Hinnebusch, 2000). The binding of Gcn1 to Gcn2 is absolutely required for the activation of Gcn2 and thus the amino acid starvation response (Sattlegger & Hinnebusch, 2000). Deletion of Gcn1 in yeast leads to absolutely no phosphorylation of eIF2α *in vivo*, and completely inhibits the ability of yeast to grow on starvation media (Marton, Crouch, & Hinnebusch, 1993). However, Gcn1 is not required for the catalytic activity of Gcn2, as extracts of *gcn1*Δ strain show phosphorylation *in vivo* (Marton et al., 1993). A constitutively activated mutant of Gcn2 ($Gcn2^{c}$) cannot activate the amino acid starvation response in a *gcn1*Δ strain, suggesting that the function of Gcn1 is to transfer uncharged tRNAs to Gcn2 as opposed to activating Gcn2 (Marton et al., 1993; Qiu et al., 2002).

The N-terminal 2052 amino acids of the 2672 amino acids (77% of all amino acids in Gcn1) of Gcn1, consisting of the majority of the protein, have been shown to be involved in ribosomal binding (Sattlegger & Hinnebusch, 2000). The contacts between Gcn1 and the ribosome have been shown to be required for activation of Gcn2 (Sattlegger & Hinnebusch, 2000). However, whether Gcn1-ribomal binding is absolutely required for Gcn2 activation is yet to be determined because to date no mutations in Gcn1 have been identified which completely dissociate Gcn1 from the

ribosome (Sattlegger & Hinnebusch, 2000; Sattlegger & Hinnebusch, 2005). Two separate sets of mutations, located in two separate locations within Gcn1, termed M7 and M1 reduce the ability of yeast to grow on starvation media (Sattlegger & Hinnebusch, 2005). The M7 and M1 mutations also reduce the association between Gcn1 and the ribosome and reduce eIF2α-P levels as shown by polysome and western blot analysis. The large size of Gcn1, its large ribosomal binding domain and the fact that physically distinct mutations (M7 and M1) both reduce Gcn1 ribosomal association, lead to the reasoning that Gcn1 contacts the ribosome at several distinct locations (Sattlegger & Hinnebusch, 2005).

The middle portion of Gcn1 consisting of amino acids 1330-1641 shares homology to **HEAT** repeats (the acronym arising from the presence of these repeats in the proteins **H**untingtin, e**E**F3, protein phosphatase **A**, and **T**or) have homology to the N-terminal portion of eEF3 (eukaryotic elongation factor 3), for which this region in Gcn1 is termed the eEF3 like region (Marton et al., 1993; Rakesh, Krishnan, Sattlegger, & Srinivasan, 2017). Recent results obtained from structural analysis are highly indicative that the C-terminus of Gcn1 consists of HEAT repeats (Rakesh et al., 2017). The HEAT repeats have been suggested to serve as interaction platform for other proteins. This could mean that Gcn1, with its HEAT repeats (over 20 repeats are present), acts as a scaffold which possibly allows an interaction between Gcn2 and the ribosome (Andrade, Petosa, O'Donoghue, Müller, & Bork, 2001; Castilho et al., 2014; Marton et al., 1993).

Also contained within the eEF3 like region of Gcn1 is the binding domain to Gcn20, where Gcn1 binds to the N-terminal 189 amino acids of Gcn20. The complex formation between Gcn1 and Gcn20 is not absolutely required for Gcn2 activation, but required for the full activation of Gcn2 (Marton et al., 1997; Vazquez de Aldana et al., 1995). Located within the C-terminal region of Gcn20, consisting of 84% of the protein, are two ATP binding cassettes (ABC), ABCI and ABCII (Vazquez de Aldana et al., 1995). The ABC's are also found within the C- terminal region of eEF3, meaning the complex of Gcn1 and Gcn20 together shares a high degree of homology to the entire length of eEF3.

The activation of Gcn2 is known to be reduced by the overexpression of eEF3 (Visweswaraiah, Lee, Hinnebusch, & Sattlegger, 2012). This was scored by observing yeast overexpressing eEF3 having reduced growth on starvation media. It has been suggested that this occurs due to binding of eEF3 to the ribosome, via its HEAT domain and the CTD (see section 1.6 below), as

overexpression of the HEAT domain and CTD of eEF3 alone cause reduced growth of yeast on starvation media. This growth defect is exacerbated when eEF3 is overexpressed in the *gcn1-M7A* strain, leading to a growth defect greater than that seen for a strain only harbouring *gcn1-M7A* or eEF3 overexpressed (Visweswaraiah et al., 2012). It has been suggested therefore, that Gcn1 (possibly in complex with Gcn20) binds to similar ribosomal contacts as eEF3 and Gcn1 executes a similar function to that of eEF3 (Visweswaraiah et al., 2012).

Gcn1 is known to directly contact the small ribosomal protein Rps10A and Rps10B with several lines of evidence supporting this finding (Lee, Swanson, & Sattlegger, 2015). Yeast two-hybrid experiments show that Rps10A directly interacts with a fragment of Gcn1 consisting of amino acids 1060-1777 *in vivo*. *In vitro* co-precipitation of both paralogues of Rps10 with Gcn1[1060-1777] has also shown that Rps10 directly interacts with Gcn1 (Lee et al., 2015). Deletion of either paralogue of *RPS10* in yeast, thereby reducing Rps10 protein levels in the cell, leads to reduced eIF2α-P under non-starvation and starvation conditions (Lee et al., 2015). This reduction in eIF2α-P levels indicates a reduction in Gcn2 activation and suggests Gcn1 must contact Rps10 in order to convey its full function with respect to mediating Gcn2 activation (Lee et al., 2015). Furthermore, when eEF3 is overexpressed in yeast strains deleted of either Rps10A Rps10B, the growth defect on starvation media is greater than that seen with eEF3 overexpression or Rps10 deletion alone. This supports the idea that the Rps10 knockdown reduces Gcn1-ribosmal association and Gcn1 ribosomal function. Taken together, data obtained so far strongly suggests that Gcn1-Gcn20 contact must occur for the efficient activation of Gcn2.

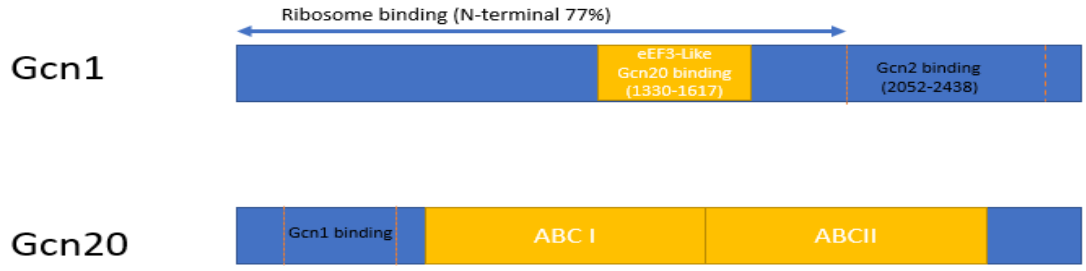

Figure 1.6 *Schematic of regions located in Gcn1 and Gcn20*

Gcn1: Binding to Gcn2 occurs with amino acids 2052-2438. The middle portion of amino acids 1330-1617 contains an eEF3 like region, involved in Gcn20 binding. 77% of the N-terminal end is involved in binding to the ribosome Gcn20: The N-terminal portion is involved in Gcn1 binding. Two ABC domains, ABCI and ABCII are located at the C-terminal end, homologous to those found in eEF3. Figure 1.6 is adapted from (Castilho et al., 2014)

1.6 eEF3 function, similarity to Gcn1 and Gcn20 and its involvement in the amino acid starvation response

eEF3 (Figure 1.7 below) is found only in yeast and other fungus. Studies however suggest an eEF3 equivalent exists in other eukaryotes, along with in prokaryotes (Kiel & Ganoza, 2001; Mateyak et al., 2018). eEF3 facilitates release of the uncharged tRNA from the E site of the ribosome during the elongation stage of translation. eEF3 is also involved in the delivery of the complex of tRNA-GTP-eEF1A to the A site of the ribosome (Andersen et al., 2006). Along with Gcn20, eEF3 is part of the ATP binding cassette family. eEF3 contains two regions, each homologous to the either Gcn1 or Gcn20, HEAT repeats (Gcn1) and the two ABC domains ABCI and ABC2 (Gcn20) (Marton et al., 1997). Located in the C-terminal end of ABC2 domain is a chromodomain, unique to eEF3 (Andersen et al., 2006). The eEF3 HEAT domain binds to the small ribosomal subunit via rRNA. The ABC2 domain and the chromodomain of eEF3 make contact to the ribosome on both the small and large subunit (Andersen et al., 2006; Gontarek, Li, Nurse, & Prescott, 1998) . The CTD of eEF3 has also been shown to co-sediment with polysomes (Lee et al., 2015; Visweswaraiah et al., 2012).

From eEF3s homology to the Gcn1-Gcn20 complex, along with the fact that overexpression of eEF3 reduces the ability of yeast to grow on starvation media (which is exacerbated by the overexpression of both Gcn1-M7A and Rps10) it is suggested that during amino acid starvation the complex of Gcn1-Gcn20 executes a function similar to that of eEF3 (Visweswaraiah et al., 2012) The Gcn1-Gcn20 complex may facilitate a release of uncharged tRNAs accumulating in the A-site of the ribosome, as opposed to eEF3 facilitating a release of uncharged tRNAs from the E-site during translation (Marton et al., 1993).

Figure 1.7 *Schematic of domains located in eEF3*

Two ABC domains are located at the C-terminal end. Heat repeats are located at the N-terminal end. The ABCII domain is involved in binding to the ribosome.

1.7 Ribosome structure, Gcn1-Gcn2 binding and its involvement in Gcn2 activation

The ribosome (represented as a surface model below in Figure 1.8) is a large molecular complex with approximately 3300 kDa in size, made up of many individual proteins and ribosomal RNA (rRNA). The yeast 80S ribosome consists of two subunits, a large 60S subunit and a small 40S subunit. The large subunit is made up of 46 large ribosomal proteins (Rpl), while the small subunit is made up of 32 small ribosomal proteins (Rps) (Spahn et al., 2001). The ribosome carries out the critical process of proteins synthesis where mRNAs are translated into proteins. Charged amino acids enter the A-site of the ribosome, are then linked together to form an ever-growing polypeptide chain in the P-site and resulting uncharged t-RNAs exit the ribosome at the E-site. It has been proposed that during amino acid starvation, when the cognate charged tRNA is not present, the cognate uncharged tRNA enters the A-site in a codon specific manner. (Lee et al., 2015; Marton et al., 1997; Murchie & Leader, 1978; Sattlegger & Hinnebusch, 2000).

The ribosome is known to directly contact both Gcn1 and Gcn2 (Marton et al., 1997; Ramirez et al., 1991). Ribosomal association with Gcn2 occurs predominately with 80S ribosomes and polysomes (actively translating ribosomes) as shown by co-sedimentation assays. When the formation of the 80S ribosome is prevented, the affinity of Gcn2 for 60S subunits is strong while for 40S subunits it is comparatively very weak. Gcn2 has been shown to associate with pre-initiation complexes which could provide Gcn2 access directly to eIF2α (Ramirez et al., 1991).

Ribosomal P-stalk proteins form an important part of the ribosome which protrude laterally from the large ribosomal subunit as a pentameric complex which consists of uL10 and two heterodimers of the protein complex of P1 and P10 (uL10 $(P1P2)_2$) (Jiménez-Díaz, Remacha, Ballesta, & Berlanga, 2013; Remacha et al., 1995). The P-stalk proteins play a crucial role in protein synthesis where they are involved in the recruitment and interaction of translation initiation and translation elongation factors required for efficient protein synthesis (Ito et al., 2014; Murakami et al., 2018)

One of the major roles of ribosomal stalk proteins is their interaction and recruitment of several translation elongation and translation initiation factors and the involvement of GTPase activity of these factors. This recruitment and interaction of these factors is vital to efficient protein synthesis. (see section “1.10. Elongation factors and their involvement in placing Gcn2 in a latent state under

nutrient replete conditions" below) (Baba, Tumuraya, Tanaka, Yao, & Uchiumi, 2013; Ito et al., 2014; Murakami et al., 2018; Remacha et al., 1995; Tanzawa et al., 2018).

Ribosomal P-stalk proteins have been shown to activate Gcn2 *in vitro* with purified mammalian components and play a role on the activation of Gcn2 *in vivo* in yeast under certain stress conditions (Inglis et al., 2019; Jiménez-Díaz et al., 2013). Using the purified mammalian components in an *in vitro* assay, Gcn2 was shown to bind to and be activated by ribosomes. The proteins of the ribosome responsible for activation of Gcn2 in this *in vitro* system were shown to be specifically those that make up the pentameric complex of the P-stalk. With co-immunoprecipitation assays using the purified mammalian components, it was also shown that Gcn2 binds to ribosomes and more specifically to the P-stalk complex (Inglis et al., 2019). Interestingly, the rate and extent at which ribosome-activated Gcn2 phosphorylates eIF2α was found to be far greater than that achieved with tRNA using the purified components *in vitro* (Inglis et al., 2019).

Ribosomal stalk proteins have also been shown to activate Gcn2 when yeast is subjected to glucose starvation and osmotic stress. This may indicate the 60S stalk proteins as possible Gcn2 ribosomal contacts under these conditions (Jiménez-Díaz et al., 2013). However, the ribosomal stalk proteins have not been shown to activate Gcn2 under amino acid starvation *in vivo*, and activation under the other stress conditions has not been shown to be a result of a direct interaction between Gcn2 and the ribosomal stalk proteins (Castilho et al., 2014; Jiménez-Díaz et al., 2013).

Like Gcn2, Gcn1 and Gcn20 associate with 80S ribosomes and polysomes, with a greater affinity of both for polysomes (Marton et al., 1997). The association of Gcn20 with polysomes is highly dependent on Gcn1 (Marton et al., 1997).. However, it is suggested that the presence of Gcn20 increases ribosomal association of Gcn1 and Gcn20 (Marton et al., 1997). This is suggested due to the fact that in co-sedimentation assays, in the presence of ATP, the complex of Gcn1 and Gcn20 associate with ribosomes with a higher affinity than either protein alone (Marton et al., 1997). The small ribosomal protein Rps10 contacts Gcn1, however this is the only confirmed specific ribosomal contact to date to be required for the full function of the amino acid starvation response (see "1.5. Gcn1 and Gcn20: domains and function" above) (Lee et al., 2015).

Furthering the knowledge as to where exactly on the ribosome Gcn1 and Gcn2 bind and how they carry out their function, is important to better understand the full involvement of the ribosome in the activation of Gcn2.

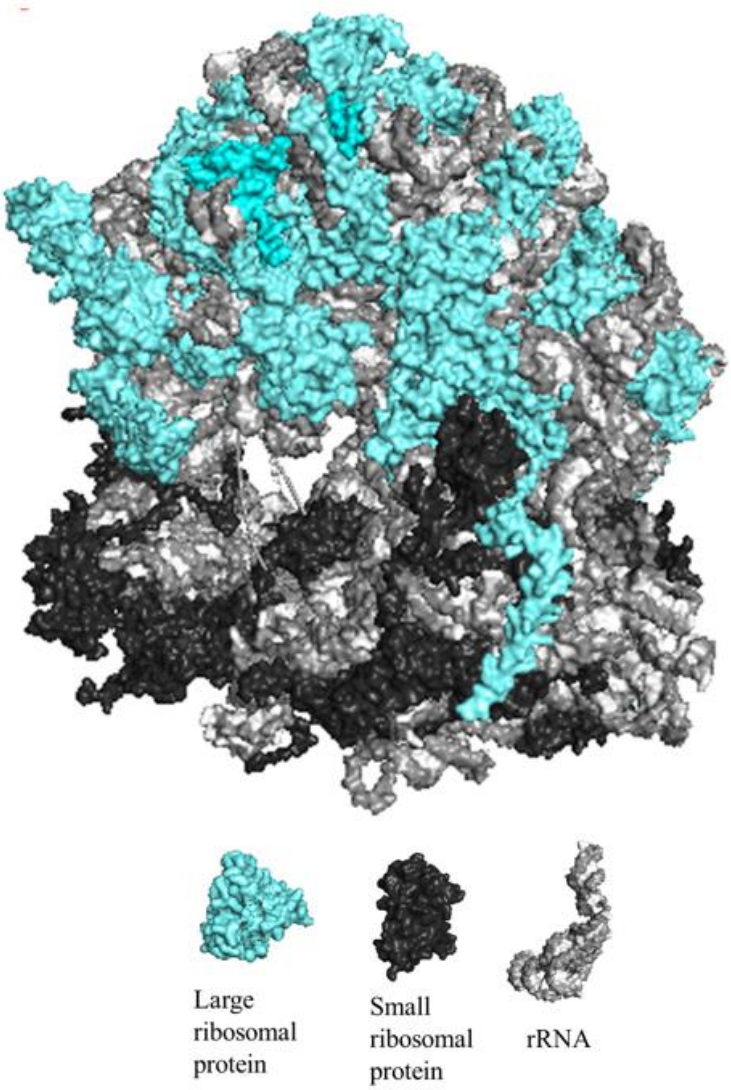

Figure 1.8 Surface representation of the 80S ribosome of S. cerevisiae

The proteins of the large ribosomal subunit are highlighted in light blue. The proteins of the small ribosomal subunit are highlighted in red. rRNAs are highlighted in light and dark grey.
Surface representation of S. cerevisiae 80S ribosome created with PyMOL Molecular Graphics System, Version 1.8 Schrödinger, LLC using data obtained from "The structure of the eukaryotic ribosome at 3.0 Å resolution." (Ben-Shem et al., 2011)

1.8 Elongation factors and their involvement in placing Gcn2 in a latent state under nutrient replete conditions

Ribosome-associated translation elongation factors including eEF1A, eEF2 and eEF3 are suggested to play important roles in the activity of Gcn2 (Castilho et al., 2014; Inglis et al., 2019; Visweswaraiah et al., 2011; Visweswaraiah et al., 2012). The translation elongation factors eEF1A and eEF3 are suggested to place Gcn2 into a latent state under non-starvation conditions in yeast (Visweswaraiah et al., 2011; Visweswaraiah et al., 2012).

From *in vivo* and *in vitro* studies it has been shown eEF1A binds to Gcn2 and reduces Gcn2 activity as seen by the reduction in the phosphorylation levels of eIF2α (Visweswaraiah et al., 2011). Under amino acid starvation conditions there is a reduction in the binding of eEF1A to Gcn2, and *in vivo* studies showed that the presence of uncharged tRNAs reduces this association (Castilho et al., 2014; Visweswaraiah et al., 2011).

eEF3 is suggested to play a more indirect role in inhibition of Gcn2 activity under non-starvation conditions. It is suggest that eEF3 and Gcn1 share similar binding sites on the ribosome (Castilho et al., 2014; Visweswaraiah et al., 2012). Studies suggest eEF3 prevents Gcn1 from forming a functional interaction with the ribosome, thereby prevents transfer of the starvation signal to Gcn2 (see sections 1.5 and 1.6 for more detail) (Castilho et al., 2014; Visweswaraiah et al., 2012)

Ribosomal P-stalk proteins have been shown to activate Gcn2 *in vivo* and *in vitro* under certain conditions which has led to the suggestion that eEF2, eEF1A and other translation elongation factors place Gcn2 in a latent state by competing with Gcn2 for binding to the P-stalk proteins. The structure of the P-stalk complex extends into the A-site of the ribosome, where elongation factors would be present under non-starvation conditions, or on stalled ribosomal complexes. (Inglis et al., 2019; Jiménez-Díaz et al., 2013). This would mean in absence elongation factors, which would occur with reduced charged tRNA levels associated with amino acid starvation, the P-stalk would be free to bind to Gcn2 and allow for its activation. When elongation factors are present and bound to the P-stalk, occurring under non-starvation conditions, the activation of Gcn2 would be prevented as Gcn2 would not have access to P-stalk proteins.

1.9 The current working model for Gcn2 activation and detection of uncharged tRNA

As mentioned above, the direct activating ligand for Gcn2 are uncharged tRNAs in eukaryotes subjected to amino acid starvation. However, how this stress signal is received by Gcn2 and the process and pathways involved are yet to be fully elucidated. Research thus far has led to a working model for this activation of Gcn2 and how uncharged tRNAs are delivered to Gcn2 (Castilho et al., 2014; Lee et al., 2015; Marton et al., 1997; Ramirez et al., 1991; Sattlegger & Hinnebusch, 2000).

The working model proposes that Gcn2, Gcn1 (and Gcn20 with its association with Gcn1) and the ribosome together form a trimeric complex (Figure 1.9 below). Gcn1 and Gcn2 likely contact the ribosome at physically distinct regions. This is proposed due to the facts the ribosomal binding domains of both Gcn1 and Gcn2 are physically distinct from that required for binding between Gcn2 and Gcn1 (Sattlegger & Hinnebusch, 2000).

As stated by the above model, uncharged tRNAs accumulating during amino acid starvation first enter the A-site of the ribosome in a codon specific manner. These uncharged tRNAs are then transferred to Gcn2. Their binding to the HisRS-like domain of Gcn2 induces auto-phosphorylation of Gcn2 causing the activation of Gcn2 and leading to phosphorylation of eIF2α. The model states that Gcn1 plays a crucial role in the transfer of uncharged tRNAs to Gcn2, where Gcn1 binds close to the A-site of the ribosome (binding to Rps10, which is in relatively proximity to the A-site, being confirmed). The process of transfer is stated to either be a direct transfer to Gcn2 via Gcn1, or Gcn1 places Gcn2 in a position where it is closely exposed to uncharged tRNAs in the A-site

Gcn1 has been shown so far to bind to Rps10, although this does not show Gcn1 contacts the A-site directly, it indicates Gcn1 makes contact near to the A-site. Considering the large size of Gcn1, and the fact the majority of the protein is involved in ribosomal contact, it would stand to reason Gcn1 makes other ribosomal contacts closer to the A-site (Lee et al., 2015). Furthermore, Paromomycin sensitivity is elicited upon overexpression of Gcn1 in yeast as compared to wild type. Whereas a deletion of Gcn1 leads to resistances against Paromomycin. As Paromomycin

binds to the A-site this is further claim to the model dictating Gcn1 binding near to the A-site (Sattlegger & Hinnebusch, 2000).

The model proposes that uncharged tRNAs are released from the A-site to, or by Gcn1. In support of Gcn1 releasing the uncharged tRNAs from the A-site is the homology Gcn1 and Gcn20 share together with eEF3, which releases uncharged tRNAs from the E-site of the ribosome. It has been hypothesized that Gcn1 shares also a similar function to eEF3 whereby it releases uncharged tRNAs from the A-site of the ribosome.

The formulation of the assumption that uncharged tRNAs activating Gcn2 are coming from the ribosomal A -site was based on the stringent response in bacteria. The stringent response involves the ribosome-associated protein relA, which synthesises (p)ppGpp, an alarmone that leads to the detection of amino acid starvation in bacteria (Wendrich, Blaha, Wilson, Marahiel, & Nierhaus, 2002). *In vitro* studies conducted in bacteria show a codon specific association of uncharged tRNAs, accumulating due to amino acid starvation, entering the A-site of the ribosome. Increases in the cellular concentration of uncharged tRNA in turn leads to the entrance of uncharged tRNAs to the A-site in bacteria (Wendrich et al., 2002). For eukaryotes, it has been shown similarly that uncharged tRNAs enter the A-site of the ribosome in a codon specific manner; this gives crucial support to the current working model dictating that uncharged tRNAs that activate the amino acid starvation response first enter the A-site of the ribosome (Murchie & Leader, 1978).

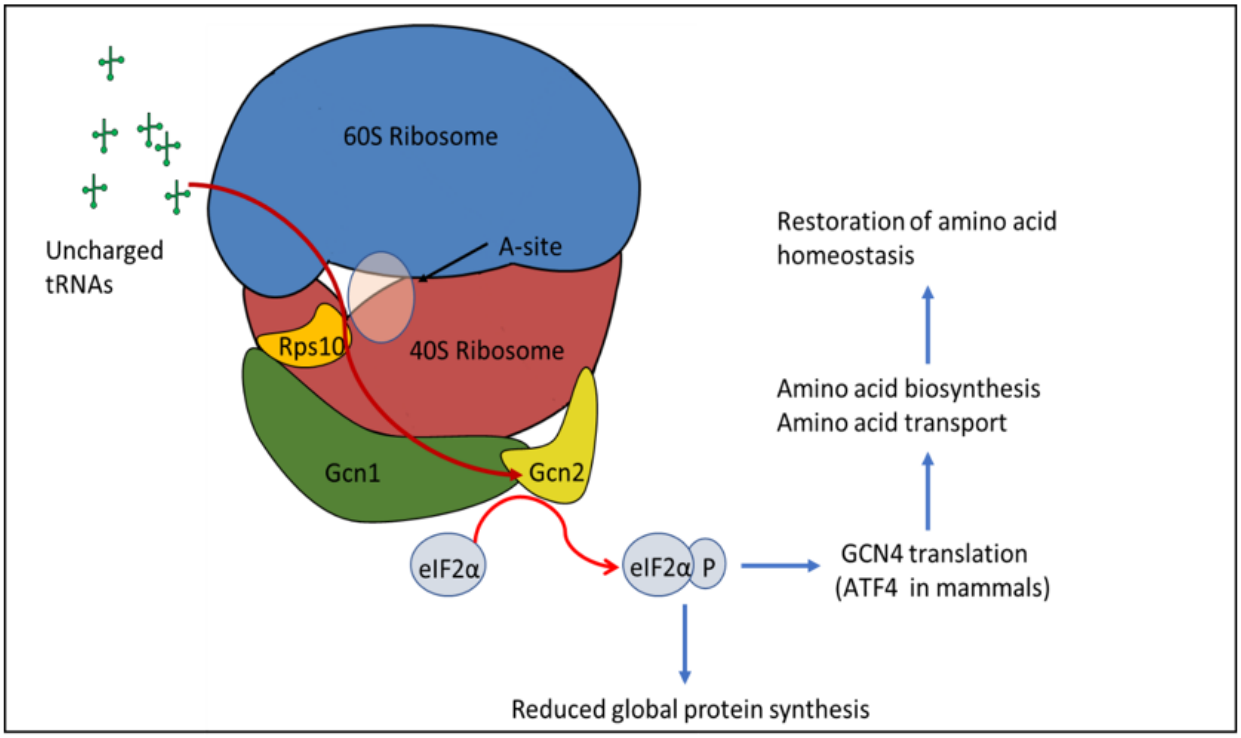

Figure 1.9 *Proposed working model for Gcn2 activation by uncharged tRNA, requiring Gcn1 and its interaction with the ribosome*

During amino acid starvation, levels of uncharged tRNA increase in the cell. In a codon dependent manner, uncharged tRNAs enter the ribosomal A-site. Gcn1 is required for the transfer of uncharged tRNA to and/or from the ribosomal A-site. Direct binding occurs between Gcn1 and Gcn2 and both are in contact with the ribosome, with 77% of Gcn1 involved in ribosomal binding. Transfer of uncharged tRNAs to Gcn2 causes Gcn2 auto-phosphorylation resulting in activation Gcn2. Activated Gcn2 phosphorylates the α sub-unit of eIF2 leading to decreased global protein synthesis. Conversely Gcn4 translation increases, and ultimately restoration of amino acid homeostasis occurs via transcription of amino acid biosynthesis genes.

1.10 Testing the working model of Gcn2 activation

To test the working model where on the ribosome Gcn1 and Gcn2 bind to carry out their functions needs to be fully mapped. The binding of Gcn1 to Rps10 is the only publicised and confirmed Gcn1 ribosomal protein binding site which has also been shown to be required for the full function of Gcn2 under amino acid starvation conditions (Lee et al., 2015). Gcn2 ribosomal contacts have so far been shown only *in vivo* in a purified mammalian component system where Gcn2 is shown to interact and be activated by ribosomal P-stalk proteins. Knowledge of exactly where on the ribosome these regulatory proteins are located and carry out their functions will allow for the formation of a more accurate understanding of how exactly uncharged tRNAs are delivered to Gcn2.

Considering the large size of Gcn1, at 2672 amino acids, together with the fact that 77% of the protein binds to the ribosome, infers that the contacts on the ribosome are multiple and vast. As separate mutations in vastly separate regions of Gcn1 infer reduced ribosomal binding and activity, this implies that the contact points on the ribosome are also greatly vast. Gcn1 is in fact $1/10^{th}$ the size of the ribosome, supports the idea that a large portion of the ribosome and its ribosomal proteins must be contacted by Gcn1. The one confirmed ribosomal protein to bind to Gcn1, Rps10 is only 105 amino acids in size, implying that at the very least, roughly only $1/20^{th}$ of Gcn1 ribosomal contacts have been identified (assuming all 105 amino acids of Rps10 interact with the approximate 2000 amino acids of Gcn1 involved in ribosomal binding).

A recent study by Jochmann (2014), a previous master's student of the Sattlegger lab, investigated the effects of deletion of each small and large ribosomal protein on the ability of the resulting deletion strains to overcome amino acid starvation. Several small and large ribosomal proteins were identified as potential Gcn1 or Gcn2 binding sites in this screening including; Rps18, Rps26, Rps28, Rpl21 and Rpl34. Ribosomal proteins are essential. The advantage of in that a large number of Rpls are encoded by two genes. Deletion of one of the genes leads to the reduction (knockdown) of the corresponding Rpls, allowing that gene to be viable Strains with knock down of the above of these proteins displayed sensitivity to amino acid starvation inducing drugs and some displayed reduced eIF2-α phosphorylation levels (Jochmann, 2014). A limitation to this approach however is that it cannot be used to investigate ribosomal proteins encoded by only one gene. Furthermore, knockdown of some RP can mass affect cell viability, making it impossible to score for effects on

Gcn2 activation. An alternative approach to deleting genes is the overexpression of ribosomal proteins. This has been shown to be an effective method previously by Lee et al. (2015) where Rps10 overexpression causes yeast strains to be sensitive to amino acid starvation inducing drugs (Lee et al., 2015).

Gcn1 binds to 60S has not been investigated to date. Gcn1 is very large, making it likely that it also contacts 60S. In additions Gcn2 is already known to associate with the large ribosomal subunit and polysomes, and to contact the P-stalk of the large ribosomal subunit *in vivo.* Therefore, it would stand to reason that contact to multiple small and large ribosomal proteins in unison is critical to elicit the full level of Gcn2 activation. Thus, to get a more insight into the contribution of the large ribosomal subunit in Gcn2 activation, this current research aims to screen for possible ribosomal contacts between Gcn1 and Gcn2 and the ribosome by the over expression of each large ribosomal protein individually.

1.11 Research hypothesis and objectives

It is known that uncharged tRNAs which accumulate during amino acid starvation activate Gcn2 and this initiates the amino acid starvation response. The process of Gcn2 activation by uncharged tRNAs is known to involve the contact of Gcn2 to Gcn1 to the ribosomes. This interaction is vital in the full functioning amino acid starvation response.

I hypothesise that Gcn1 and Gcn2 bind to several large ribosomal subunit proteins, in addition to Gcn2 binding to the P-stalk, and that these interactions are critical for Gcn2 activation.

This hypothesis will be tested and refined by addressing the following three objectives:

1: Identify large ribosomal proteins that are putatively in contact with Gcn1 or Gcn2.

This will be investigated by screening a library of yeast strains that are each overexpressing one of the 46 large ribosomal proteins individually for their ability to grow on amino acid starvation media. Reduced growth on amino acid starvation is indicative of impaired ability to activate Gcn2.

2: Confirm whether reduced growth associated with overexpression of an Rpl is truly due to impaired Gcn2 activation.

This will be achieved by scoring for the phosphorylation levels of eIF2α, the substrate of Gcn2. Reduced levels of eIF2α-P is indicative of reduced Gcn2 activity. Confirm results from objective one checking overexpression levels.

3: Determine where on the large ribosome Gcn1 and Gcn2 reside.

With knowing which Rpl identified to impair Gcn2 activation when overexpressed, this will allow for the determination of a footprint (outline of interaction site for Gcn1 or Gcn2 on the ribosome) of Gcn2 and Gcn1 on the ribosome. The footprint will be compared with the location of the A-site and the P-stalk of the ribosome.

This will allow for the refinement of the current working model for the molecular mechanisms involved in the activation of Gcn2 under amino acid starvation.

1.12 Relevance of research

Information revealed on the molecular mechanisms involved in the transfer of the stress signal to Gcn2 in yeast can be applied to higher eukaryotes including Humans. Gcn2 and Gcn1 have been found in all eukaryotes studied to date, implying that the amino acid response pathways is highly conserved (Castilho et al., 2014).

Gcn2 has been shown to play an important role in the response to many other cellular processes besides amino acid starvation, including UV stress, oxidative stress and glucose starvation (Chaveroux et al., 2011; Deng et al., 2002; Yang, Wek, & Wek, 2000). Gcn2 is also found to be involved in the defence against DNA and RNA viruses, which themselves have developed counter defences against Gcn2 (Berlanga et al., 2006; del Pino et al., 2012; Won et al., 2012). Furthermore, Gcn2 plays an important role in neurobiology (Costa-Mattioli et al., 2005; Hao et al., 2005; Ma et al., 2013; Maurin et al., 2005). It is found to play a role in the formation of memories including the switch between long- and short-term memories (Costa-Mattioli et al., 2005; Trinh & Klann, 2013) . Gcn2 is also involved in neuronal development and feeding behaviours (Maurin et al., 2005). Gcn2 has been found to play a role in Alzheimer's disease, where it contributes to neuronal dysfunction associated with this disease (Ma et al., 2013)

A large focus of research into the effects of Gcn2 on health and physiology is the well-established link between Gcn2 and cancer. In solid human tumours, Gcn2 is found to be hyperactivated and this is related to cancer cell survival and proliferation (Wang et al., 2013; Ye et al., 2010). As Gcn2 is not required in healthy, well feed cells, this makes the inhibition of Gcn2 activation an attractive means of cancer treatment (Bunpo et al., 2009; Koromilas, 2015).

Knowledge gained in this study with respect to the involvement of the ribosomal binding sites of Gcn1 and Gcn2 required for Gcn2 activation may help further our understanding of the starvation response. As Gcn2 is found active in many diseases including Alzheimer’s and cancers, knowledge on how Gcn2 is activated may help lead to the development of effective treatment strategies against these diseases.

Chapter 2 Materials and Methods

2.1 Yeast strains used in this study

Table 2.1 *Yeast strains used in this study*

Strain	Genotype	Source
H1511	MATα ura3-52 trp1-63 leu2-3,112, GAL2 +	(Foiani, Cigan, Paddon, Harashima, & Hinnebusch, 1991)
H2556	MATα ura3-52 trp1-63 leu2-3,112, GAL2 +, gcn1Δ	(Sattlegger & Hinnebusch, 2000)

2.2 Plasmids used in this study

Table 2.2 *Plasmids used in this study*

Plasmid name	**Gene**	**Selectable marker**	**Vector**	**Source**
pES124-B2	*GST-gcn1(*2052–2428)	*URA3*, *leu2-d*, 2μ	pEG(KT)	(Sattlegger & Hinnebusch, 2000)
pES128-9-1	*GST* alone	*URA3*, *leu2Δ*, 2μ	pEG(KT)	(Sattlegger & Hinnebusch, 2000)
pRPL1A	*RPL1A**	URA3, Amp^R	BG1805	(Dharmacon, 2019)
pRPL2A	*RPL2A**	URA3, Amp^R	BG1805	(Dharmacon, 2019)
pRPL4B	*RPL4B**	URA3, Amp^R	BG1805	(Dharmacon, 2019)
pRPL5	*RPL5**	URA3, Amp^R	BG1805	(Dharmacon, 2019)
pRPL6A	*RPL6A**	URA3, Amp^R	BG1805	(Dharmacon, 2019)
pRPL7A	*RPL7A**	URA3, Amp^R	BG1805	(Dharmacon, 2019)
pRPL7B	*RPL7B**	URA3, Amp^R	BG1805	(Dharmacon, 2019)
pRPL8A	*RPL8A**	URA3, Amp^R	BG1805	(Dharmacon, 2019)
pRPL9A	*RPL9A**	URA3, Amp^R	BG1805	(Dharmacon, 2019)
pRPL10	*RPL10**	URA3, Amp^R	BG1805	(Dharmacon, 2019)
pRPL11A	*RPL11A**	URA3, Amp^R	BG1805	(Dharmacon, 2019)
pRPL12A	*RPL12A**	URA3, Amp^R	BG1805	(Dharmacon, 2019)
pRPL13A	*RPL13A**	URA3, Amp^R	BG1805	(Dharmacon, 2019)

pRPL15A	*RPL15A**	URA3, Amp^R	BG1805	(Dharmacon, 2019)
pRPL16A	*RPL16A**	URA3, Amp^R	BG1805	(Dharmacon, 2019)
pRPL17A	*RPL17A**	URA3, Amp^R	BG1805	(Dharmacon, 2019)
pRPL18B	*RPL18B**	URA3, Amp^R	BG1805	(Dharmacon, 2019)
pRPL19A	*RPL19A**	URA3, Amp^R	BG1805	(Dharmacon, 2019)
pRPL20A	*RPL20A**	URA3, Amp^R	BG1805	(Dharmacon, 2019)
pRPL21A	*RPL21A**	URA3, Amp^R	BG1805	(Dharmacon, 2019)
pRPL23A	*RPL23A**	URA3, Amp^R	BG1805	(Dharmacon, 2019)
pRPL24A	*RPL24A**	URA3, Amp^R	BG1805	(Dharmacon, 2019)
pRPL25	*RPL25**	URA3, Amp^R	BG1805	(Dharmacon, 2019)
pRPL26A	*RPL26A**	URA3, Amp^R	BG1805	(Dharmacon, 2019)
pRPL27A	*RPL27A**	URA3, Amp^R	BG1805	(Dharmacon, 2019)
pRPL28	*RPL28**	URA3, Amp^R	BG1805	(Dharmacon, 2019)
pRPL29	*RPL29**	URA3, Amp^R	BG1806	(Dharmacon, 2019)
pRPL30	*RPL30**	URA3, Amp^R	BG1807	(Dharmacon, 2019)
pRPL31A	*RPL31A**	URA3, Amp^R	BG1808	(Dharmacon, 2019)
pRPL33A	*RPL33A**	URA3, Amp^R	BG1809	(Dharmacon, 2019)
pRPL34A	*RPL34A**	URA3, Amp^R	BG1805	(Dharmacon, 2019)
pRPL34B	*RPL34B**	URA3, Amp^R	BG1805	(Dharmacon, 2019)
pRPL35A	*RPL35A**	URA3, Amp^R	BG1805	(Dharmacon, 2019)
pRPL36A	*RPL36A**	URA3, Amp^R	BG1805	(Dharmacon, 2019)
pRPL37A	*RPL37A**	URA3, Amp^R	BG1805	(Dharmacon, 2019)
pRPL38	*RPL38**	URA3, Amp^R	BG1805	(Dharmacon, 2019)
pRPL39	*RPL39**	URA3, Amp^R	BG1805	(Dharmacon, 2019)
pRPL40A	*RPL40A**	URA3, Amp^R	BG1805	(Dharmacon, 2019)
pRPL41A	*RPL41A**	URA3, Amp^R	BG1805	(Dharmacon, 2019)
pRPL42B	*RPL42B**	URA3, Amp^R	BG1805	(Dharmacon, 2019)
pRPL43A	*RPL43A**	URA3, Amp^R	BG1805	(Dharmacon, 2019)

*each *RPL* gene is tagged with a c-terminal fusion tag containing: His6, HA epitope, protease 3C site and a protein A ZZ domain.

2.3 Media

All media and solutions, unless otherwise stated, were prepared using double de-ioinsed water, made up to 1 L (unless otherwise stated) and sterilized for 20 minutes at 121^{o}C or by passing through a 0.2 µm cellulose acetate filter (Sartorius Stedim Biotech).

Glucose and galactose stock solutions

40% weight by volume glucose (FORMEDIUM^{TM}) or galactose (FORMEDIUM^{TM}) was dissolved in water

YPD (Yeast Peptone Dextrose)

10 g yeast extract (FORMEDIUM^{TM})

20 g peptone (FORMEDIUM^{TM})

20 g agar (for solid media only) (FORMEDIUM^{TM})

50mL sterile 40% stock added after sterilization.

YPG (Yeast Peptone Glycerol)

10 g yeast extract (FORMEDIUM^{TM})

20 g peptone (FORMEDIUM^{TM})

20 g agar (for solid media only) (FORMEDIUM^{TM})

15 mL glycerol (FORMEDIUM^{TM})

Synthetic defined media (SD)

1.9 g yeast nitrogen base without amino acids (FORMEDIUM^{TM})

5 g ammonium sulphate (Ajax)

20 g agar (for solid media only) (FORMEDIUM^{TM})

Synthetic complete media (SC)

1.9 g yeast nitrogen base without amino acids (FORMEDIUM™)

5 g ammonium sulphate (Ajax)

20 g agar (for solid media only) (FORMEDIUM™)

2.0 g amino acid mix (Kaiser synthetic complete drop-out mixture) (FORMEDIUM™)

Luria Bertani media (LB)

10 g bacto tryptone (FORMEDIUM™)

5 g yeast extract (FORMEDIUM™)

10 g Sodium chloride (Ajax)

2.4 Amino acid and nucleobases stock solutions

Amino acid	Solvent	Final concentration (g/100mLs)
Leucine (FORMEDIUM™)	water	1.31
Isoleucine (FORMEDIUM™)	water	0.656
Valine (FORMEDIUM™)	water	0.586
Tryptophan* (FORMEDIUM™)	water	0.8
Uracil (FORMEDIUM™)	water	0.224
Histidine (FORMEDIUM™)	water	2.09

*Tryptophan was filter sterilised and stored in a light proof container at 4°C

2.5 Drug stock solutions used

2 M 3-Amino-1,2,4-triazole (3AT) (FORMEDIUM™)

2 µg/ml Sulfometuron methyl (SM) (CHEM SERVICE)

Drug	**Solvent**	**Final concentration**
3 AT (* (FORMEDIUM™)	Water	16.816 g/100mLs
SM (CHEM SERVICE)	DMSO	2 µg/ml

*3AT was filter sterilised and stored in a light proof container at 4°C

2.6 Antibiotics used

Antibiotic	**Solvent**	**Final concentration (µl/100mLs)**
Ampicillin (FORMEDIUM™)	water	50

2.7 Permanent storage of yeast cultures

Yeast strains were streaked on SD glucose media and grown for 2-3 days at 30°C. Cells were then transferred from the plate to 2ml tubes with 500µl of sterile 30% v/v glycerol. Tubes were stored at -80°C.

30% v/v glycerol

15mLs of glycerol was added to 35mLs of water, distributed into 2 mL screw cap tubes, and then autoclaved.

2.8 Permanent storage of bacterial cultures

500µl of fresh overnight bacterial cultures were added to 1 mL of 100% v/v glycerol. Permed yeast strains were stored at -80^{o}C.

70% v/v glycerol

35mLs of glycerol was added to 15mLs of water, distributed into 2 mL screw cap tubes, and then autoclaved.

2.9 Plasmid isolation using alkaline lysis method

4 mL of overnight cultures of bacteria were grown on LB media with ampicillin. 1mL of each culture was added to a 1.5mL Eppendorf tube and centrifuged at 14,000 rpm at 4^{o}C for 1 minute. The supernatant was discarded. A further 1 ml of the overnight culture was added, and the procedure was repeated until all the overnight culture was pelleted. 150 µl of resuspension buffer containing RNase was added to the pellet and vortexed until the pellet was fully dissolved. 200 µl of lysis solution was added and the tubes were inverted several times until the solution became homogenous. 400 µl of ice-cold neutralisation solution was added to each tube and then inverted several times. Each tube was centrifuged at 14,000 rpm at 4^{o}C for 5 minutes. 600 µl of the supernatant from each tube was removed and added to a new Eppendorf tube. 600 µl ice cold isopropanol was added to the supernatant and each tube was inverted several times. Tubes were incubated at -80^{o}C for 30 minutes. Then each tube was centrifuged at 14,000 rpm at 4^{o}C for 5 minutes. The supernatant was removed and 600 µl of ice cold 70% ethanol was added, followed by centrifugation at 14,000 rpm at 4^{o}C for 5 minutes. The supernatant was removed, and the pellet was dried for 30 minutes. The pellet was re-suspended in 40 µl of TE pH 8.0 and stored at -20^{o}C.

Resuspension buffer*

Solution	Volume
1 M glucose	5 mL
1 M Tris-HCl	2.5 mL
0.5 M EDTA	1 mL
Water	90.5mL
total volume	100mLs

***10 µL of RNAse was added per 10 mL of buffer prior to use

1M glucose stock solution
9 grams of glucose was dissolved in 50mLs of water

1 M Tris-HCL stock solution
6.057 g of Tris base (Invitrogen) was dissolved in 50 mL of water and the pH was adjusted to 8.0 with concentrated HCl

0.5 M EDTA stock solution
14.612 g of EDTA (FORMEDIUM) was dissolved in 100 mL of water and the pH was adjusted to 8.0 with NaOH

Neutralisation buffer

Solution	volume
10 M NaOH	200 µl
1% SDS	1 mL
Water	8.8 mL
Total volume	10 mL

10 N NaOH stock solution

20 g of NaOH was dissolved in 50 mL of water

1% w/v SDS stock solution

0.3 grams of SDS dissolved in 30 mL water

Lysis buffer

Solution	Volume
5M Potassium acetate	60 mL
Glacial acetic acid	11.5 mL
Water	28.5 mL
Total volume	100 mL

2.10 DNA agarose gel electrophoresis

5 µl of isolated plasmid DNA was mixed with 1 µl of 6X loading dye and then loaded on a 1% agarose gel along with a 2-log DNA ladder. The gel was run for 30 minutes at a constant voltage of 100V.

1% agarose gel

1 g of agarose was dissolved in 100 mL of 1X TAE buffer and then 10 µl of ethidium bromide was added. The gel was poured into the gel tray and cooled for 20 minutes until set.

50X Tris Acetate EDTA (TAE)

Tris	276 g
Acetic acid	57.1 mL
EDTA	18.6 g
Water	Added up to 1 L

6X DNA loading dye

Bromophenol blue	0.25mg
Glycerol	3 mL
Water	7 mL

2.11 Yeast transformation

Making yeast competent

An overnight culture of yeast was grown in a glass tube containing 3 mL of YPD liquid media, at 30C in a roller. 1 mL of the overnight culture was used to inoculate a 250ml flask containing 50 mL of YPD liquid media and grown to an optical density of 0.8 at 30C and shaking at 160rpm. The culture was transferred to a 50 mL falcon tube and spun at 4000 rpm for 5 minutes at 4^{o}C. The supernatant was discarded, and the pellet re-suspended with 8 mL of solution 1, then incubated at 30^{o}C shaking for 30 minutes, to make the cells competent.

Transformation

The competent yeast cells were spun at 4000 rpm for 5 minutes at 4^{o}C. The supernatant was discarded, and the pellet re-suspend in 500µL of solution 1. Herring sperm DNA (10mg/ml) was denatured at 100^{o}C for 10 minutes, then quickly cooled ice-water. To an Eppendorf tube 5µL of denatured herring sperm DNA was added along with 5µL of plasmid DNA. 100µL of yeast culture was added and pipetted up and down. The culture was incubated for 30 min at 30^{o}C. 700µl of solution 2 was added, followed by an incubation at 30^{o}C for 45 minutes and shaking at 160 rpm.

The culture was heat shocked at 42°C for 10 minutes, and then cooled on ice for 5 minutes. Cultures were then spun at 1000 rpm for 5 minutes. The supernatant was removed, and the pellet re-suspended with 50µL of SD media. The cell suspension was spread on SD galactose plates using sterile glass beads (protocol outlined below) and incubated for 3 to 4 days at 30°C.

Solution 1

Solution	Volume
10X TE pH 7.4	1 mL
1M lithium acetate in TE	1 mL
Water	8 mL

10X TE

1.211g of Tris base and .372g of EDTA were dissolved in 100 mL of water and the pH was adjusted to 7.4 with concentrated HCL

1M Lithium acetate

10.2 g of lithium acetate was dissolved in 100 mL of water. Solution was filter sterilised.

Solution 2

Solution	**Volume**
44% PEG in 1X TE	9 mL
1M Lithium acetate in 1 X TE	1 mL

44% PEG in 1X TE

44g of poly ethylene glycol was dissolved in 10 mL of 10X TE then the volume was made up to 100mL with H_2O.

2.12 Sterile Glass bead procedure for distribution of transformants onto solid media

Following the transformation procedure outlined above, the resulting transformation solutions were placed on to solid media of SDGlucose containing appropriate amino acids. Sterile glass beads were added (approximately 20 beads per plate) and the plates were firmly shaken side to side on a flat surface, allowing the glass beads to transfer and distribute the suspended transformation solution across the places allowing for the formation of single colonies

2.13 Semi-quantitative growth assay

Two single colonies from each yeast transformation were picked, streaked for single colonies then grown on SD glucose plates. Each single colony was then grown to saturation in glass tubes containing SD glucose media in a roller at room temperature for 1-2 days. A 10-fold serial dilution was preformed 4 times on each culture. 5µl of the undiluted culture and of each of these 44 dilutions were transferred to plates containing solid media. Solid media used included the following: YPD, YPG, SD glucose, SD galactose and SD galactose containing 3AT ranging in concentration of 15mM to 150mM. The yeast strains were grown on the solid media at 30ºC for two to three weeks or until no growth changes were observed any more. The plates were scanned daily on a document scanner to document the growth of each yeast strain.

2.14 Conformation of plasmid expressing protein of interest in yeast using PCR

50 µL PCR reactions were carried out on colonies used for growth assays

Component	Volume
PCR-grade water	Up to 50µL
10X KAPA buffer	5 µL
10 mM dNTP mix	1 µL
10 µM Forward primer	2 µL
10 µM Reverse primer	2 µL
5 U/µl KAPA Taq DNA polymerase	0.2 µL
Template DNA (streak of colony)	Approximately $1/10^{th}$ of a colony

*a small streak of each colony was collected from colonies grown in solid media using a sterile pipette tip which was placed in each reaction mixture and mixed until dissolved.

PCR reaction mixes containing colony streaks were pulse vortexed prior to carrying out PCR analysis. PCR reactions were carried out with the following cycling protocol, using an Applied Biosystems® Veriti® 96-Well Thermal Cycler.

Step	Temperature	Duration	Cycles
Initial denaturation	95ºC	3 minutes	1
Denaturation	9ºC	30 seconds	
Annealing	55ºC	30 seconds	35
Extension	72ºC	1 minute	
Final Extension	72ºC	1 minute	1

2.15 Primers used in this study

Table 2.3. *Primers used in this study*

Primer	**Sequence**
Forward primer	5'-ATACCTCTATACTTTAACGTCAA-3'
Reverse primer	5'-ATAAT'CAGGAACATCGTATGGA-3'

2.16 Generation of whole cell extracts treated with formaldehyde

Cell growth

This procedure was conducted according to the protocol outlined by Lee et al. (Lee et al., 2017). Yeast strains were grown to saturation at 30^{o}C for 2 to 3 days in 4mls of SD medium containing glucose and supplements to cover auxotrophies. 250ml flasks containing 25mls of the same medium but galactose instead of glucose were inoculated with x ml of overnight cultures. Cultures were grown overnight at 26^{o}C and 160rpm until exponential phase was reached. Each strain was harvested at an OD_{600nm} around 0.8by by transferring them to 50ml falcon tubes containing 10 g of clean ice flakes and 0.675mls of x% formaldehyde. Tubes were left on ice for an hour with shaking every 15 minutes. 1ml of 2.5M glycine was added to each falcon tube to quench unreacted formaldehyde. Falcon tubes were spun at 4500rpm for 5 minutes. Supernatant was poured off and the pellet was re-suspended with 1ml of ice-cold double de-ionisesd water. 100µl aliquots were added to 0.6ml tubes and were spun at 12500 rpm for 10 minutes. The supernatant was poured off and the resulting pellets were frozen and stored at -18^{o}C.

For the generation of cell extracts originating from amino acid starved cells, SM was added at a final concentration of 1µg/ml 2 minutes prior to harvesting.

Cell lysis

200µl of 0.1M NaOH was added to the cell pellet, the pellet re-suspended, and left for 5 minutes. Tubes were spun at 4000 rpm for 5 minutes at 21^{o}C. The resulting supernatant was poured off and

the pellet re-suspended with 100µl of 2x denaturing gel loading dye. The tubes were then immediately heated to 80^{o}C for 8 minutes and spun vortexed briefly. The resulting denatured cell extracts were then subjected to SDS PAGE.

2X denaturing gel loading dye*

Solution	Volume/weight
0.5M TrisHCL (pH 6.8)	25 ml
SDS	4g
Glycerol	20ml
water	55ml

*10% 2-Mercaptoethanol was added prior to use.

0.5 TrisHCL pH 6.8

6.05 g Tris was dissolved in 80 ml water. The pH was adjusted to 8.8 with the addition of concentrated HCL (Unilab) acid. Water was added to a final volume of 100 ml

2.17 SDS PAGE

Sodium dodecyl sulphate polyacrylamide gel electrophoresis (SDS PAGE) gradient gels were prepared using 4% and 20% acrylamide and reused precast Bio-Rad Criterion™ gel cassettes, and the gel cassettes were then placed in a Bio-Rad Criterion™ electrophoresis cell unit. 8 µg to 1.5 µg of sample was added to each well. Alongside samples, 10 µL of See blue plus 2 MW marker (Invitrogen) was loaded in the first well to observe the migration of proteins and determine approximate protein sizes. Gels were run at 180V and 120 mA until the dye front reached the bottom of the gel cassette, or until the desired separation of proteins had occurred as judged by the separation of the MW marker

Gradient SDS PAGE gel solutions

	40% bis-acrylamide	10% SDS	1.5M Tris-HCL pH 8.8	H_2O	Total volume
4%	10mls	1ml	25ml	74ml	100ml
20%	50ml	1ml	25ml	24ml	100ml

40% stock bis-acrylamide: acrylamide (29:1) solution

193.4 g of acrylamide (Invitrogen) and 6.6 grams of bis-acrylamide (Invitrogen) was weighed out and water added to 500mls.

1.5M Tris-HCL pH 8.8

18.171 g UltraPure™ Tris base (Invitrogen) was dissolved in 80mls water, the pH was adjusted to 8.8 with the addition of concentrated HCL (Unilab) acid. Water was added to a final volume of 100mls

2.18 Western blotting

Western transfer

After electrophoresis, the gradient gels were then placed on a 0.2µm nitrocellulose membrane (Bio-rad) and the separated proteins were transferred to the membrane using the Bio-Rad transfer unit containing chilled transfer buffer, for 1 hour 20 minutes at 100V and 1A. Equal loading of each sample was determined by staining resulting transferred nitrocellulose membranes with 0.8% Ponceau S followed by washing with 5% glacial acetic acid. Membranes were then scanned on a document scanner to record the results. After that, membranes were blocked in 5% (w/v) fat free milk powder or 3% (w/v) BSA (for detecting phosphorylated proteins) dissolved in TBS-T solution, for 1 hour. The blocking solution was discarded and the appropriate primary antibody solution was added as outlined in the Table below. The primary antibody was recovered after

incubation for future use. The membranes were washed in TBS-T three times over the course of 25 minutes. The washed membranes were then placed in a TBS-T solution containing the corresponding secondary antibody conjugated to horseradish peroxidase (HRP) that can be used to detect any bound primary antibody to the membrane. Antibodies were used at the concentrations outlined in the Table below, for 1 hour with shaking. The secondary antibody solution was discarded, then membranes were washed in TBS-T for 40 minutes with the TBS-T solution being changed 4 times. Bound antibodies were then detected as outlined below.

Transfer buffer

1X Tris-Glycine	100 mL
Methanol	200 mL
Water	700 mL

10X Tis-Glycine

Tris	151.5 g
Glycine	720 g
Water	Made up to 5 L

0.8% (w/v) Ponceau S stain

0.8 g of Ponceau (Helena)	100mls of 5% acetic acid

5% acetic acid

50 ml of glacial acetic (Unilab)	950mls of de-ionised H_20

10X TBS

24 g Tris and 80 g of NaCl (Univar) was dissolved in 900 ml of H_20 with the pH being adjusted to 7.4 with conc. HCL and H_20 added to a total volume of 1000 ml

TBS-T

Water	899 mL
10X TBS	100 mL
Tween-20	1 mL

Blocking solutions

5% (w/v) non-fat milk powder in TBS-T

0.5 g was of non-fat milk powder (Pams) was dissolved in 10 mL of TBS-T

3% (w/v) BSA in TBS-T

0.3 g was of BSA (Life technologies) powder was dissolved in 10 mL of TBS-T

Primary antibodies and concentrations used in this study

Antibody	Concentration	Source
Anti-EIF2 alpha/EIF2S1 [p Ser51] Antibody (E90)	1:5000	Thermo Fisher
PGK1	1:5000	Santa Cruz

Secondary antibodies used in this study

Antibody	Concentration	Source
Goat anti mouse	1:50,000	Thermo Fisher
Goat anti rabbit	1:100,000	Thermo Fisher

Detection of bound antibodies

Equal volumes of prepared detection solutions A and B were mixed immediately prior to detection at a total volume of 20µl per 1cm^2 of nitrocellulose membrane. The detection solution mixture was pipetted evenly over the surface of the membrane and a thin piece of plastic film was placed on

top. The HRP bound to the secondary antibody was then detected using a Bio-Rad ChemiDoc™ imaging system with chemiluminescence detection mode selected. Resulting images were saved and then analysed with Bio-Rad Image Lab software.

Solution A*	**Solution B***
13 mL 1.5M Tris pH 8.8	13 mL 1.5M Tris pH 8.8
187 mL water	187 mL water
0.088 g Luminol powder	134 µL H_20_2
0.013 g p-Coumaric acid	

*Solutions were kept at 4^{o}C in a light proof bottle

Re-probing membranes

Membranes requiring further re-probing with subsequent primary antibodies were first incubated for 30 minutes using equal volumes of hydrogen peroxide and ddH_20, using a volume sufficient to cover the membranes. The membranes were then washed a further two times in TBS-T for 15-minute. Washed membranes were then probed with the next primary antibody following the western blotting protocol outlined above.

2.19 Analysis and quantification of western signals

Resulting images from western blotting protocol above were analysed using Image Lab software (Version 6.0.0 build 25 standard edition). Molecular weights of detected bands were estimated with the molecular weight analysis tool and with the use of the molecular weight marker transferred on to membranes. Signal intensities were determined for each detected band on the blotted membranes. Signal intensities were normalised across the membranes by adjusting the signal intensities with the signal intensities obtained from probing the membranes for a housekeeping protein.

Chapter 3 Results

3.1 Identification of large ribosomal proteins required for the full activation of Gcn2

As mentioned in the introduction, the mechanism by which the sensing of amino acid starvation occurs is far from being fully understood. Important steps in the process remain unclear, including how uncharged tRNAs are directed to Gcn2 during amino acid starvation. Research thus far has helped formulate a working model on molecular mechanisms involved in the activation of Gcn2 under amino acid starvation. It has become clear that the interaction of both Gcn1 and Gcn2 with ribosomes plays a vital role in the fully functioning amino acid starvation response.

To gain a better understanding of the detailed mechanisms of how Gcn1 and Gcn2 are involved in sensing amino acid starvation and subsequent Gcn2 activation, a complete footprint of Gcn1 and Gcn2 on the ribosome is required. This can be achieved by assessing individually which of the large ribosomal proteins Gcn1 or Gcn2 are required for the full activation of Gcn2.

A previous student (Jochmann, 2014) from the Sattlegger lab carried out an investigation of ribosomal proteins required for the full functioning of the amino acid starvation response by using a library of yeast strains that each lack one of the genes coding for an individual ribosomal protein. Possible Gcn1-Gcn2 contacts to both small and large ribosomal proteins were identified. In this screen, reduced growth and eIF2α-P levels of strains growing on starvation media was indicative of impaired Gcn2 activity. This indicates that the deletion of certain ribosomal proteins results in a dissociation of either Gcn1 or Gcn2 from the ribosome, either of which would lead to the reduced Gcn2 activity seen with the reduced growth and reduced eIF2α-P levels.

More recently Yeast-Two Hybrid Y2H studies have been carried out with a library of small ribosomal proteins as prey and Gcn1 as bait, with Rps10 being successfully identified as binding to Gcn1 (Lee et al., 2015). Reduction in levels of Rps10 by deletion of one of the gene paralogues coding for Rpl10 was found to interfere with the ability of yeast to grow and respond to amino acid starvation media. This was confirmed with reduced eIF2α-P levels, indicating a reduction in the function of Gcn2. This study also identified that overexpression of Rps10 is an effective means of identifying the requirement of a ribosomal protein for the fully functioning amino acid starvation response (Lee et al., 2015).

As the overexpression of Rps10 was seen to be an effective approach at identifying possible Gcn1-ribosomal contact, this led to this current study aimed to investigate the effect of overexpressing large ribosomal proteins on the amino acid starvation response

The reasoning of how overexpression of a Rpls affect Gcn2 function in that it leads to excessive amounts of this exogenous protein in the cells which are non-ribosome bound. If Gcn1 or Gcn2 binds to this Rpls, they will likely bind to the non-ribosome bound versions, thereby preventing them to bind the Rpls that is incorporated in the ribosome. Therefore, Gcn1 or Gcn2 are hampered in ribosome association. Since ribosome association is essential for Gcn2 activation, this will lead to reduced Gcn2 function. Since the overexpression of the Rpls renders the otherwise WT cell incapable of Gcn2 activation, this phenomenon is called a dominant negative effect.

3.2 Construction of a yeast library overexpressing large ribosomal proteins

In order to determine the possible effect of overexpression of each large ribosomal protein on Gcn2 activation in yeast, a library of yeast strains each overexpressing one of the large ribosomal proteins needs to be created. This library can be created by transforming plasmids, each containing one of the large ribosomal protein genes, into a wild type yeast strain, with their expression being under the control of an inducible promoter.

Plasmids were available from the Yeast ORF collection provided from Dharmacon each containing one of the large ribosomal protein genes (Dharmacon, 2019). Each of the large ribosomal proteins ORFs have been cloned into the Gateway destination vector of BG1805 with a *URA3* marker. The large Rpl ORFs are under the promoter of the yeast *GAL1* gene, which allows induced expression in the presence of galactose. The ORFs are also fused with a tandem affinity tag at the C-terminus. The affinity tag consists of a Protein A (ZZ domain), a protease 3C site, HA and a 6xHis tag. A plasmid map is depicted below in Figure 3.1. *E. coli* cells containing these plasmids were obtained with ampicillin resistance for selection. Of the 46 large ribosomal protein genes, 39 of them were available for use in this current study. One paralogue for each large ribosomal protein gene was

used in this study except for, RPL*7* and *RLl34* where both paralogues were used.

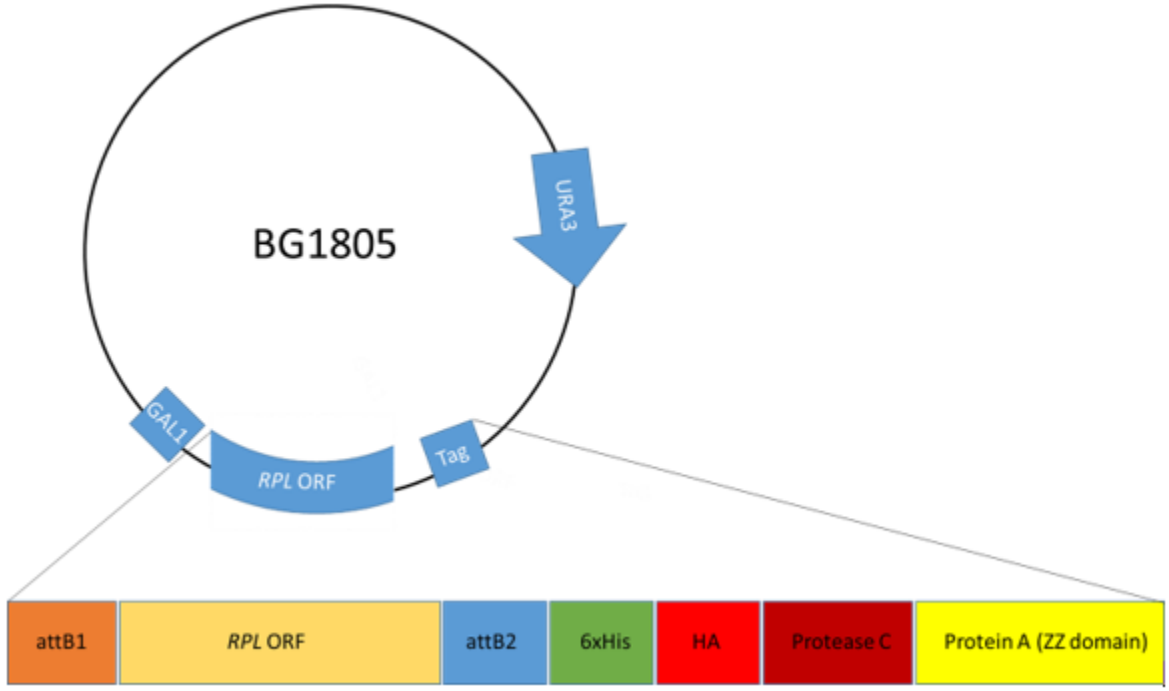

Figure 3.1 *Plasmid map of BG1805*

RPL ORF are gateway cloned into URA3 vector. RPL ORF is under the control of GAL1 inducible promoter. RPL ORF are expressed a c-terminal tandem affinity tag consisting of; Protein A (ZZ domain), protease 3C, HA and a 6xHis tag.

The plasmids containing one of the large ribosomal proteins (Table 2.2) present in the provided *E.coli* strains were isolated as outlined in materials and methods. Each isolated plasmid was then transformed into the WT strain H1511 (Table 2.1), this led to a library of yeast strains where each strain contains a specific over-expressible *RPL* gene. For each Rpl, four independent colonies (a, b, c and d) were streaked on solid media as well as being placed in permanent storage as outline in material and methods. The presence of the plasmid containing the expected large ribosomal protein ORF in the newly formed yeast strains was confirmed with colony PCR analysis on two of the four colonies (using primers from Table 2.3 in materials and methods) using protocol outlined in materials and methods. The forward primer annealed to the plasmid between 16 and 39 bp upstream of attB1. The reverse primer annealed to the plasmid between 45 and 67 bp downstream of attB2. This led to the amplicons from colony PCR containing the ORF of the gene

as well as 156 bp flanking both sides of this region. The PCR amplicons were resolved on a 1% agarose gel. A 2-log DNA ladder was run next to the PCR amplicons.

A representative of the PCR analysis is shown below for yeast strains overexpressing Rpl1A, Rpl2A, Rpl4b, RPL5, Rpl6A and Rpl7B in Figure 3.2. (PCR analysis of all Rpl overexpressing strains is in appendix). Sizes in base pairs (bp) found for bands for colony a and b from each Rpl overexpressing strains was determined with molecular weight analysis tools using image lab software, where amplicon sizes were determined against the 2-log ladder loaded with each agarose gel. The determined sizes of each amplicon are listed in Figures 5.1 to 5.7 in the appendix.

A)

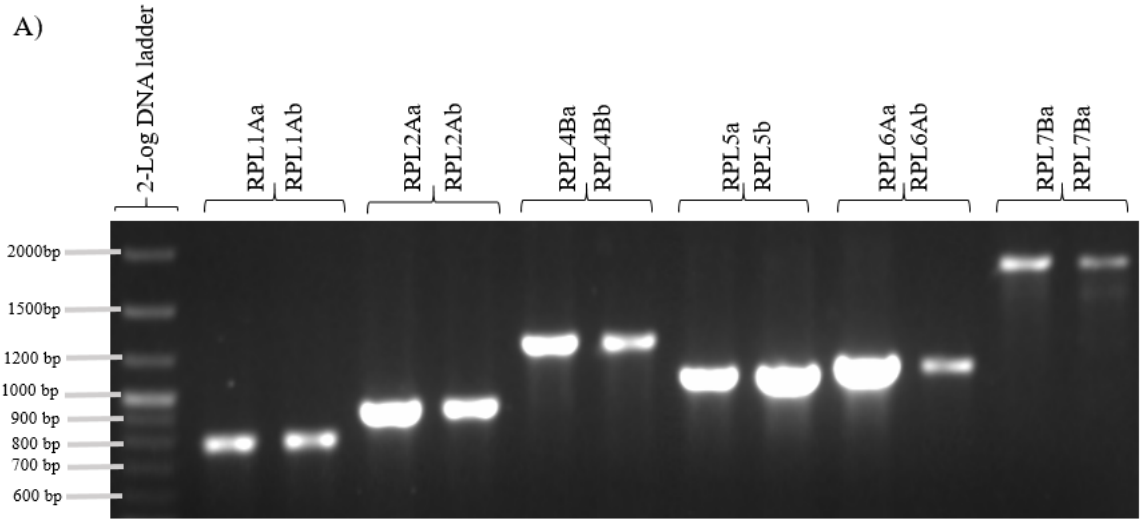

B)

yeast containing plasmid borne gene as indicated	Expected size (bp)	Found size (bp)
RPL1A	807	a) 789 b) 812
RPL2A	918	a) 932 b) 954
RPL4B	1242	a) 1287 b) 1302
RPL5	1047	a) 1102 b) 1088
RPL6A	684	a) 1129 b) 1171
RPL7B	888	a) 1898 b) 1923

Figure 3.2 *PCR analysis of RPL strains 1A to 7B (two colonies, a and b, of each strain were analysed), confirming the correct size for the respective RPL genes in the BG1805 vector*

A) Shown is PCR analysis of RPL strains 1Aa to 7Bb loaded on a 1% agarose gel (lanes 2-11) compared against 2-log DNA ladder (lane 1). **B)** Table indicates the expected size in bp of each respective RPL gene and the found size obtained by molecular weight analysis using image lab software.

The expected size of the amplicon was determined based on the yeast genome database, that is the intron-less ORF for each respective gene (Cherry et al., 2011; Saccharomyces Genome Database, 2019, March 17). As can be seen from the analysis of these colony PCR amplicons, colony PCR of a and b from RPL1A, RPL2A, RPL3A, RPL4B, RPL5, RPL8A, RPL9A, RPL1A0, RPL11A, RPL12A, RPL13A, RPL15A, RPL20A, RPL21A, RPL24A, RPL29A, RPL30, RPL35A, RPL37A, RPL38A, RPL39A, RPL41A, RPL42A, and RPL 43A all yielded PCR amplicons with estimated size similar to that which is expected Interestingly the PCR amplicons strains RPL 6A, 7A, 7b, 16A, 17A, 18B, 23A, 25A, 26A, 27A, 28, 31A, 33A, 34A, 34B and RPL40A significantly differ from the expected length of the coding sequence (Saccharomyces Genome Database, 2019, March 17). However, when the size of the intronic DNA is added to the coding sequence of these

larger than expected PCR amplicons, the found sizes matched similarly with that of the amplicon. A summary of expected and found amplicon lengths is shown in Table 3.1.

To verify the identity of the RPL reads from several of the above PCR products were sequenced commercially. Results of analysis of obtained sequencing data is displayed in Figures 5.8 to 5.12 in the appendix. As is seen in Figure 5.9 in the appendix, the colony PCR product from Rpl18 sequenced commercially does indeed contain intronic DNA in the PCR product as was predicted from the found size in Figure 5.3 and in displayed in Table 3.1 b

Table 3.1 (following page) Analysis of RPL genes and determined PCR sizes of amplicons from colony PCR of colonies a and b of Rpl overexpressing strains as indicated

Dark green indicates where the found size is of the expected size from coding sequence (CDS) only and does not appear to include intronic DNA. Light green indicates where the genomic DNA of the RPL *gene* does not contain any intronic DNA. Light red indicates where the found size corresponds to genomic DNA with the inclusion of intronic DNA. All sizes are in base pairs (bp).

Strain	genomic DNA contains intron	genomic DNA	CDS	expected size with genomic DNA (intronic and CDS) plus 156 bp gateway	expected size with CDS only plus 156 bp gateway	determined PCR size from each colony
RPL1A	no	651	651	807	807	a) 789 b) 812
RPL2A	yes	909	762	1065	918	a) 932 b) 954
RPL4B	no	1086	1086	1242	1242	a) 1287 b) 1302
RPL5	no	891	891	1047	1047	a) 1102 b) 1088
RPL6A	yes	943	528	1099	684	a) 1129 b) 1171
RPL7A	yes	1659	732	1815	888	a) 1772 b) 1799
RPL7B	yes	1548	732	1704	888	a) 1898 b) 1923
RPL8A	no	768	768	924	924	a) 941 b) 956
RPL9A	no	573	573	729	729	a) 736 b) 736
RPL10	no	663	663	819	819	a) 827 b) 814
RPL11A	no	522	522	678	678	a) 665 b) 643
RPL12A	no	495	495	651	651	a) 610 b) 610
RPL13A	yes	962	597	1118	753	a) 725 b) 719
RPL15A	no	612	612	768	768	a) 725 b) 713
RPL16A	yes	887	597	1043	753	a) 971 b) 962
RPL17A	yes	968	552	1124	708	a) 917 b) 908
RPL18B	yes	990	558	1146	714	a) 1016 b) 1008
RPL19A	yes	1073	567	1229	723	a) 618 b) 618
RPL20A	yes	993	516	1149	672	a) 681 b) 681
RPL21A	yes	868	480	1024	636	a) 634 b) 634
RPL23A	yes	915	411	1071	567	a) 1049 b) 1024
RPL24A	no	465	465	621	621	a) 591 b) 573
RPL25A	yes	840	426	996	582	a) 924 b) 900
RPL26A	yes	828	381	984	537	a) 861 b) 848
RPL27A	yes	969	408	1125	564	a) 1095 b) 1073
RPL28	yes	958	447	1114	603	a) 1073 b) 1073
RPL29	no	177	177	333	333	a) 334 b) 344
RPL30	yes	545	315	701	471	a) 474 b) 487
RPL31A	yes	760	439	916	595	a) 929 b) 938
RPL33A	yes	846	321	1002	477	a) 1041 b) 1062
RPL34A	yes	760	363	916	519	a) 900 b) 910
RPL34B	yes	835	363	991	519	a) 976 b) 988
RPL35A	yes	851	360	1007	516	a) 506 b) 506
RPL36A	yes	763	300	919	456	a) 921 b) 932
RPL37A	yes	623	264	779	420	a) 441 b) 441
RPL38	no	234	234	390	390	a) 417 b) 417
RPL39	yes	539	153	695	309	a) 283 b) 272
RPL40A	yes	818	384	974	540	a) 1000 b) 968
RPL41A	no	75	75	231	231	a) 173 b) 168
RPL42B	yes	759	318	915	474	a) 388 b) 400
RPL43A	yes	679	276	835	432	a) 371 b) 371

	Found size is of expected size from coding sequence only.		Genomic DNA does not contain any intronic DNA.		Found size appears to include intronic DNA.

3.3 Assessing growth of Rpl overexpressing strains on 3AT containing starvation media

To identify putative Gcn1 or Gcn2 ribosomal contacts, the effect of overexpressing each large ribosomal protein on yeast growth on starvation media can be assessed, as done previously for the overexpression of Rps10 (Lee et al., 2015). This assessment can be carried out by conducting a semi-quantitative growth assay for each Rpl overexpressing strain.

Colonies a and b overexpressing *RPL* gene were grown to saturation to carry out a semi-quantitative growth assay. Using the saturated overnight cultures, a series of four 10-fold dilutions was carried out, giving a total of five concentrations of cultures. Next 5 µl of each of the overnight cultures and the four dilutions were transferred to solid media, as illustrated in Figure 3.3 below.

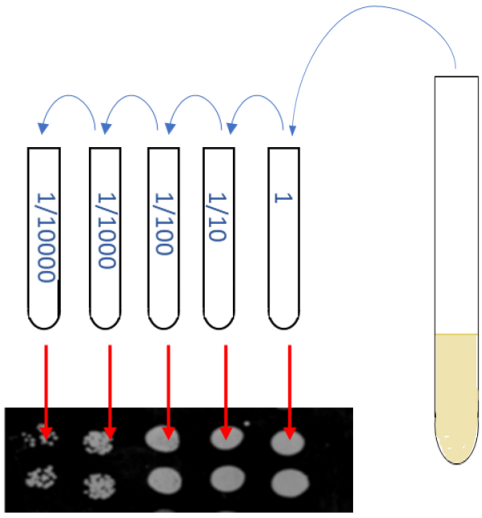

Figure 3.3 *Experimental procedure for semi-quantitative growth essay.*

Saturated culture (test tube located to the right of the diagram) was subjected to 10-fold serial dilutions as indicated by the blue arrows (resulting dilution factor s of; 1:10, 1:100, 1:1000 and 1:10,000). 5 µl of each dilution was then spotted and grown on solid media as indicated.

Growth assays for each Rpl overexpressing strain were conducted on solid Synthetic Defined (SD) medium containing glucose, solid SD medium containing galactose (SGal), and SGal medium containing the drug 3-Amino-1,2,4-triazole (3AT) at four different concentrations of 15 mM, 30 mM, 60 mM and 90 mM. The use of the four different concentrations allows for the assessment of the degree of sensitivity to 3AT. SGal plates without 3AT were used to test whether overexpression

of a RPL gene leads to a growth defect. Plates containing SD with glucose were used to assess the growth of the yeast strains on SD media without inducing expression of the large ribosomal proteins. Plates containing Yeast Peptone Dextrose (YPD) a nutrient rich medium, were used as reference for the yeast Peptone Glycerol (YPG) plates. The YPG plates were used to verify cells have functional mitochondria as mutations can occur during transformation. Yeast cells with damaged mitochondria are identifiable by their inability to grow on media containing glycerol. Growth was monitored and recorded over three to four weeks or until no change in growth was observed. All growth was carried out in a 30^{o}C incubator.

A wild type yeast strain transformed with an empty vector was used as a control because Gcn2 should be fully functional in this strain. Growth of this strain can be referred to indicate the growth expected when there is no impairment on the starvation response. A yeast strain deleted for *GCN1* (*gcn1Δ*) was used as another control strain as this strain is unable to grow under starvation conditions due to inability to activate Gcn2. A final control used was a yeast strain overexpressing the Gcn1 C-terminal fragment encompassing amino acids 2052-2428 (*gcn1*- [2052-2428]) under the control of a galactose inducible promoter. Overexpression of *gcn1*[2052-2428] is known to compete with Gcn1 for Gcn2 binding, thus reducing the amino acid starvation response (Sattlegger & Hinnebusch, 2000). This is used as a control as there should be a reduced ability of this strain to grow on starvation media, which would confirm that the Gal promoter within the plasmids used is functional and successfully led to overexpression of the ribosomal protein.

The two independent colonies of a and b from each Rpl overexpressing strains were subject to the semi-quantitative growth assay. Each growth assay contained the four 3AT concentrations mentioned above with the control plates mentioned above. On each plate two representative colonies (a and b) of strain overexpressing *gcn1*[2052-2428], Rpls and vector alone. The control strain of *gcn1Δ* strain was spotted to the left of the plate, vertically.

When grown on SDGal media containing no 3AT (non-starvation conditions) it was found that many of the strains had reduced growth when compared to the same strains grown on glucose containing no 3AT. This indicates that the overexpression of the large ribosomal proteins induced by galactose, causes the growth defect. This may be due to the fact that some large ribosomal proteins are involved in ribosomal biogenesis and this was taken into consideration when assessing the growth differences on the starvation containing media.

As expected, WT yeast strains containing the empty vector were able to grow on all plates including the starvation plates containing 3AT, because Gcn2 is fully functional and is able to sense and overcome amino acid starvation conditions. The *gcn1Δ* strain had severely reduced growth on the starvation plates (as compared to the control plates), as expected, as Gcn2 is not able to be activated due to the absence of Gcn1 and therefore cannot overcome starvation. Impaired growth therefore confirmed that the 3AT used in this study was potent and effective in triggering amino acid starvation. The strain overexpressing the *gcn1*Δ2052-2428 fragment displayed increasing sensitivity to 3AT as the concentration increased. This is indicative of the *gcn1*Δ2052-2428 fragment interfering with the contact between Gcn1 and Gcn2, reducing the amino acid starvation response as the function of Gcn2 is impaired. This result also confirmed that the different 3AT concentration can indicate the degree to which the amino acid starvation response is affected.

If overexpressing a large ribosomal protein leads to a reduced ability for that strain to grow on 3AT containing media compared to the WT strain overexpressing vector alone, then the strain is said to have the phenotype of 3AT sensitivity ($3AT^s$). Of the assessed strains seven strains displayed a $3AT^s$ phenotype. The $3AT^s$ phenotype was given to all strains displaying 80% or less growth at one 3AT concentration or more compared to the WT strains. The six strains displaying the $3AT^s$ include those overexpressing Rpl18, Rpl20, Rpl30, Rpl39, Rpl40 and Rpl43. The growth of these strains is displayed below in Figure 3.4 where $3AT^s$ strains are typed in bold red text to the right of the Figure. Growth of all strains are displayed in Figures 5.8 to 5.10 in the appendix.

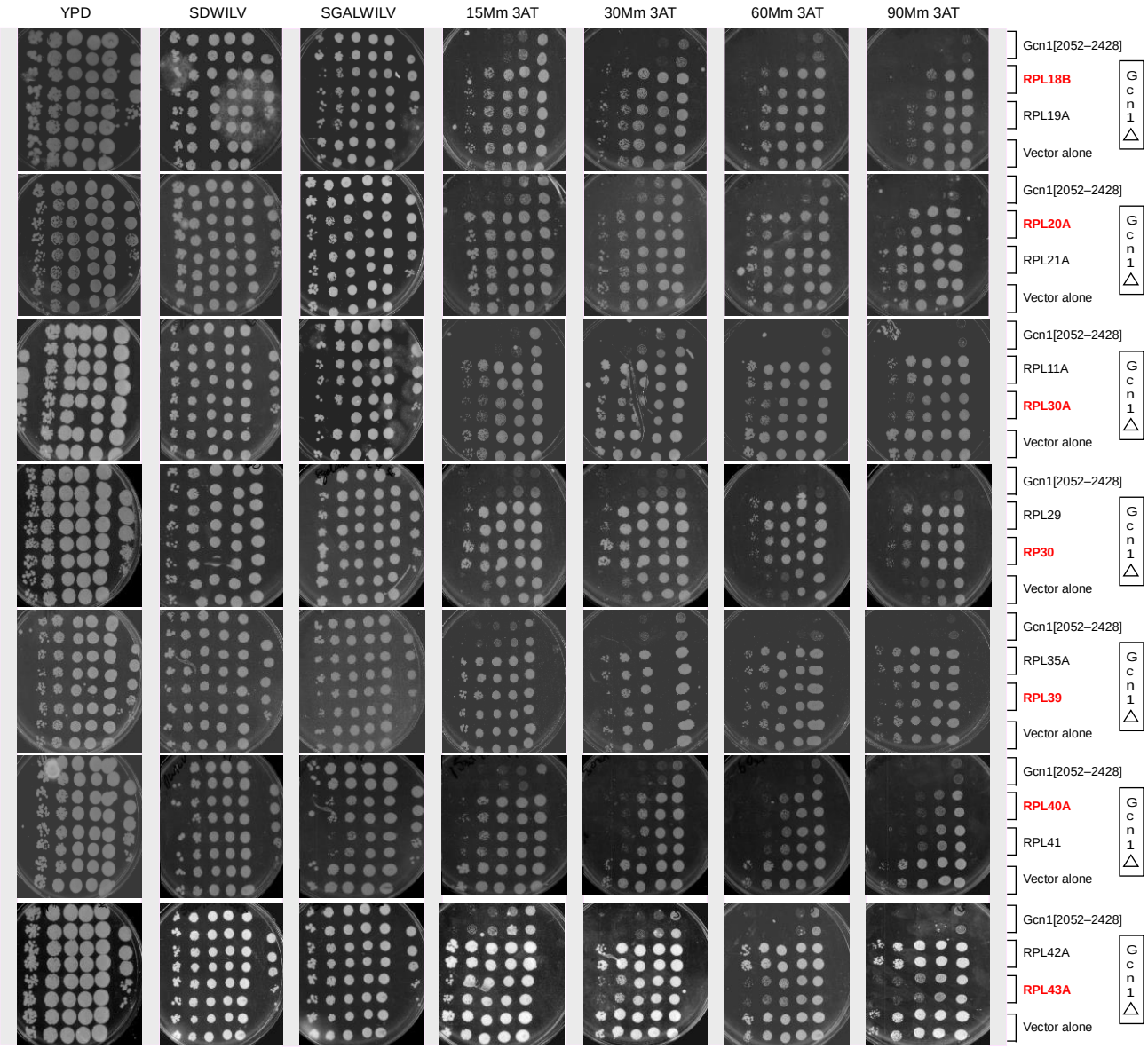

Figure 3.4 *Large ribosomal proteins displaying reduced growth when subjected to amino acid starvation*

Semi-quantitative growth assays were performed with the yeast strains as indicated to the right of the images. Plates used included YPD, SD (SDWILV) with glucose, SGal (SGALWILV) and SD with galactose containing four different concentrations of 3AT (15 mM, 30 mM, 60 mM, and 90 mM). Strains assessed for growth on starvation media are indicated to the right of the figure. Stains displaying sensitivity to amino acid starvation when a Rpl is overexpressed are indicated by bold red text to the right of the Figure.

3.4 Quantitative analysis of growth differences caused by Rpl overexpression

In order to quantify and gauge more objectively the observed growth differences, growth scores were calculated for each strain. The growth seen for each strain was converted to a numerical value, where the growth of each strain at each of the five dilutions was scored as indicate below. Full growth (100%) is scored as 10, 75% growth scored 7.5, 50% growth scored 5, 25% scored 2.5 and no growth scored 0 (see Figure 3.5 below). The growth scores were totaled, where the maximum possible score is 50 (5 times a score of ten). The growth scores were calculated for all Rpl overexpressing strains and the WT control on all 4 concentrations of starvation plates and the SDGal control plate (no 3AT) and are presented in Table 5.1 found in the index. The growth for each representative colony (a and b) from each strain was found to be almost identical across all strains therefore a total growth score was given for each strain and not for the individual representative colonies. Where any small differences were observed, an average between the two colonies was calculated.

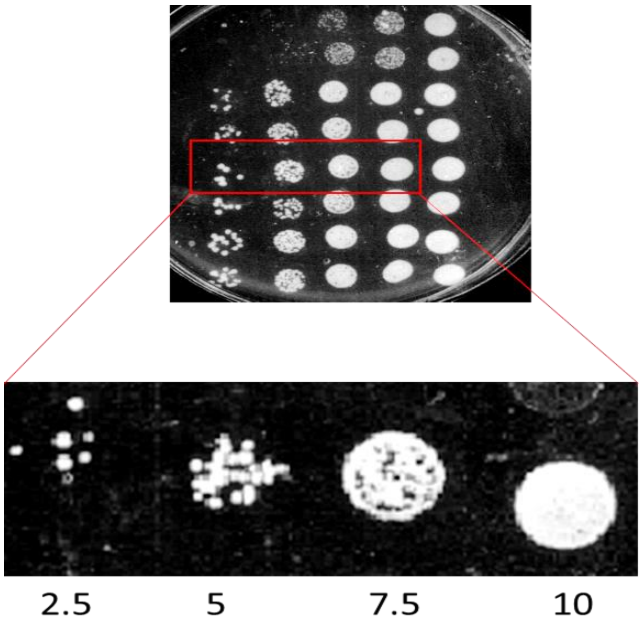

Figure 3.5 *Scoring system of yeast growth*

Represented growth of a yeast strain is highlighted and enlarged. Full growth is given a growth score of 10, 75% growth is given a score of 7.5, 50% growth is given a score of 5, 25% growth is given a score of 2.5 and no growth is given a score of 0.

The scores obtained on each of the 3AT plates were then divided by that of the control plate (SD galactose), to consider any growth defects that are unrelated to the effects on the amino acid starvation response. This value then was further divided by the value of the WT from each plate, allowing for direct comparison between different growth assays, as there may be some growth difference depending on the batch of media used (Figure 5.2, appendix). The final adjusted growth scores of each strain at each 3AT concentration was plotted in the bar graph below in Figure 3.6 to allow for the easy visual comparison of the growth rates between strains overexpressing different Rpls.

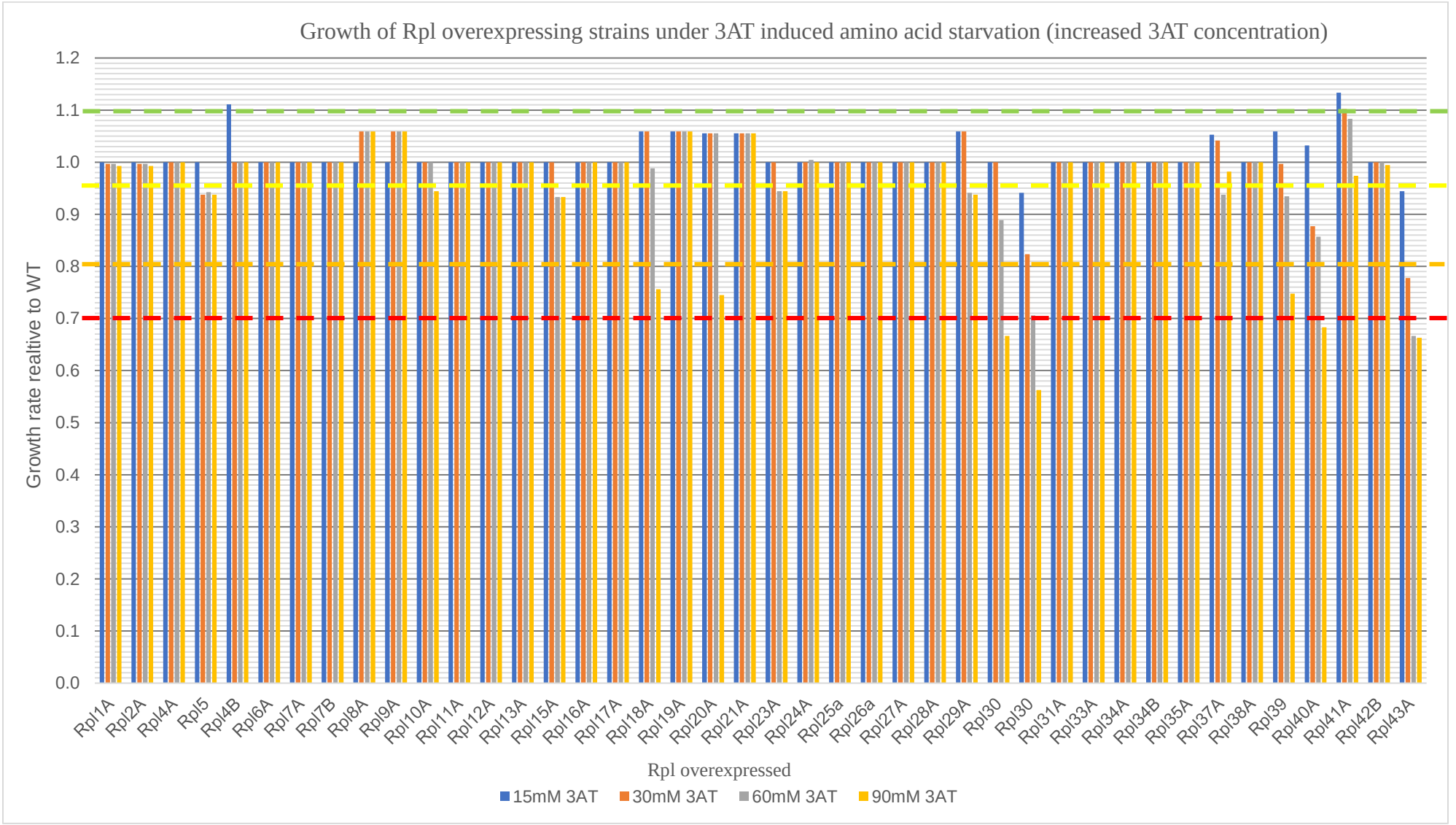

Figure 3.6 *Quantitative assessment of growth of RPL overexpressing yeast strains growing on starvation media.*

The bar graph shows the relative growth of yeast overexpressing each Rpl over expressing strain as indicated on the x axis. Relative growth is shown for each 3AT concentration as indicated by the key at the bottom of the graph. A growth rate of 1 corresponds to full growth as seen for WT with fully functioning Gcn2.

As can be seen above in Figure 3.6 there was considerable difference in the relative growth rates across all Rpl overexpressing strains, suggesting that Rpl overexpressing strains differ in their degree of $3AT^S$. Three degrees of sensitivity were assigned to those Rpl overexpressing strains with a relative growth of at least 95% of that of the WT strain. These degrees were classed as either strong, moderate or weak. High $3AT^S$ was assigned to those overexpressing strains where the growth was 70% or less than that of the WT strain (with fully functional Gcn2) on at least one of the four concentrations of 3AT (those strain below the dashed red line in Figure 3.6). Strong $3AT^S$ was found for Rpl30, Rpl40A and Rpl43A. Moderate $3AT^S$ was assigned to those overexpressing strains where the growth was between 70% and 80% less than that of the WT strain on at least one of the four concentrations of 3AT (those strain found between the dashed red and orange lines in Figure 3.6). Moderate $3AT^S$ was found for Rpl20A, Rpl39 and Rpl18A. Weak $3AT^S$ was assigned to those overexpressing strains where the growth was between 85% and 95% less than that of the WT strain on at least one of the four concentrations of 3AT (those strain found between the dashed yellow and orange lines in Figure 3.6). Weak $3AT^S$ was found for Rpl5A, Rpl11A, Rpl23A, Rpl29A and Rpl37A. Those Rpl overexpressing strains with 95% or more relative growth than the WT were not considered $3AT^S$. The degree of sensitivity is summarised below in Table 3.2

Table 3.2 *Degrees of $3AT^S$ for the indicated Rpl overexpressing strains grown on plates containing 15mM 3AT to 90mM 3AT.*

Degree of 3AT sensitivity		
weak	moderate	strong
Rpl5	Rpl20A	Rpl30
Rpl15A	Rpl39A	RPl40A
Rpl11A	Rpl18A	Rpl43A
Rpl23A		
Rpl29A		
Rpl37A		

Interestingly from the data displayed in the graph of Figure 3.6 above, some Rpl over expressing yeast strains displayed a 3AT resistance phenotype $3AT^R$ at some or all 3AT concentrations. This is where these Rpl over expressing strain appear to grow better on 3AT as compared to the WT strain on the starvation media. $3AT^R$ Rpl overexpressing (those displaying increased growth above

110% compared to WT) strains identified from this quantitative analysis include Rpl4B, and Rpl41A ($3AT^R$ strains are those with growth scores above the dashed green line in Figure 3.6). Possible reasons for the identified Rpls displaying $3AT^R$ when overexpressed will be explored in the discussion section.

3.5 Reassessing $3AT^S$ with higher concentrations of 3AT

Following the results obtained from the semi-quantitative growth assay using the four 3AT concentrations ranging from 15-90 mM, it became apparent that the most observable $3AT^s$ phenotypes were observed at the higher concentrations. Therefore, to this end the experiment was repeated with all strains using additional higher 3AT concentration plates. This second screen also allowed the limits of reducibility of the screening assay to be assessed. The plates with concentrations of 120 mM and 150 mM 3AT were used to further evaluate the sensitivities seen with the lower concentrations in the first set of growth assay using 15 mM to 90 mM 3AT. The aim was that strains that only showed a weak $3AT^s$ phenotype may display more convincingly a $3AT^s$ phenotype at higher 3AT concentrations. Growth assays were carried out for all Rpl overexpressing strains on the plates containing 3AT concentrations of 15 mM to 150 mM and are displayed in Figures 5.11 to 5.13 in the appendix. Similarly, as for the first set of growth assay using 3AT concentrations of 15 mM to 90mM, this second set of growth assays at higher 3AT concentrations was quantified as above. In this assay growth scores were counted in factors of 10 (10%-100%) to give a more accurate assessment of growth, as growth on the higher concentration 3AT plates was harder to assess when assigning values in 25% increments. Growth scores calculated are displayed in Table 5.3 in the appendix. The growth scores were then converted into the adjusted scores as it was done for the growth assay conducted at 15 mM to 90 mM. Adjusted growth scores are displayed in Table 5.4 in the appendix. Resulting adjusted growth scores are displayed below in Figure 3.7

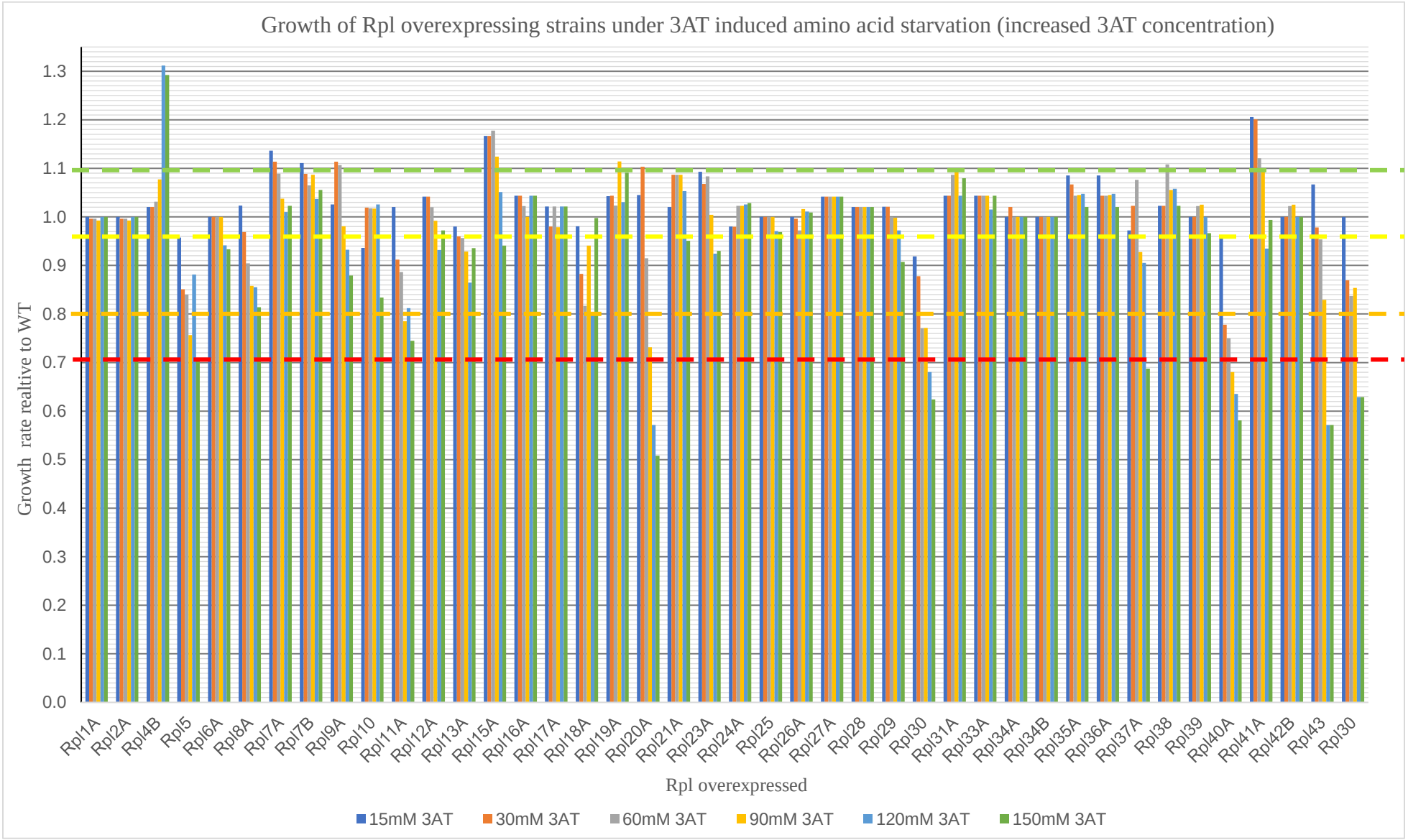

Figure 3.7 *Quantitative assessment of growth of Rpl overexpressing yeast strains growing on starvation media (higher concentration).*

The bar graph shows the relative growth of yeast overexpressing each Rpl over expressing strain as indicated on the x axis. Relative growth is shown for each 3AT concentration as indicated by the key at the bottom of the graph. A growth rate of 1 corresponds to full growth as seen for WT with fully functioning Gcn2.

Degrees of 3AT^S for each Rpl overexpressing strain were assigned similarly as for the growth assay above in section 3.4, with the exception that the degree of sensitivity was assigned only when the reduced growth was seen on at least two concentrations of 3AT. This was due to some stains displaying sensitivity at low concentrations and not at the higher concentrations and were considered outliers.

Strong sensitivity was assigned to those overexpressing strains where the growth was 70% or less than that of the WT strain on at least two of the six concentrations of 3AT (those strains found below the dashed red line in Figure 3.7). Strong 3AT^S was found for Rpl20A, Rpl330, Rpl40A and Rpl43A. Moderate 3AT^S was assigned to those overexpressing strains where the growth was between 70% and 80% less than that of the WT strain on at least two of the six concentrations of 3AT (those strain found between the dashed red and orange lines in Figure 3.7). Moderate 3AT^S was found for Rpl5, Rpl8A, Rpl11A and Rpl18B. Weak 3AT^S was assigned to those overexpressing strains where the growth was between 85% and 95% less than that of the WT strain on at least two of the six concentrations of 3AT (those strain found between the dashed orange and yellow lines in Figure 3.6).. Weak 3AT^S was found for Rpl6A, Rpl10A, Rpl13A, Rpl23A and Rpl37A. Those Rpl overexpressing strains with 95% or more relative growth than the WT were not considered 3AT^S. The degree of sensitivity is summarised below in Table 3.3

Table 3.3 *Degrees of 3AT^S for the indicated Rpl overexpressing strains grown on plates containing 15 mM 3AT to 150 mM 3AT.*

Degree of 3AT sensitivity		
weak	moderate	strong
Rpl6A	Rpl5	Rpl20A
Rpl10A	Rpl8A	Rpl30
Rpl13A	Rpl11A	RPl40A
Rpl23A	Rpl18A	Rpl43A
Rpl37A		

Comparing the two growth assays from sections 3.3 to 3.5 it was found Rpl overexpressing strains identified from both sets of growth assays with strong $3AT^S$ included Rpl30, 40A and 43A. Strains overexpressing Rpls giving at least moderate 3AT sensitivity was found for Rpl18A and Rpl20A on both assays. And those with weak sensitivity included Rpl5, Rpl11A, Rpl23A, and Rpl37A were found on both assays. Considering both sets of growth assays agree with each other in these results, it gives strength to the reproducibility of results from the semi-quantitative growth assay conducted.

Rpl6A (weak $3AT^S$), Rpl10 (weak $3AT^S$), Rpl13A (moderate $3AT^S$) and Rpl 8A (moderate $3AT^S$) were only identified on the second assay using higher concentrations. Identification of these different Rpls causing $3AT^S$ when overexpressed, would indicate that using higher concentrations of 3AT can indeed identify more $3AT^S$ over expressing strains not found at the lower 3AT concentrations. Rpl 15A (weak $3AT^S$), Rpl 29 (weak $3AT^S$) and Rpl39 (moderate $3AT^S$) however, were only identified on the first assay using lower concentrations. A possible reason for the differences could be variations in the strength of 3AT contained in the plates. 3AT can degrade with exposure to light, which may have been the case for some plates which did not display a $3AT^S$ phenotype (National Center for Biotechnology Information, 2019).

The Rpls identified from both sets of assays which gave $3AT^S$ when overexpressed are displayed below in Table 3.4. For simplicity, where two different degrees of $3AT^S$ are found for one Rpl overexpressing strain across the two sets of growth assays, the highest degree of $3AT^S$ found has been assigned.

Table 3.4 *Summary of degrees of sensitivity for indicated Rpl overexpressing strains for growth assays in chapter 3.3 to 3.5*

Degree of 3AT sensitivity		
weak	moderate	strong
Rpl6A	Rpl5	Rpl20A
Rpl10A	Rpl8A	Rpl30
Rpl15A	Rpl11A	RPl40A
Rpl13A	Rpl18B	Rpl43A
Rpl23A	Rpl39A	
Rpl29A		
Rpl37A		

Interestingly, several more Rpl overexpressing strains displayed a $3AT^R$ phenotype in this second set of growth assay assessing higher concentrations of 3AT. $3AT^R$ was assigned similarly as for the first growth assay set with the exception $3AT^R$ was only assigned to Rpl overexpressing strains displaying 110% or more growth on at least two of the six 3AT concentrations of the WT strain. Strains displaying $3AT^R$ here were Rpl4 Rpl7, Rpl9, Rpl15 and Rpl41. In agreement with the first growth assay set, Rpl4 and Rpl41 were identified. Although the degree of $3AT^R$ was significantly higher here, with growth increasing roughly 20% and 30% that of the WT for strains overexpressing Rpl4 and Rpl41 respectively. Again, reasons for Rpl overexpressing strains displaying $3AT^R$ will be discussed in the discussion section.

Interestingly, Rpl15, which was identified as weakly $3AT^S$ in the first growth assay set was not identified to have any $3AT^S$ in the second growth assay set. This contradiction in results may indicate the limitation of distinguishing between lower degrees of $3AT^S$ when quantifying growth differences by eye.

3.6 Attempting to assess levels of Gcn2 activation in 3AT^{s} strains

In order to determine whether a 3AT^{S} elicited by the overexpression of a Rpls, Rpl5, Rpl11, Rpl15, Rpl23, Rpl, Rpl37, Rpl30, Rpl40a, Rpl43a Rpl18a, 20a, 39a and 41a, are truly due to an impairment of Gcn2 activity, the degree of Gcn2 activation needs to be determined. A direct measure for the level of Gcn2 activation is the amount of eIF2α phosphorylated (eIF2-P) in a cell, as eIF2α is the substrate for Gcn2. Therefore, reduced eIF2-P level suggests that a 3AT^{S} phenotype is truly due to reduced Gcn2 activation. The method of scoring eIF2-P levels has been used in a recent study by Lee et al. (2015) as an effective means to determine differences in eIF2-P levels between yeast strains with reduced or overexpressed levels of small ribosomal proteins. For this, yeast strains are grown on nutrient rich Synthetic Complete (SC) medium containing all amino acids and grown at 26^{o} C to an OD of 0.8 at 160 rpm. Then 3AT was added, and the strains harvested after 2 minutes, which was identified as the optimal time to observe the level of eIF2-P immediately following the beginning of amino acid starvation. The reduced temperature of 26^{o} C from 30^{o} C was used also to slow down the reaction kinetics to enable the detection in the delay of eIF2 phosphorylation due to the impaired ability to detect the starvation signal.

To test whether overexpression of a Rpls impaired Gcn2 activity, the above-mentioned protocol was conducted on the yeast strains overexpressing and Rpl the elected a 3AT^{S} phenotype. Samples were collected under nutrient replete conditions and compared to those under starvation conditions for all strains displaying 3AT^{S} phenotype. Overnight cultures of each strain were grown to saturation on SC medium containing glucose. For each culture two flasks containing SGal medium were inoculated, one flask for replete conditions and one for starvation conditions and grown at 26^{o}C and 160 rpm. Once the culture reached an OD of around 0.8, 3AT was added at a final concentration of 30 mM/ml to one flask. After exactly 2 minutes the culture was subjected to formaldehyde cross-linking before being harvested. The non-starved culture was harvested shortly thereafter. Whole cell extracts were generated and then subject to SDS-PAGE and western blotting. Membranes were probed with anti eIF2α-P antibody as outlined in materials and methods. The membrane was also probed for the protein Pgk1 as a loading control. Pgk1 is a house keeping gene, where levels have been shown previously to be independent of amino acid starvation and do not change due to the starvation. Pgk1 level also correlated with amount of cell

extract loaded, so can be used to adjust amount of protein loaded and to take into account when quantifying relative eIF2α-P levels.

Surprisingly, the eIF2-P antibody did not detect a signal at the molecular weight of eIF2, but instead detected proteins that differed in size depending on the Rpls being expressed with the addition of the 19 kDa affinity tag these proteins are expressed with (Figure 3.8 below). Given that no band was detected when the Rpls were not present (for the control strains) it would appear the antibody was binding to the affinity tag of the overexpressed Rpls. The overexpressed Rpls were tagged with an approximate 19 kDa 6xHis, HA epitope, and a Protein A (ZZ domain) affinity tag. As the fragmented crystal (FC) region of protein A is known to bind to many immunoglobulins, it is likely that this is un-specifically detected by the eIF2α-P antibody. This makes it difficult to detect eIF2-P levels, considering that some tagged Rpl30 and Rpl43 proteins have the same molecular weight as eIF2α-P. However, one advantage of the eIF2α-P antibody un-specifically binding to the tagged Rpls is that it can be now used for determining the expression levels of the overexpressed Rpls, as well as verifying whether their molecular weight is as expected.

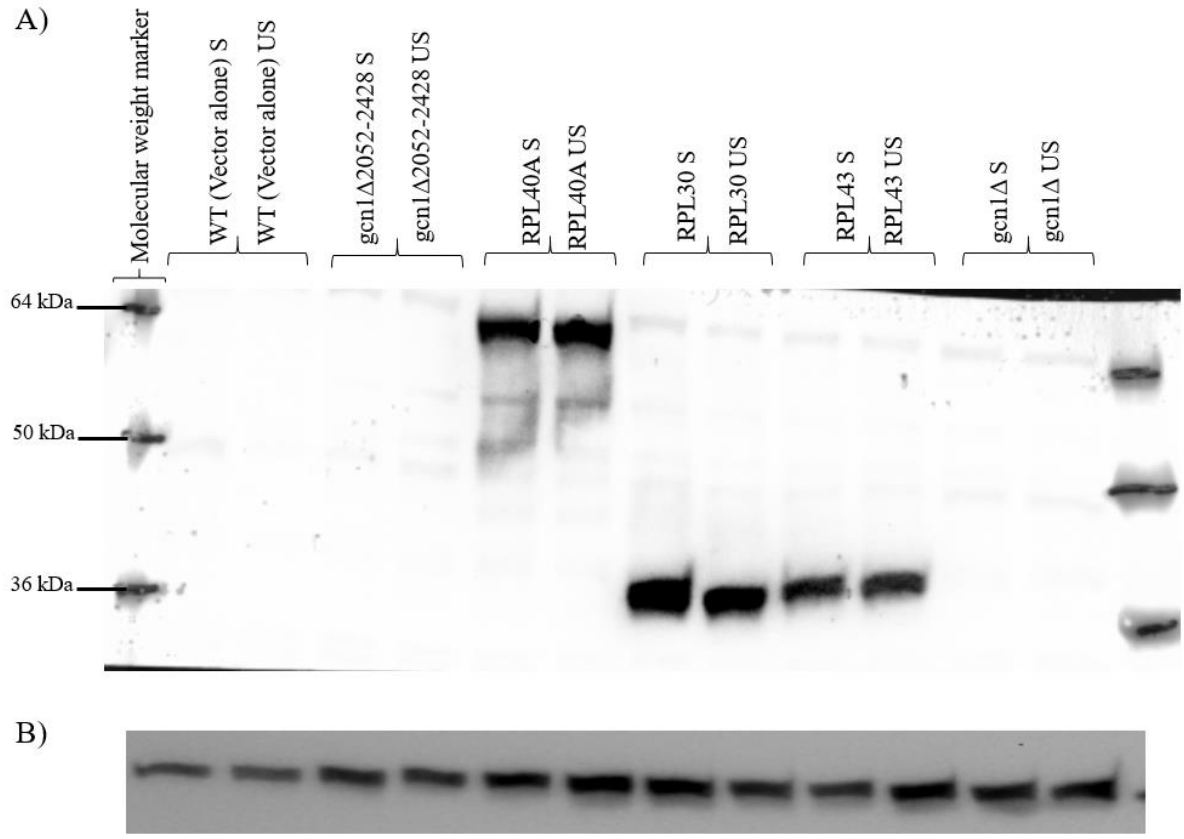

Figure 3.8 *The attempt to detect eIF2α-P levels*

A) Samples as indicated were loaded on the gel. Starved (S) and un-starved (US) samples for each strain were loaded next to each other. Samples were starved for 2 minutes with 30 mM 3AT. Molecular weight marker was loaded in the first and last lanes as indicated. B) Pgk1 levels

3.7 Determining the expression level and size of each large ribosomal protein

As was found in the previous chapter it is very likely that the FC portion of the eIF2A-P antibody binds to the Protein A tag of the Rpls. The eIF2α-P antibody therefore can be used for the direct detection of protein A, without the use of a primary antibody specific to protein A.

To confirm the large ribosomal proteins are all expressed and at the expected size, colonies a and b of each Rpl overexpressing strain were grown as above for detection of eIF2α-P, with the exception samples were not exposed to amino acid starvation. Loaded samples were subject to the same western blot analysis above. Detected bands of all Rpls are displayed in the appendix in Figures 5.14 to 5.17. The molecular weights of the detected signals detected with the western blotting of each strain overexpressing a large ribosomal protein can be determined with the help of molecular weight marker loaded with the samples on the SDS gel to confirm the proteins are being expressed and are at the height expected. As the Rpls are tagged with a fusion tag of approximately 19 kDa in size (Figure 3.1), then it would be expected the protein size of each protein is 19 kDa larger. Membranes were detected for chemiluminescence as outlined in materials and methods. Resulting images were analysed for molecular weights by comparing the heights to those of the molecular weight marker using image lab software as outlined in materials and methods. Table 3.5 below shows the size of each Rpl, the expected size with the addition of the 19 kDa fusion tag and the found sizes from colonies a and b of each Rpl overexpressing strains. Where a sample was loaded on more than one gel (Rpl5, Rpl37A and Rpl30) the determined molecular weights were averaged across all gels.

Table 3.5 *Found size in kDa of each large ribosomal protein*

The molecular weight was determined using image lab software and comparing to molecular weight marker. Found sizes are shown for representative colonies a and b. When no protein was detected this is indicated with ND "Not Detected".

Protein overexpressed	Protein size (kDa)	Expected protein size (protein size + 19 kDa tandem fusion tag) (kDa)	Found size (a)	Found size (b)
Rpl1A	24.5021	43.5021	47.34	46.68
Rpl2A	27.4371	46.4371	49.03	48.35
Rpl4B	39.0968	58.0968	56.52	56.78
Rpl5	33.7131	52.7131	59.35	58.79
Rpl6A	19.9808	38.9808	ND	ND
Rpl7A	27.6627	46.6627	45.21	45.52
Rpl7B	27.7208	46.7208	46.17	46.17
Rpl8A	28.1502	47.1502	51.89	51.63
Rpl9A	21.5803	40.5803	44.27	44.58
Rpl10	25.3829	44.3829	45.52	45.66
Rpl11A	19.732	38.732	39.42	39.98
Rpl12A	17.8289	36.8289	38.34	38.88
Rpl13A	22.5806	41.5806	46.95	47.95
Rpl15A	24.4639	43.4639	ND	ND
Rpl16A	22.2286	41.2286	44.47	44.75
Rpl17A	20.5729	39.5729	36.15	36.02
Rpl18B	20.5937	39.5937	42.96	43.23
Rpl19A	21.7368	40.7368	44.35	44.64
Rpl20A	20.4571	39.4571	44.05	44.20
Rpl21A	18.2626	37.2626	40.30	40.42
Rpl23A	14.4853	33.4853	35.12	35.47
Rpl24A	17.6471	36.6471	41.48	41.37
Rpl25	15.7759	34.7759	30.30	30.06
Rpl26A	14.252	33.252	30.16	29.73
Rpl27A	15.5516	34.5516	37.18	36.96
Rpl28	16.7419	35.7419	37.34	37.83
Rpl29	6.685	25.685	25.63	25.72
Rpl30	11.4235	30.4235	31.72	31.02
Rpl31A	12.9623	31.9623	34.30	35.00
Rpl33A	12.1707	31.1707	34.01	ND
Rpl34A	13.6645	32.6645	36.63	36.39
Rpl34B	13.6665	32.6665	36.15	36.02
Rpl35A	13.9329	32.9329	35.12	35.47
Rpl36A	11.1445	30.1445	30.30	30.06
Rpl37A	9.8727	28.8727	32.02	31.67
Rpl38	8.8407	27.8407	ND	ND
Rpl39	6.3589	25.3589	22.34	22.83
Rpl40A	14.5683	33.5683	54.17	54.22
Rpl41A	3.3544	22.3544	19.64	19.81
Rpl42B	12.239	31.239	ND	ND
Rpl43A	10.1082	29.1082	32.14	34.73

As can be seen, molecular weights closely fit the expected size, where generally the sizes are only a few kDa larger, this may be due to running conditions of gels and limitations of the accuracies of the molecular weight marker. However, Rpl40A significantly differed from the expected size. Rpl 40A has an expected size of around 33.57 kDa, but detected signals gave signals around 54 kDa. Rpl6Aa, Rpl6Ab, Rpl15Aa, Rpl15Ab, Rpl33Ab, Rpl38a, RPl38b, Rpl42Ba, RPl42Bb were not detected as indicated in the Table above. It is possible the expression levels of these proteins are too low to be detected with the amount of cell extract used.

The degree in $3AT^{s}$ caused by a Rpls may indicate which large ribosomal protein binds to Gcn1 or Gcn2 in the strongest way, and thus is most important for Gcn2 activation. However, the degree of $3AT^{S}$ also depends on the levels to which each large ribosomal protein is overexpressed. The more overexpressed the more potential in preventing Gcn1 and Gcn2 ribosome binding

To determine the relationship between the overexpression levels of the tagged Rpl and the degree to which it affects the amino acid starvation response, the expression levels of each large ribosomal protein was determined. For this, the signals from the above membranes were quantified using image lab analysis software as described in materials and methods. For each sample, the intensity of signals for tagged Rpls were normalised to the signal obtained from the house keeping gene of Pgk1. These levels were normalised by that of one Rpl that was loaded on every gel as reference. Expression levels relative to Rpl5a (Table 5.9 in appendix) were plotted on the bar graph below in Figure 3.9. As Rpl6Aa, Rpl6Ab, Rpl15Aa, Rpl15Ab, Rpl33Ab, Rpl38a, Rpl38b, Rpl42Ba, Rpl42Bb did not give a detectable signal, it is possible that these were not overexpressed, or their expression was too low to be detected. As can be seen in the graph below a vast array of different expression levels are seen for each Rpl overexpressing strain. As seen in Table 5.9 in the appendix, the expression levels ranged from as little as 0.33% (Rpl23Aa) to 176% (Rpl5a) as compared to Rpl5.

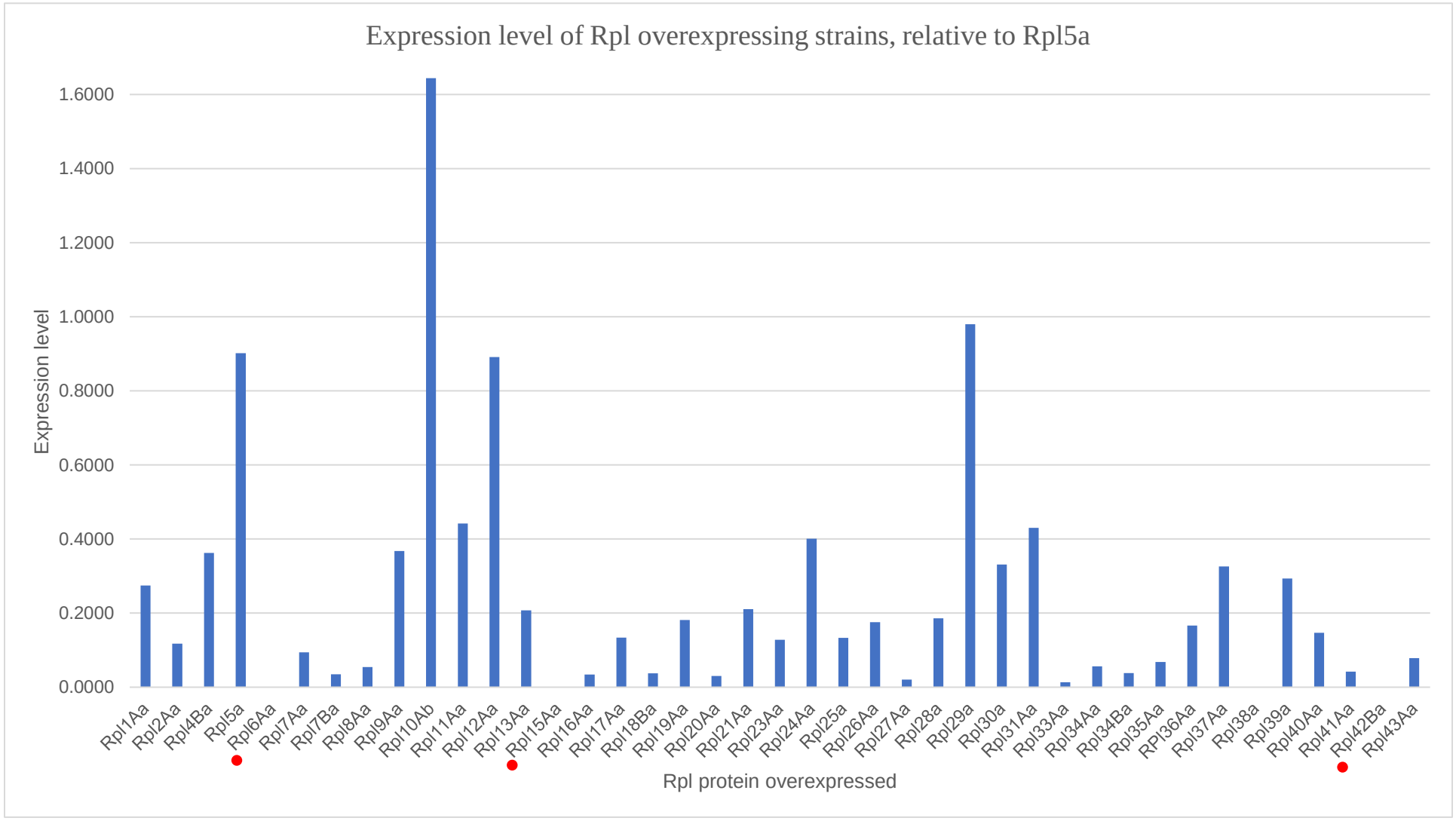

Figure 3.9 *Graph displaying expression level of Rpl overexpressing strains.*

Expression level of each Rpl overexpressing strain. Expression levels were determined by normalising western signals for each strain to pgk1 levels. Expression levels are all relative to Rpl5a. Strains marked with a red dot failed to give any signal to determine expression level.

3.8 Correlation between $3AT^S$ and level of Rpl overexpression

To determine the relationship between the cellular amount of exogenous large ribosomal proteins and the degree to which it affects the amino acid starvation response, the expression levels determined in chapter 3.7 above were compared to the growth scores obtained in the two sets of semi-quantitative growth assays from sections 3.4 and 3.5.

First the expression levels relative to Rpl5 were ranked from smallest to highest to give an indication of the trend seen for increasing expression levels (displayed in the graph below in Figure 3.10). The same ordering of Rpl overexpressing strains was applied to the relative growth scores obtained from the growth assays from section 3.4 (3AT concentrations of 15 mM to 90 mM) and the second growth assay from section 3.5 (3AT concentrations of 15 mM to 150 mM). This allowed for the reordering of strains relative from graphs displayed in Figures 3.6 and 3.5. This results in all growth scores ordered with respect to their increasing expression levels. The graph from Figure 3.10, displaying ordered expression levels, was then overlaid on the reordered growth score graphs, this allows for the observation of any correlation between growth scores and increasing expression levels. The resulting graphs are displayed below in Figures 3.11 and 3.12. Trendlines were added to both data sets in each graph to give an indication of the trend displayed by the ordering of the Rpl overexpressing strains.

If the expression levels of Rpls (concentration of the exogenous Rpls in the cell) is the sole reason for the varying degrees of $3AT^S$, then an inverse correlation would be expected. That is, as expression levels increase, growth scores would decrease. If this was the case, then growth scores would follow the same increasing trend that the ordered expression levels display. As can be clearly seen from the two graphs displayed in Figures 3.11 to 3.12 there appears to be no similar trend, which is the 3AT sensitivity does not appear to increase with increasing expression levels. Also seen in the graphs, the R^2 values for the growth scores ordered according to the increasing expression level values is very low for all graphs. It can be concluded that there is no significant statistical correlation between the found growth scores for the growth of Rpl overexpressing strains on 3AT and their respective expression levels. This supports idea that degrees of overexpression are not the sole reason for the differing $3AT^S$.

This could indicate that strains inducing stronger $3AT^S$ phenotypes (lower growth scores) with lower expression levels, may indicate a more functionally important Rpl with respect to its importance in the response to amino acid starvation (observing strains further to the left in Figures 3.11 and 3.12).

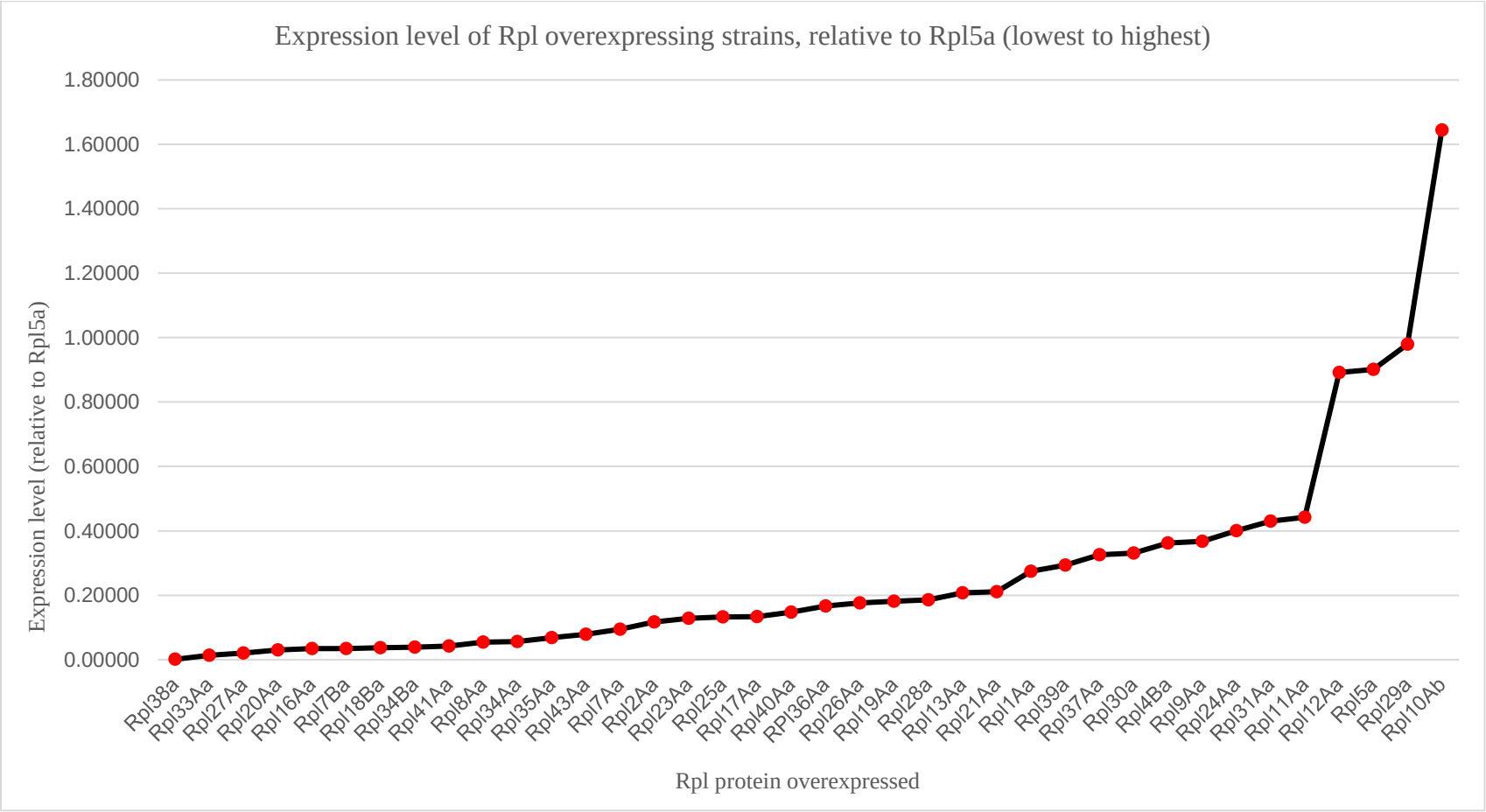

Figure 3.10 *Graph displaying expression level of Rpl overexpressing strains.*

Expression level of each Rpl overexpressing strain. Expression levels were determined by normalising western signals for each strain to pgk1 levels. Expression levels are all relative to Rpl5a. Strains marked with a red dot failed to give any signal to determine expression level.

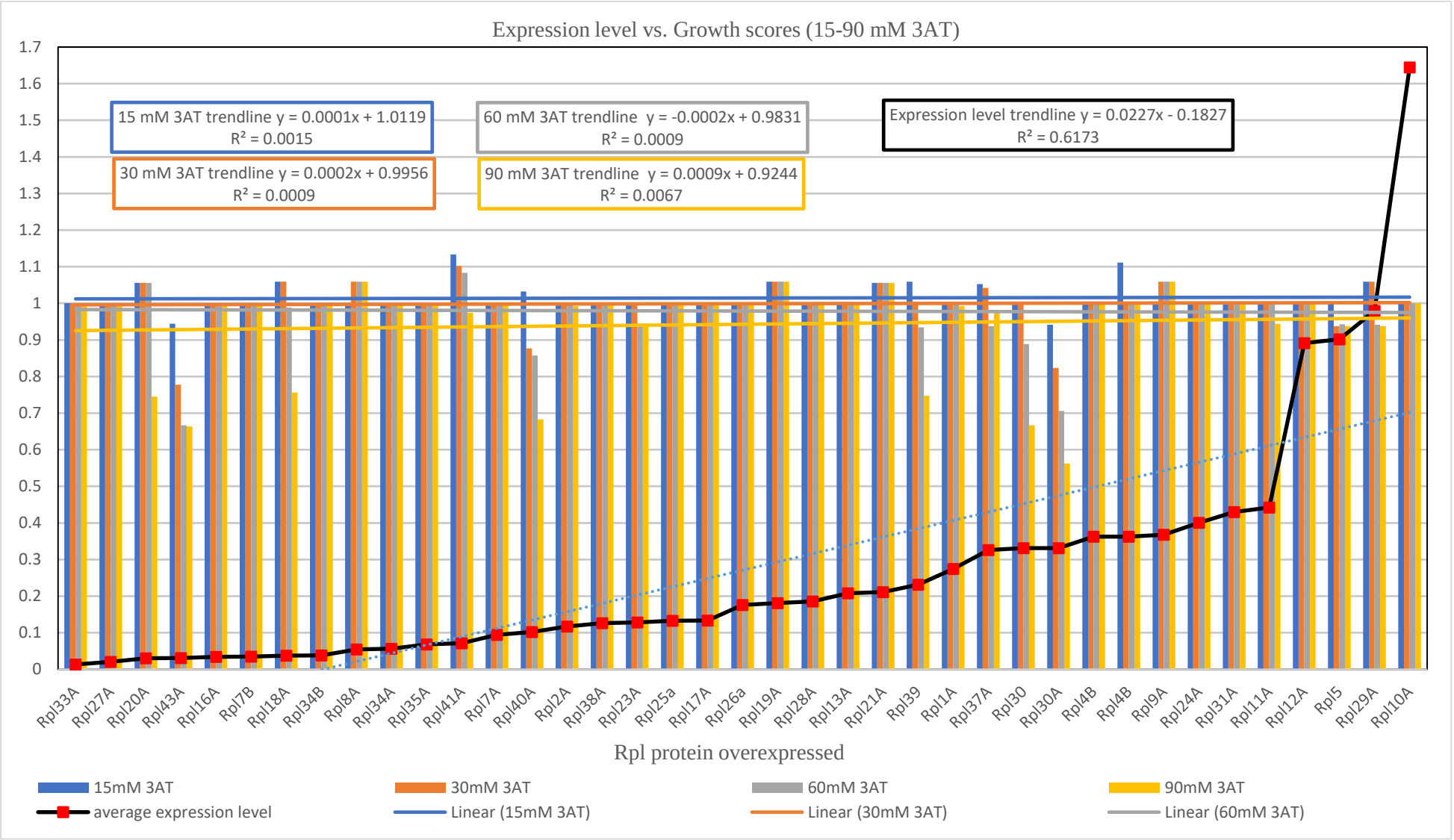

Figure 3.11 *Graph displaying ranked expression levels of Rpl overexpressing strains and their corresponding growth scores (from growth assay set one).*

Red squares displayed indicate expression levels, relative to Rpl 5a, for each Rpl overexpressing strain. Corresponding growth scores found for Rpl overexpressing strains on each 3AT concentration is displayed in the blue, orange, grey and yellow bars (see Figure key below graph). Trendlines for expression levels and for growth scores for each 3AT concentration are also displayed as indicated by the Figure key below the graph (correlating trendline equations displayed in the top left of the graph).

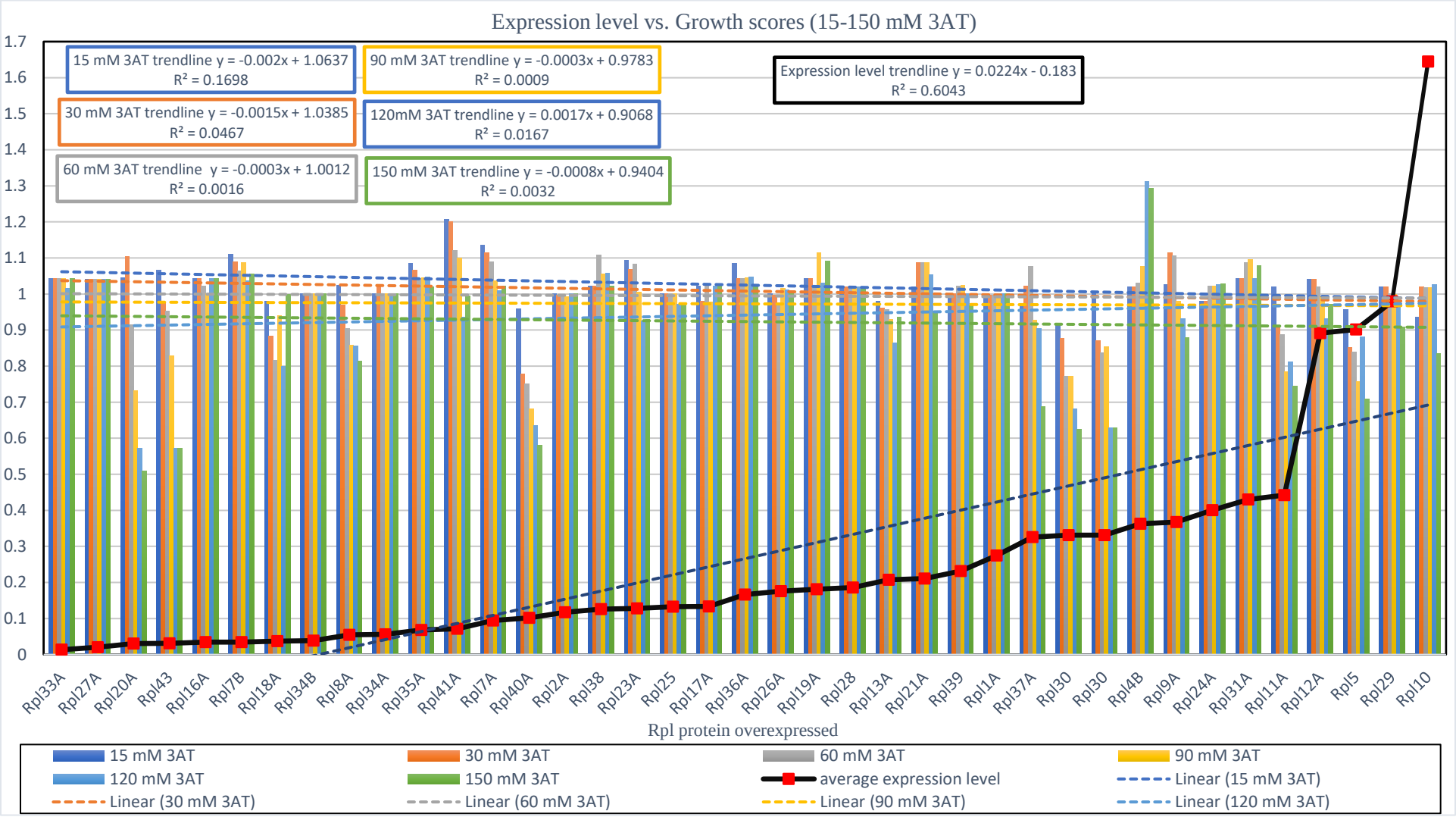

Figure 3.12 *Graph displaying ranked expression levels of Rpl overexpressing strains and their corresponding growth scores (from growth assay set two).*

Red squares indicate expression levels, relative to Rpl 5a, for each Rpl overexpressing strain. Corresponding growth scores found for Rpl overexpressing strains on each 3AT concentration is displayed in the dark blue, orange, grey, yellow, light blue and green bars (see Figure key below graph). Trendlines for expression levels and for growth scores for each 3AT concentration are also displayed as indicated by the Figure key below the graph (correlating trendline equations displayed in the top left of the graph).

3.9 Attempt to compensate for variation in expression levels

All Rpls inducing $3AT^S$ have varying levels of overexpression, meaning growth defects caused occurred with differing amounts of the exogenously expressed Rpls present in the cell. As mentioned above this does not dictate the level of $3AT^S$, however this still needs to be considered when assigning the functional significance of a potential Gcn1-Gcn2 ribosomal contact.

In an attempt compensate for the expression levels, and to possibly reveal any true functional significance of Rpls, degrees of $3AT^S$ were recalculated whereby expression levels were considered. As for degrees of $3AT^S$, the $3AT^S$ strains were assigned three degrees of expression level. Strains with expression levels below that of 10% compared Rpl5 were assigned as having low expression levels. Strains with expression levels between 10% and 30% of Rpl5 were assigned as having moderate degrees of expression. Strains with expression levels above 30% that of Rpl5 were assigned to having high expression levels. Degrees of expression for Rpl overexpressing strains are displayed below in Table 3.6 below. For recalculating $3AT^S$, numerical values were first assigned to degrees of $3AT^S$ and for degrees of expression levels. Values of 3, 2 and 1 were assigned to strong, moderate and weak degrees of $3AT^S$ respectively. Values of 1, 2 and 3 were assigned to high, medium and low degrees of expression. The numerical value of the degree of $3AT^S$ was then divided by the numerical value of the degree of expression level to give an adjusted 3AT values. All values are displayed in Table 3.6 below

These values were then used to reallocate degrees of $3AT^S$. A calculated value of 0.33 was deemed as weak $3AT^S$, 0.5 to 0.67 was deemed as moderate, 1 to 2 was deemed as strong and 2 to 3 was deemed as very strong $3AT^S$. These reallocated degrees of $3AT^S$ are summarised in Table 3.7 below.

Table 3.6 *Calculation of adjusted degrees of 3AT^S*

Strain	Degree 3AT^S	Expression level	Expression level degree	3AT^S numerical value	Expression level numerical value	Adjusted 3AT^S value	Adjusted degree of 3AT^S
Rpl20Aa	strong	3.0	high	3	1	3.00	Very strong
Rpl18Ba	moderate	3.7	high	2	1	2.00	Strong
Rpl8Aa	moderate	5.4	high	2	1	2.00	Strong
Rpl43Aa	strong	7.8	high	3	1	3.00	Very strong
Rpl23Aa	weak	12.8	moderate	1	2	0.50	Moderate
Rpl40Aa	strong	14.7	moderate	3	2	1.50	Strong
Rpl13Aa	weak	20.8	moderate	1	2	0.50	Moderate
Rpl39a	weak	29.4	moderate	1	2	0.50	Moderate
Rpl37Aa	weak	32.6	low	1	3	0.33	Weak
Rpl30a	strong	33.1	low	3	3	1.00	Strong
Rpl11Aa	moderate	44.2	low	2	3	0.67	Moderate
Rpl5a	moderate	90.2	low	2	3	0.67	Moderate
Rpl29a	weak	98.0	low	1	3	0.33	Weak
Rpl10Ab	weak	164.4	low	1	3	0.33	Weak

Table 3.7 *Comparison between degrees of 3AT^S compared to reallocated degrees of 3AT^S taking expression levels into account.*

Degree of 3AT^S			Reallocated degrees of 3AT^S taking expression levels into account		
Weak	Moderate	Strong	Weak (0.33)	Moderate (0.5-0.6)	Strong (1-2)
Rpl6A	Rpl5	Rpl20A	Rpl10	Rpl5	Rpl18
Rpl10A	Rpl8A	Rpl30	Rpl29	Rpl11	Rpl8
Rpl15A	Rpl11A	RPl40A	Rpl37	Rpl13	Rpl40
Rpl13A	Rpl18B	Rpl43A		Rpl23	Rpl30
Rpl23A	Rpl39A			Rpl39	
Rpl29A					
Rpl37A					

Chapter 4 Discussion

4.1 Identification of Rpls required for the full activation of the amino acid starvation response

It is known that both Gcn1 and Gcn2 contact ribosomes, and that this is important for Gcn2 (Inglis et al., 2019; Lee et al., 2015; Ramirez et al., 1991; Sattlegger & Hinnebusch, 2000; Visweswaraiah et al., 2012). Exactly where on the ribosome contacts are made however, is yet to be fully elucidated. Experimentally, very few specific ribosomal contact points with Gcn1 or Gcn2 have been reported and confirmed so far (Inglis et al., 2019; Lee et al., 2015). This research aimed to determine more comprehensively which individual large ribosomal proteins are contacted by Gcn1 and Gcn2. Furthering the knowledge of Gcn1 and Gcn2 ribosomal contacts is critical in fully understanding the mechanisms of the transfer of the starvation signal to Gcn2 during amino acid starvation.

For the investigation into Gcn1 and Gcn2 ribosomal contacts, a genetic approach was taken whereby a library of yeast strains were generated that contained plasmids overexpressing each large ribosomal protein from a galactose inducible promoter. All strains from this library were assessed for the effects of the overexpression of each large ribosomal protein on Gcn2 activation. If a Rpl binds to Gcn1 or Gcn2 then its overabundance caused by overexpression is expected to lead to its binding to Gcn1 or Gcn2 and thereby prevent their binding to ribosome bound endogenous Rpls. As a result, these Rpl overexpressing strains would have reduced ability to respond to amino acid starvation, by preventing the full function of Gcn2.

In sections 3.3 to 3.5 of this thesis, overexpressed Rpls were investigated for their effect on strain growth under amino acid starvation induced by 3AT. Reduced ability to respond to amino acid starvation was indicative of impaired contact of Gcn1 or Gcn2 to the ribosome.

Overexpressing a Rpl as a means to score for its involvement in Gcn2 activation has been shown previously as being a suitable approach (Lee et al., 2015). Rps10 overexpression in yeast results in their reduced ability to grow under amino acid starvation induced by 3AT (Lee et al., 2015). Rps10 was verified *in vitro* to be a true binding partner of Gcn1 and to be required for Gcn2 activation (Lee et al., 2015). This supports the suitability of the overexpression approach to identify possible ribosomal contacts.

From the semi-quantitative growth assays (refer to sections 3.3 to 3.5) several Rpls were identified, which when overexpressed led to the reduced ability of strains to grow on the starvation media. These strains were termed as sensitive to the amino acid starvation inducing drug of 3AT ($3AT^S$). Refer to Tables 3.2 to 3.4 in results section for identified Rpls.

A higher $3AT^S$, compared to a lower $3AT^S$, should indicate a more functionally significant contact between the Rpls and either Gcn1 or Gcn2 in terms of Gcn2 activation. Differences in importance of Rpls could be explained by the fact Gcn1 has several ribosomal contacts, where some may be more functionally significant than others. The M7 and M1 mutations in Gcn1, located in physically distinct regions, differentially affect the amount of polysome binding affinity between Gcn1 and polysomes and also differ in the effects they have on the amino acid starvation response (Sattlegger & Hinnebusch, 2005). As the M7 and M1 mutations are in physically distinct regions within Gcn1, it would be expected they contact also physically distinct regions on the ribosome (Sattlegger & Hinnebusch, 2000; Zhu & Wek, 1998). Therefore, interference of physically distinct regions of the ribosome where Gcn1 contacts, could also differentially affect the function of Gcn1 and the activation of Gcn2. In a similar manner, interference of potentially different Gcn2 ribosome contacts will also vary in the degree of the effects on Gcn2 activation and the amino acid starvation response, but to a lesser degree considering a much smaller region of Gcn2 contacts the ribosome compared to Gcn1 (compare Figures 1.5 to 1.6).

Before relating degrees of $3AT^S$ to the possible significance of a potential ribosomal contact to Gcn1 or Gcn2, overexpression levels needed to be taken into account, as each Rpl was overexpressed with vastly varying degrees. As was explored in section 3.8 of the results, it was concluded that the variations in growth scores and resulting assigned $3AT^S$ for each Rpl overexpressing strain was not solely due to expression levels. This would mean the variation in $3AT^S$ may have arisen due to the functional significance of a Rpl with respect to its importance in Gcn1 or Gcn2 ribosomal binding, and not solely due to its cellular concentration. For example, the overexpression of Rpl20A had expression levels of approximately 2% that of Rpl5, but overexpression of Rpl20A was able to infer a stronger degree of $3AT^S$ than Rpl5 (refer to section 3.8 and Table 3.5). Also, Rpl43 had approximately tenfold higher expression level (expression level 3% that of Rpl5a) than Rpl30 (expression level 33% that of Rpl5a) while both infer strong $3AT^S$ when overexpressed.

All Rpls inducing $3AT^S$ have vastly varying levels of overexpression (see Table 3.6), meaning growth defects caused occurred with differing amounts of the exogenously expressed Rpls present in the cell. As mentioned above this does not dictate the level of $3AT^S$, however this still needs to be considered when assigning the functional significance of a potential Gcn1-Gcn2 ribosomal contact. An attempt to compensating for the variation in expression levels of Rpls causing $3AT^S$, was conducted in section 3.9 of the results section. Recalculated $3AT^S$ (Table 3.7) should be considered when analysing any functional significance of a Rpl with respect to its effect on Gcn1/Gcn2 function or binding to the ribosome. This will be needed to be taken into account for any possible effect expression levels may have had on influencing degrees of $3AT^S$. However, it is possible that the lowest levels of expression of Rpls was already high enough to saturate any possible contacts to Gcn1 or Gcn2, meaning expression levels above that may have had little to no effect on degrees of $3AT^S$. Therefore, careful consideration must be taken when considering if these adjusted degrees of $3AT^S$ accurately represent the functional significance of Rpls with respect to their effects on Gcn2 activation.

4.2 Overexpressed Rpls affecting growth on starvation medium

Besides causing $3AT^S$, some Rpl overexpressing strains displayed a phenotype of resistance to 3AT ($3AT^R$) and the seemingly increased ability to more strongly respond to amino acids starvation compared to the WT strain. Rpls identified as causing $3AT^R$ when overexpressed include Rpl4 Rpl7, Rpl9, Rpl15 and Rpl41. This could be due to the overexpressed Rpls influencing Gcn4 translation down stream of Gcn2. As is seen in research by Martín-Marcos, Hinnebusch, and Tamame (2007), a mutation to Rpl33 leads to a resistance to 3AT which is concluded to involve a reduced ability of 60S ribosomes to join the 43S preinitiation complex, which is required for initiation of translation (see Figure 1.3 to 1.4 in the introduction) (Martín-Marcos et al., 2007). This allows a bypassing of uORF4 and then the subsequent increased translation of Gcn4 (comparing steps 3 and 4 between Figures 1.3 and 1.4 in the introduction). It is possible the overexpression of Rpls which gave a $3AT^R$ phenotype may have similarly caused a level of Gcn4 translation. This would lead to increased growth on starvation media compared to

the WT strain and would explain an increased ability to grow when amino acid starvation is induced.

Along with Rpl33, some Rpls which include Rpl5, Rpl11, Rpl25, Rpl28, and Rpl30 also have been shown to have effects on the production of mature ribosomes and processing of pre-rRNA (Deshmukh, Tsay, Paulovich, & Woolford, 1993; Moritz, Pulaski, & Woolford, 1991; Underwood & Fried, 1990; van Beekvelt et al., 2001; Vilardell & Warner, 1997). This can occur with the interaction of the above mentioned Rpls with trans-acting factors or directly with translation machinery. An overexpression of these proteins therefore could stimulate an increase in mature ribosome production and pre-mRNA processing, leading to an increased ability to grow compared to WT, at least under replete conditions. None of the $3AT^R$ Rpl overexpressing strains identified in this current research however are included in the above-mentioned list of Rpls involved in ribosome production and pre-rRNA processing. Interestingly however Rpl5, Rpl11 and Rpl30, identified as possible stimulators of ribosome production were identified as $3AT^S$, but not $3AT^R$ when overexpressed in yeast in this current study. The overexpression of these Rpls could interfere in some way with the endogenous Rpls preventing their regulatory role in ribosome production. This could explain why Rpl5, Rpl11 and Rpl30 displayed $3AT^S$ phenotypes. However as this would also lead to reduced growth on non-starvation media, and this was compensated for when calculating relative growth scores, this is an unlikely explanation for these $3AT^S$ phenotypes.

The elongation factor eEF1A is known to bind to ribosomes. eEF1A is known to interact with P-stalk proteins and with the A-site of the ribosome during the delivery of charged tRNAs to the A-site (Mateyak & Kinzy, 2010; Visweswaraiah et al., 2011) From proteome complex and co-immunoprecipitation studies, possible interactions between eEF1A and many Rpls have been shown (Gavin et al., 2006). eEF1A is known to bind to and interfere with the function of Gcn2, with binding of eEF1A to the C terminus of Gcn2. (Gavin et al., 2006; Visweswaraiah et al., 2011). Overexpression of ribosomal proteins may interact with eEF1A and prevent eEF1A binding Gcn2, increasing the function of Gcn2 and leading to an increased ability to grow on starvation media. Rpl7A, Rpl13A, Rpl17A, Rpl24, Rpl25A, Rpl30 and Rpl35A were found in complexes associated with eEF1A in the proteome complex study by Gavin et al. (2006) and eEF1A co-precipitates with Rpl39 (association of Rpls with eEF1A is indicate in Table 4.2) (Gavin et al., 2006; Visweswaraiah

et al., 2011). Indeed, Rpl7A was identified in this current research as causing $3AT^R$ when overexpressed and its association with eEF1A possibly explains this phenomenon.

It needs to be considered that the overexpression of Rpls which lead to a $3AT^S$ phenotype could have negatively affected the amino acid starvation response downstream of Gcn2. This could possibly have been due to decreased translation of Gcn4 which may occur by way of affecting the way ribosomes interact with the uORFs of Gcn4. This means the $3AT^S$ phenotypes may not have been due to impairment of Gcn2 function but instead affects downstream of Gcn2. This will need to be addressed in the future to verify if $3AT^S$ phenotypes revealed in this research are due to impairment of Gcn2. Suggestions on how this can be done will be discussed further in section 4.8.

4.3 Mapping Gcn1 and Gcn2 possible contacts on the ribosome

Gcn1 and Gcn2 must directly contact each other for the activation of Gcn2 under amino acid starvation conditions (Sattlegger & Hinnebusch, 2000). Also, Gcn1 and Gcn2 both require association to the ribosome for the full function of the amino acid starvation response (Sattlegger & Hinnebusch, 2000). As the domains required for binding between Gcn1 and Gcn2 are physically separate from the ribosomal binding domains of Gcn1 and Gcn2, this would imply that Gcn1 and Gcn2 bind separately to the ribosome at distinctly different sites (Ramirez et al., 1991; Sattlegger & Hinnebusch, 2000; Zhu & Wek, 1998). In support of this Gcn1 and Gcn2 have been shown to contact physically distinct locations on the ribosome, where Gcn1 binds to the small ribosomal protein Rps10 and under certain conditions, Gcn2 binds to the P-Stalk proteins of the large ribosomal subunit (Inglis et al., 2019; Lee et al., 2015). Therefore, it would appear that separate groups of Rpls are involved in the binding of Gcn1 and Gcn2. Although it has not been confirmed that Gcn1 may also contact the stalk and Gcn2 may contact Rps10. Considering Rps10 and P-stalk proteins are the only determined contacts to the ribosome which have been confirmed and given the functional significance of Gcn1 and Gcn2 ribosomal binding, Gcn1 and Gcn2 need to be fully mapped on the ribosome. This mapping would help to add to the working model, and the understanding, of how Gcn2 is activated by uncharged tRNAs (see Figure 1.9). As the $3AT^S$ phenotypes caused by overexpression of Rpls are indicative of a possible impairment of Gcn1 or

Gcn2 ribosomal binding, the findings from this current research can be used to give some insight into the possible placement of both Gcn1 and Gcn2 on the ribosome.

To this end *in silico* analysis was performed on a model of the 80S ribosome of *S. cerevisiae* using data obtained from: "The structure of the eukaryotic ribosome at 3.0 Å resolution.", where the structures and location of all ribosomal proteins in the yeast 80S ribosome are available. The location of each large ribosomal protein, which when overexpressed caused $3AT^s$, was mapped by highlighting each protein as indicated in Figures 4.1 to 4.5 on a surface representation model of the 80S yeast ribosome. Given the fact that Rps10 and P-stalk proteins are confirmed contacts to Gcn1 and Gcn2 respectively, these proteins are also indicated. Considering that Rps10 and the P-stalk proteins are both located close to interface between the two ribosomal subunits it would stand to reason that both Gcn1 and Gcn2 could contact the large and the small ribosomal subunit.

4.4 Attempt to allocate Gcn1 and Gcn2 large ribosomal contacts

On observation of the location of Rpls causing $3AT^S$ it was found these proteins were located on vastly separate regions, spread out over the large ribosomal subunit, with the exception of a significantly large region on the large ribosomal subunit shown in Figure 4.1 As little to no identified Rpls are located in this region it could be concluded that possibly neither Gcn1 or Gcn2 bind to this position on the ribosome. It would appear that this region is a possible exclusion zone for Gcn1-Gcn2 ribosomal association. This possible exclusion zone is a considerable distance away from known binding partners of Gcn1 and Gcn2 (Rps10 and the P-stalk). This gives support to $3AT^S$ phenotypes caused by overexpression of Rpls are due to impairment of either Gcn1 or Gcn2 ribosomal contacts, as the majority of these Rpls are closer in vicinity to Rps10 and P-stalk proteins than the above-mentioned exclusion zone. Considering the location of these Rpls on the ribosome, their location with respect to the known binding partners of Gcn1 and Gcn2, and their interaction with other proteins, an attempt was made to assign these Rpls causing $3AT^S$ as binding partners of Gcn1 or Gcn2. This is discussed below in section 4.5 and 4.6

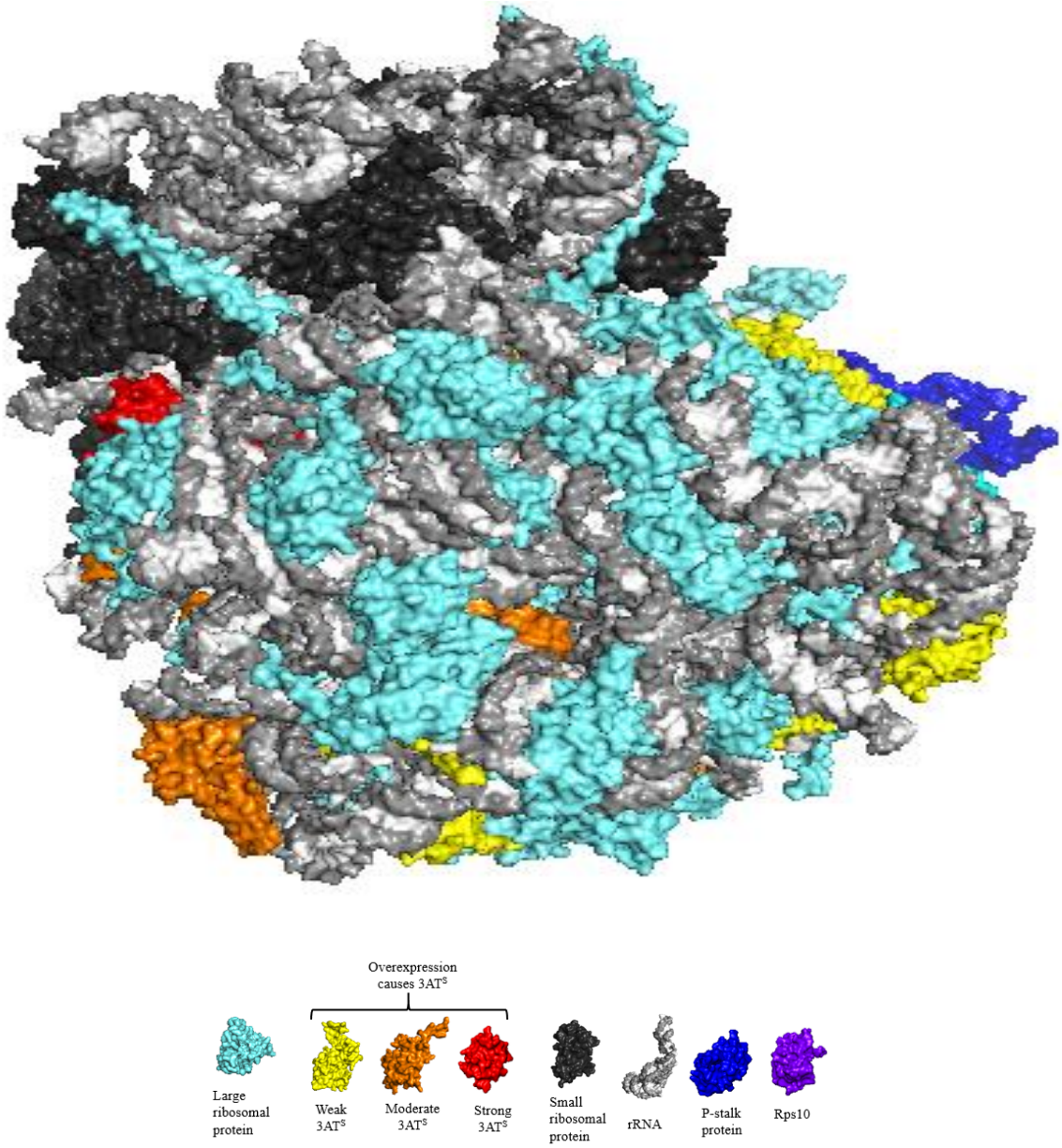

Figure 4.1 *Surface representation of the 80s ribosome of S. cerevisiae highlighting ribosomal proteins leading to 3AT sensitivity when over expressed*

The ribosomal subunit and its proteins highlighted in light blue. The small ribosomal subunit and its proteins highlighted in black. rRNA highlighted in light and dark grey. Highlighted in red are large ribosomal proteins when overexpressed cause strong $3AT^S$. Highlighted in orange are large ribosomal proteins when overexpressed cause moderate $3AT^S$. Highlighted in yellow large ribosomal proteins when overexpressed cause weak 3ATS. Highlighted in purple is Rps10, known to directly bind to Gcn1. Ribosomal P-Stalk proteins are highlighted in dark blue, known to bind to Gcn2. Surface representation of S. cerevisiae 80s ribosome created with PyMOL Molecular Graphics System, Version 1.8 Schrödinger, LLC using data obtained from "The structure of the eukaryotic ribosome at 3.0 Å resolution." (Ben-Shem et al., 2011)

4.5 Possible Gcn2 ribosomal contact points

As mentioned previously, recent research has identified *in vivo* that mammalian ribosomes specifically contact Gcn2 involving the P-stalk proteins of the large ribosomal subunit (Inglis et al., 2019). In this purified system ribosomal P-stalk proteins are shown to strongly activate Gcn2, significantly more so than uncharged tRNAs, this contradicting the suggestion that the major activating ligand to Gcn2 is uncharged tRNAs (Hinnebusch, 1997; Wek et al., 1995). It would be possible that the activation of Gcn2 by P-Stalk proteins occurs under only certain condition which has been shown *in vitro* for free cytoplasmic pools of P-stalk proteins but not ribosome associated P-stalk proteins under glucose starvation and osmotic stress conditions (Jiménez-Díaz et al., 2013). These previous studies however did not conclude that such binding and activation of Gcn2 at the P-stalk occurs under *in vitro* amino acid starvation conditions. Therefore, it is important to investigate where the identified Rpls in this current research, which when overexpressed cause $3AT^S$, may be located with respect to the P-stalk to identify any possible association of Gcn2 with the P-stalk proteins under amino acid starvation conditions. As it is known that Gcn2 contacts P-stalk proteins, this makes it likely several of the Rpls around the P-stalk might also contact Gcn2. Of course, it cannot be excluded that Gcn1 might also contact to and near to the P-stalk, as this has not been disproven experimentally.

Interestingly two of the four Rpls determined to induce a strong $3AT^S$ when overexpressed, Rpl20 and Rpl40, are located directly at the base of the P-stalk of the large ribosomal subunit (seen in Figure 4.2a and 4.2b). Given the fact that mammalian Gcn2 has been confirmed to contact ribosomal P-stalk proteins *in vivo*, this may indicate that Gcn2, rather than Gcn1, may also make contact to Rpl20 and Rpl40. Further highlighting the possible functional significance of Rpl20 is the fact it has very strong $3AT^S$ when this is readjusted for its expression level (see Table 3.6 and 3.7). Furthermore, when the ribosome is positioned to look down on the P-stalk proteins directly, the cluster of Rpls consisting of the P-stalk, Rpl20 and Rpl40 is also surrounded by other Rpls which when overexpressed cause moderate and weak $3AT^S$ in this current study (Figure 4.2b). Rpl20 is found in direct contact to Rpl10, which in turn is in contact with Rpl5 and in very close contact to Rpl11. Both Rpl10 and Rpl5 were identified to induce moderate $3AT^S$ when

overexpressed. Rpl6 is also in close contact to Rpl18 (slightly obscured by other large ribosomal proteins. Similarly, to the ribosomal stalk proteins, Rpl20 and Rpl40 may be required for complete binding of Gcn2 to the ribosome and thus the full function of Gcn2. The other Rpls identified surrounding Rpl20 and Rpl40 may also possibly play a role in enhancing or supporting the binding and activation of Gcn2 to the ribosome. Given that Rpl20 and Rpl40, identified as inducing strong $3AT^S$, are located closer to the P-stalk than other surrounding proteins with lower $3AT^S$ supports that these contacts are functionally more significant. It would be unreasonable to assume all these Rpls in Figure 4.2a and 4.2b would be involved in the binding of Gcn2, given the size of Gcn2, and the size of its binding domain (see Figure 1.5 in the introduction). However, given the small size of both Rpl20 and Rpl40, compared to Gcn2, it is reasonable to consider the possibility the Gcn2 does make direct contact to this region of the ribosome. Considering Gcn2 contacts Gcn1, it would be a likely possibility that some of the Rpls mentioned above, surrounding the cluster of the Rpl20, Rpl40 and the P-stalk proteins make contact to Gcn1 and not Gcn2.

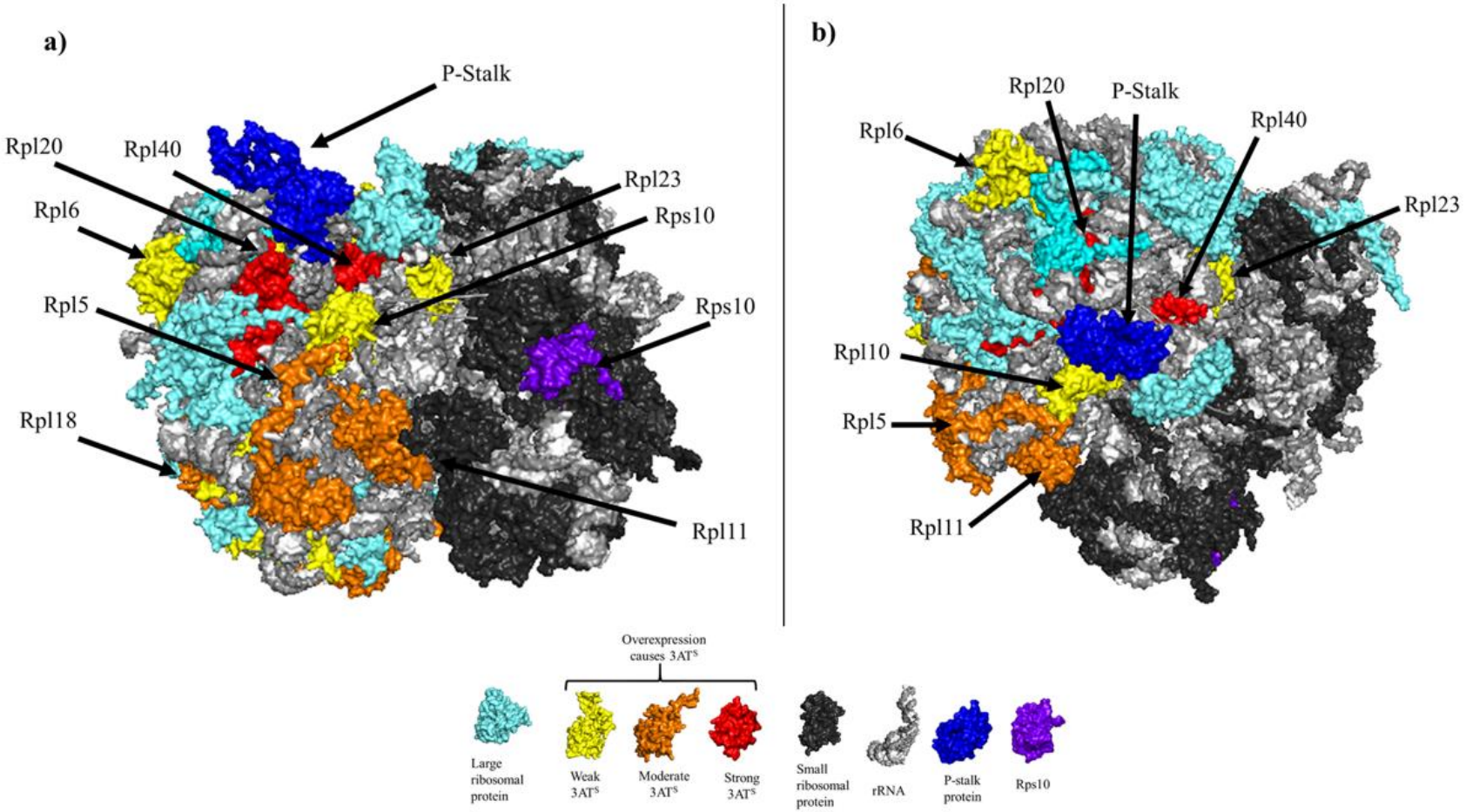

Figure 4.2 a) & b) Surface presentations of the 80s ribosome of S. cerevisiae highlighting ribosomal proteins leading to 3AT sensitivity when over expressed

The ribosomal subunit and its proteins highlighted in light blue. The small ribosomal subunit and its proteins highlighted in black. rRNA highlighted in light and dark grey. Highlighted in red are large ribosomal proteins when overexpressed cause strong $3AT^S$. Highlighted in orange are large ribosomal proteins when overexpressed cause moderate $3AT^S$. Highlighted in yellow large ribosomal proteins when overexpressed cause weak 3ATS. Highlighted in purple is Rps10, known to directly bind to Gcn1. Ribosomal P-Stalk proteins are highlighted in dark blue, known to bind to Gcn2. Surface representation of S. cerevisiae 80s ribosome created with PyMOL Molecular Graphics System, Version 1.8 Schrödinger, LLC using data obtained from "The structure of the eukaryotic ribosome at 3.0 Å resolution." (Ben-Shem et al., 2011)

4.6 Possible Gcn1-ribosmal contact points

Given the fact that Gcn1 has been shown to directly contact the small ribosome at Rps10, with this contact being required for the full function of Gcn2, it would stand to reason that some of the Rpls in this current study which induced $3AT^S$ when overexpressed, may be located close to Rps10. Also, considering the current working model states uncharged tRNAs are possibly released from the A-site of the ribosome to Gcn1, some of the identified Rpls in this study causing $3AT^S$ when overexpressed could also be expected to be in the vicinity of the A-site. In Figure 4.3a and 4.3b below, a view of the ribosome is presented displaying Rps10 and location of the A-site as indicated. As can be seen, especially in Figure 4.3b, Rpl40, Rpl23, Rpl10, Rpl11, and Rpl5, all identified to induce some level of $3AT^S$, are all located in close vicinity to the A-site of the ribosome.

From crystal structures of the 70S ribosome of *Thermus thermophilus* the bacterial large ribosomal protein L5, homologous to Rpl11 in yeast, is suggested to interact with A-site associated charged tRNAs (Yusupov et al., 2001). Cryo-EM structures of the 80S ribosome from yeast also suggest A-site associated charged tRNAs interact with Rpl11 as well as Rpl5 (Spahn et al., 2001). It would be possible that uncharged tRNAs also interact with Rpl5 and Rpl11. This is intriguing as mentioned above and shown in Figures 4.3a and 4.3b, Rpl5 and Rpl11 both induced moderate degrees of $3AT^S$ when overexpressed in this current study. If the $3AT^S$ phenotypes occurring from overexpression of Rpl5 and Rpl11 is indeed due to interference of Gcn2 activation, it would seem likely that this is due to interference of contact of Gcn1. Binding of Gcn1 to this region of the ribosome would be in support of the current working model whereby Gcn1 may be involved in release and transfer of uncharged tRNA to Gcn2.

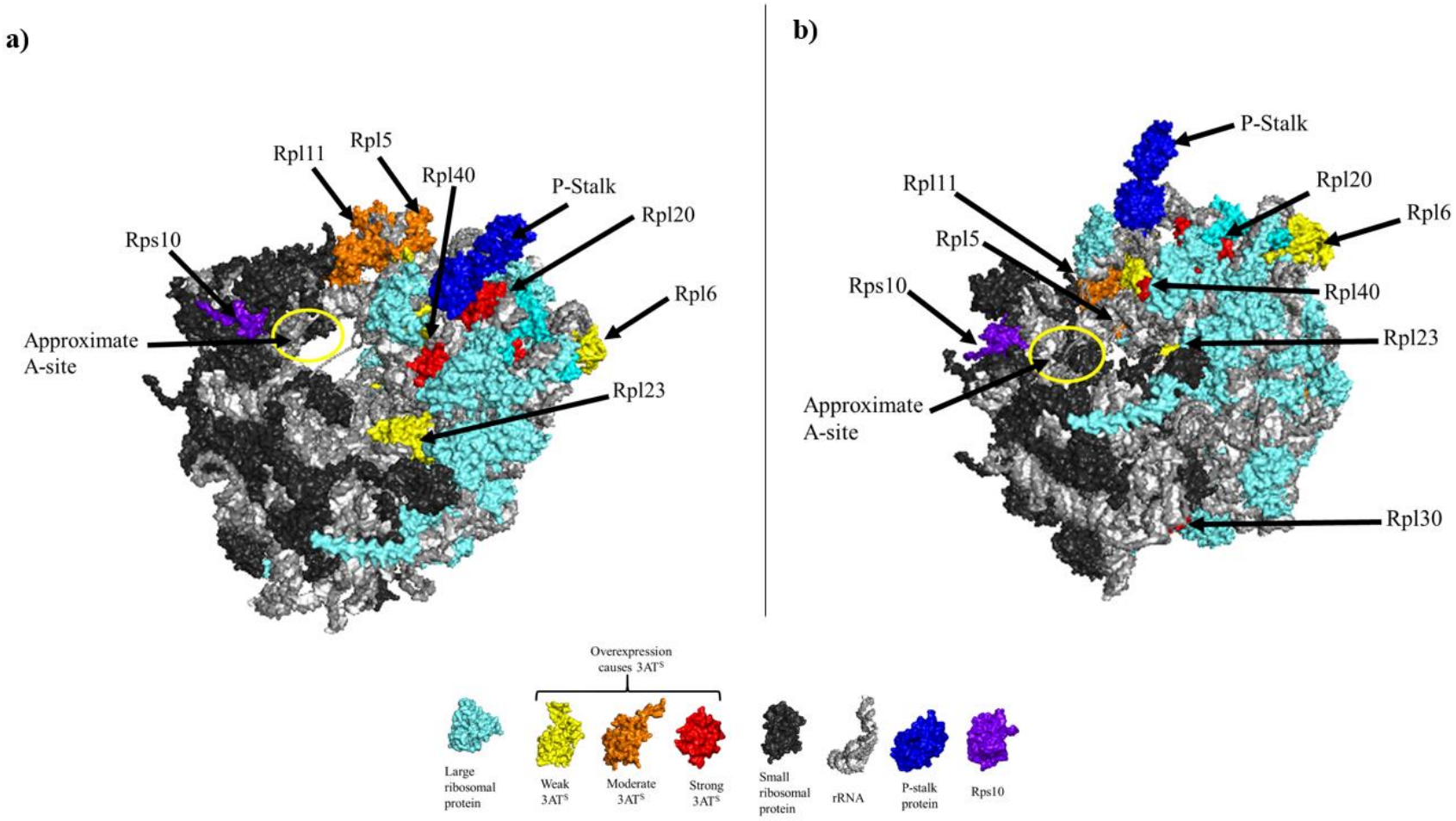

Figure 4.3 a) & b) *Surface representations of the 80s ribosome of S. cerevisiae highlighting ribosomal proteins leading to 3AT sensitivity when over expressed*

The ribosomal subunit and its proteins highlighted in light blue. The small ribosomal subunit and its proteins highlighted in black. rRNA highlighted in light and dark grey. Highlighted in red are large ribosomal proteins when overexpressed cause strong $3AT^S$. Highlighted in orange are large ribosomal proteins when overexpressed cause moderate $3AT^S$. Highlighted in yellow large ribosomal proteins when overexpressed cause weak $3AT^S$. Highlighted in purple is Rps10, known to directly bind to Gcn1. Ribosomal P-Stalk proteins are highlighted in dark blue, known to bind to Gcn2. Surface representation of S. cerevisiae 80s ribosome created with PyMOL Molecular Graphics System, Version 1.8 Schrödinger, LLC using data obtained from "The structure of the eukaryotic ribosome at 3.0 Å resolution" (Ben-Shem et al., 2011)

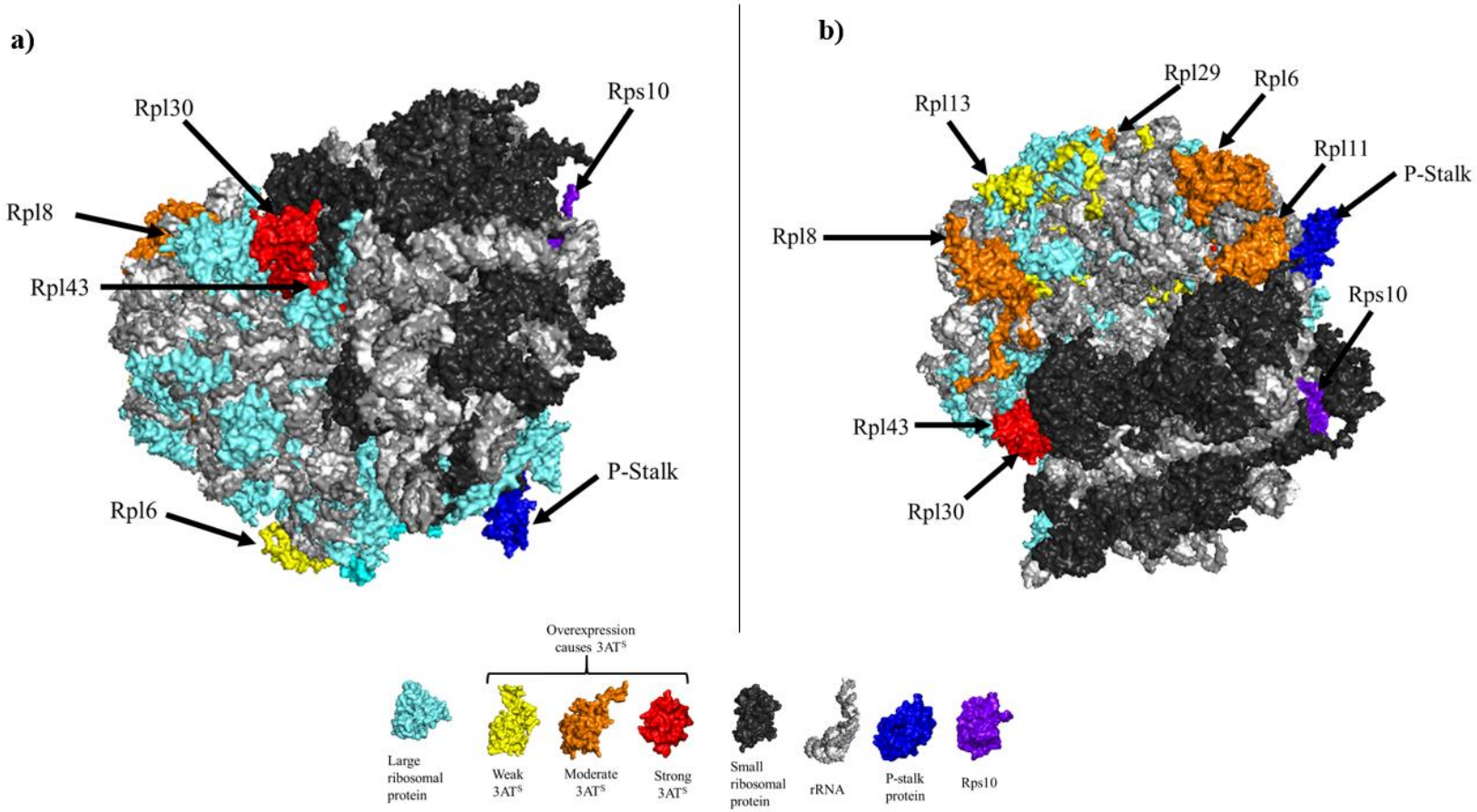

Figure 4.4 a) & b) *Surface representations of the 80s ribosome of S. cerevisiae highlighting ribosomal proteins leading to 3AT sensitivity when over expressed*

The ribosomal subunit and its proteins highlighted in light blue. The small ribosomal subunit and its proteins highlighted in black. rRNA highlighted in light and dark grey. Highlighted in red are large ribosomal proteins when overexpressed cause strong $3AT^S$. Highlighted in orange are large ribosomal proteins when overexpressed cause moderate $3AT^S$. Highlighted in yellow large ribosomal proteins when overexpressed cause weak $3AT^S$. Highlighted in purple is Rps10, known to directly bind to Gcn1. Ribosomal P-Stalk proteins are highlighted in dark blue, known to bind to Gcn2. Surface representation of S. cerevisiae 80s ribosome created with PyMOL Molecular Graphics System, Version 1.8 Schrödinger, LLC using data obtained from "The structure of the eukaryotic ribosome at 3.0 Å resolution" (Ben-Shem et al., 2011).

Gcn1 and Gcn20 together share homology to eEF3 as outlined in the introduction (see sections 1.5, 1.6 and Figures 1.6 and 1.7) (Vazquez de Aldana et al., 1995). Overexpression of the HEAT domain (similar to those found in Gcn1) and the C-terminal domain (shares homology to ABC domains in Gcn20) of eEF3 both reduce the ability of yeast to grow on starvation media. The eEF3 HEAT domain binds to the ribosome and the CTD of eEF3 has been shown to co-sediment with polysomes (Visweswaraiah et al., 2012). It has been suggested that the binding of eEF3 to the ribosome, via the HEAT domain and the CTD, impair the function of Gcn1 on the ribosome and activation of Gcn2. It is also suggested that this may be due to eEF3 bound to ribosomes affecting some of the Gcn1-ribosomal contact points. It has been suggested therefore, that Gcn1 (possibly in complex with Gcn20) binds to similar ribosomal contacts as eEF3 and Gcn1 executes a similar function to that of eEF3 (Visweswaraiah et al., 2012). If this is the case, then some of the large ribosomal proteins involved in the binding of eEF3 to the ribosome could be expected to also bind to the complex of Gcn1-Gcn20.

Cryo-electron microscopy has previously revealed that eEF3 interacts with the large ribosomal proteins Rpl5 and Rpl11 found in the E-site of the ribosome (Andersen et al., 2006; Armache et al., 2010). Interaction of eEF3 with Rpl5 and Rpl11 occurs via the ABCII domain and chromodomain of eEF3 (Andersen et al., 2006). Significantly, this current research showed that Rpl5 and Rpl11 both induce moderate $3AT^S$ phenotypes when overexpressed (position on the ribosome shown in Figures 4.3a and 4.3b). As Rpl5 and Rpl11 have been shown to interact with eEF3, and Gcn1 and eEF3 are suggested to share some ribosomal binding sites, it would be possible that Gcn1 would also contact Rpl5 and Rpl11.

A study by Gavin et al. (2006) using a tandem-affinity-purification (TAP) method in a genome wide screen of identified proteins found in protein complexes found in yeast. Protein complexes that precipitate with different attachment proteins were identified. Where the complex of Gcn1 and Gcn20 is a core module to a complex, several Rpls were found to associate in this complex with Gcn1 and Gcn20. Rpls identified to associate in complexes along with Gcn1 and Gcn20 include: Rpl1A, Rpl4A, Rpl18A, and Rpl30 (listed in Table 4.2) (Gavin et al., 2006).

Interestingly Rpl18 and Rpl30 were both identified in this current study as inducing $3AT^S$ when overexpressed. This could indicate that the $3AT^S$ phenotypes observed by overexpression of Rpl18 and Rpl30 are due to interference of a possible Gcn1-ribosmal contact point. Figure 4.4a, which displays the ribosome with the P-stalk facing away and to the right of the front view displays the location of Rpl30. Strikingly from this view, it is seen that Rpl30 is in direct contact with Rpl43, another Rpls which when overexpressed induced a strong $3AT^S$ phenotype. Upon further rotation of the ribosome, where the P-stalk is completely facing away from the surface displayed, many more Rpls identified in this region are exposed. Given the fact that Rpl30 and Rpl43 are in direct contact with each other (both causing strong $3AT^S$ when overexpressed), and a possible association of Rpl30 with Gcn1 has been shown previously, it would support this region of the ribosome may indeed be a functionally important for Gcn1. Interestingly, as displayed in Figure 4.4a and 4.4b, the cluster of proteins close to Rpl30 and Rpl43 is some distance away from Rps10, the one confirmed Gcn1-ribosmal contact point (Rps10). However, it must be considered that Gcn1 is a very large protein $1/10^{th}$ the size of the ribosome, it is still plausible that Gcn1 could be positioned in such a way where it could contact to Rpl30. In further support of the functional significance of a possible contact to Rpl43 is the fact it was reallocated as having very strong $3AT^S$ when its expression level was taken into consideration (see Table 3.6 and 3.7)

It is possible that besides Gcn1 and Gcn2, Gcn20 makes contact to large ribosomal proteins, and that loss of Gcn20 contact to the ribosome when Rpls were overexpressed is responsible for some of the observed $3AT^S$ phenotypes observed in this study. In the proteome screen by Gavin et al. (2006) Rpl30, identified in this current research to induced strong $3AT^S$ when overexpressed, is found in a complex that includes Gcn20 and this complex does not include Gcn1. It would also be possible the Gcn20 contacts Rpl5 and Rpl11. As mentioned above the complex of Gcn1 and Gcn20 have been suggested to share similar binding sites on the ribosome as eEF3 (Visweswaraiah et al., 2012). As Rpl5 and Rpl11 (both causing moderate $3AT^S$) have been shown to interact with the ABC2 domain of eEF3, which is also found in Gcn20, this could give rise to the possibility of Gcn20 making contact to Rpl5 and Rpl11 (Andersen et al., 2006; Vazquez de Aldana et al., 1995).

4.7 Relating to past findings

If Gcn1 or Gcn2 bind a ribosomal protein that is important for Gcn2 activation, then any genetic approach that prevents the interaction to this ribosomal binding point should impair growth on starvation media. Two genetic approaches have been used to assess the importance of ribosomal proteins on the activation of Gcn2. The approach used in this current study used the overexpression of Rpls. The overexpression of exogenous, non-ribosomal associated ribosomal proteins would occupy the binding site in Gcn1 and Gcn2 thereby preventing binding to the ribosome associated Rpls. The other approach is the deletion of one of the two paralogues of a Rpl thereby, knocking down Rpl levels in the cell, as a consequence, not all Ribosomes in a cell would have that Rpl, preventing Gcn1 and Gcn2 forming a functional complex with the ribosome. In both of these approached the result is a reduction in ribosomal association of either Gcn1 or Gcn2. Both approaches should have similar results, that is should discover the same Rpls as possible contact points for Gcn1 or Gcn2. Previous studies have shown that deletion and overexpression can give the same phenotype of reduced growth on starvation media with both the deletion and overexpression of Rps10 leading to reduced growth on starvation media (Lee et al., 2015).

Jochmann (2014), from the Sattlegger group, used the above-mentioned knockdown approach for the investigation of important Rpls with respect to their involvement in Gcn1 and Gcn2 binding. Several Rpls were identified as possible contacts to Gcn1 or Gcn2, these include Rpl6A, Rpl18B, Rpl21A, Rpl 34B and Rpl35. When levels of these Rpls were reduced in yeast strains by the deletion of either paralogue of the genes for the respective Rpls, sensitivity to SM (SM^S) was observed (Rpls which when deleted lead to SM^S and the resulting degrees of SM^S are summarised in Table 4.1 below). This shows that knockdown of these Rpls in yeast leads to a reduction in the ability to respond to amino acid starvation (Jochmann, 2014).

For the comparison of Rpls which when overexpressed caused $3AT^S$ to those which when knocked down caused SM^S, the Rpls identified in the study by Jochmann (2014) were mapped alongside the Rpls identified in this current study. This mapping is displayed below in Figure 4.5a, 4.5b and 4.5c. If both studied did identify Rpls which truly do contact Gcn1 and Gcn2, it would be expected that a similar footprint on the ribosome would be produced. Indeed, when comparing the knockdown screening of Rpls to this current research looking at the overexpression of Rpls it is seen that both studies identified Rpl6 and Rpl18 as reducing growth on starvation media when

overexpressed or when reduced in levels by deletion of one paralogue of the gene in yeast (highlighted by bold red text in Figure 4.5a below). As these Rpls were identified in both studies, they are both strong candidates for being true binding partners of Gnc1 and Gcn2. This is further supported by the fact interaction of Gcn1 with Rpl18 has been shown previously in the proteome complex study by (Gavin et al., 2006).

Rpl21 which was not identified to cause reduced growth on starvation media when overexpressed was however found to cause reduced growth in the knockdown study. When observing where on the ribosome Rpl21 is located, it is found in direct contact with Rpl20 near the base of the P-stalk (Figure 4.5b). Rpl20 was identified in this current research to induce strong $3AT^S$. Considering Rpl20 and Rpl21 are both in direct contact with each other, and their close proximity to the P-stalk would support this region of the ribosome making contact to Gcn1 or Gcn2. Rpl21 knockdown also causes a reduction eIF2α-P levels under amino acid starvation conditions when levels are reduced by deletion, compared to the WT (Jochmann, 2014). This further the possibility of this region of the ribosome as being involved in the binding of Gcn1 or Gcn2 and this being functionally important with respect to the activation of Gcn2.

When the ribosome is rotated to display Rpl34 (Figure 4.5c), identified in the knockdown screen by Jochmann (2014) to induce SM^S , Rpl34 is found located very close to Rpl43 as well as Rpl30, which both cause a strong degree of $3AT^S$. Furthermore as mentioned in the previous chapter, the proteome complex screening study by Gavin et al. (2006) showed that Rpl30 can form certain complex with Gcn1. Thus, the combination of findings from the knockdown screen, the over expression screen and the fact Rpl30 is found in complexes with alongside Gcn1 would suggest that Gcn1 makes contact at this point. Even though the two studies found some differing possible Gcn1-Gcn2 large ribosomal contact points, the results are still in agreement with each other in terms of a more general position on the ribosome where Gcn2 or Gcn1 may contact. An explanation for why some Rpls identified as possible Gcn1 or Gcn2 ribosomal contacts in this current study were not identified in the knock down screen could be that essential Rpls were not able to be assessed in knock down screen. Essential Rpls are those where only one gene exists for the protein (unlike the majority of Rpls which are encoded by two genes). Essential Rpls include Rpl5, Rpl10, Rpl25, Rpl28, Rpl29, Rpl30, Rpl38 and Rpl39. Rpl5, Rpl10, Rpl30 and Rpl39 were all identified in this current study as possible Gcn1 or Gcn2 contacts. This highlight the importance

of using the two differing genetic approached of overexpression and knockdown together as a powerful tool to identify possible contact points between Rpls and Gcn1 or Gcn2. Another reason why the studies are not in total agreement could be that some overexpressed Rpls may have existed misfolded in the cell. As the Rpls are usually found in complex with other Rpls in the ribosome, it could be expected that when not associated with the ribosome, their structure would not be the same. Many Rpls would have hydrophobic regions which are normally buried within the ribosome. Possible mis-folding of these proteins when overexpressed, which do indeed contact Gcn1 or Gcn2, may have prevented their ability to bind to Gcn1 or Gcn2.

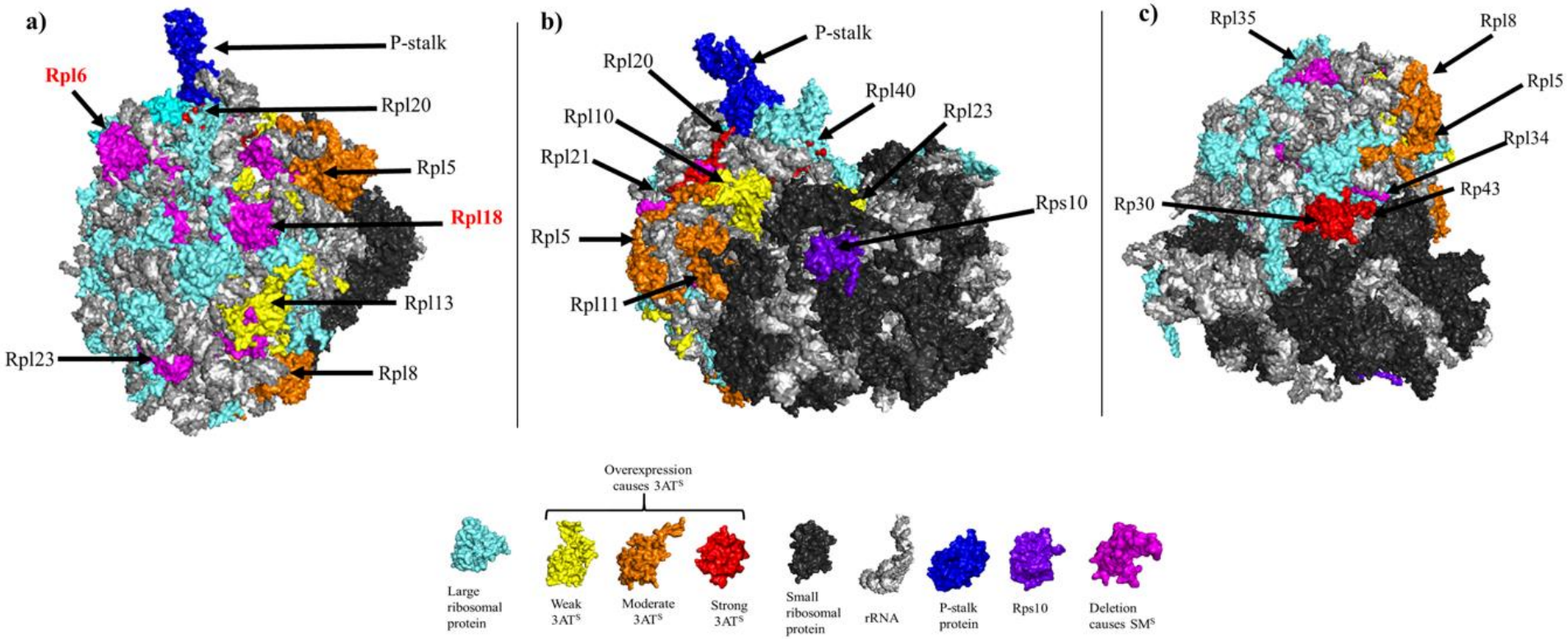

Figure 4.5 a), b) & c) *Surface representations of the 80s ribosome of S.* cerevisiae *highlighting ribosomal proteins leading to 3AT sensitivity when over expressed and large ribosomal proteins causing SM^S when knocked down.*

The ribosomal subunit and its proteins highlighted in light blue. The small ribosomal subunit and its proteins highlighted in black. rRNA highlighted in light and dark grey. Highlighted in red are large ribosomal proteins when overexpressed cause strong 3AT^S. Highlighted in orange are large ribosomal proteins when overexpressed cause moderate 3AT^S. Highlighted in yellow large ribosomal proteins when overexpressed cause weak 3AT^S. Highlighted in purple is Rps10, known to directly bind to Gcn1. Highlighted in pink are large ribosomal proteins which when knocked down cause SM^S. Ribosomal P-Stalk proteins are highlighted in dark blue, known to bind to Gcn2. Surface representation of S. cerevisiae 80s ribosome created with PyMOL Molecular Graphics System, Version 1.8 Schrödinger, LLC using data obtained from "The structure of the eukaryotic ribosome at 3.0 Å resolution." (Ben-Shem et al., 2011)

Table 4.1 *Comparison of results found in this study to those found in: deletion screen by Jochmann (2014), Co-precipitation study by Gavin. et al. (2006). Also displayed is the association of ribosomal proteins with elongation factors eEF3 and eEF1A.*

Strain	3ATS or 3ATR	Expression level	Gcn1-Gcn20 Co-precipitation	Deletion (Vivian)	eEF3 contact point	eEF1A association
Rpl1A		0.27	Yes, Gavin et al			
Rpl2A		0.12				
Rpl4B	3AT^{R}	0.36	Yes, Gavin et al			
Rpl5	Moderate 3ATS	0.90			Cryo EM	
Rpl6A	Weak 3ATS	ND		strong SM^{S}		
Rpl7A		0.09				Yes, Gavin et al.
Rpl7B	3AT^{R}	0.03				
Rpl8A	Moderate 3ATS	0.05			Yes, Gavin et al.& Armache et al	
Rpl9A	3AT^{R}	0.37				
Rpl10A	Weak 3ATS	1.64				
Rpl11A	Moderate 3ATS	0.44			Gavin et al, Armache et al & Cryo EM	
Rpl12A		0.89				
Rpl13A	Weak 3ATS	0.21				Yes*. Gavin et al.
Rpl15A	3AT^{R}	ND				
Rpl16A		0.03				
Rpl17A		0.13				Yes, Gavin et al.
Rpl18A	Moderate 3ATS	0.04	Yes, Gavin et al	strong SM^{S}	Yes, Gavin et al.	
Rpl19A		0.18				
Rpl20A	Strong 3ATS	0.03				
Rpl21A		0.21		Very strong SM^{S}		
Rpl23A	Weak 3ATS	0.13				
Rpl24A		0.40				Yes, Gavin et al.
Rpl25a		0.13				Yes, Gavin et al.
Rpl26a		0.18				
Rpl27A		0.02				
Rpl28A		0.19				
Rpl29A	Weak 3ATS	0.98				
Rpl30	Strong 3ATS	0.33	Yes Gavin et al			Yes, Gavin et al.
Rpl31A		0.43				
Rpl33A		0.01				
Rpl34A		0.06				
Rpl34B		0.04		Very strong SM^{S}		
Rpl35A		ND		Very strong SM^{S}		Yes, Gavin et al.
Rpl37A	Weak 3ATS	0.17				
Rpl36A		0.33				
Rpl38A		0.13				
Rpl39	Weak 3ATS	0.23				Yes, Gavin et al.
Rpl40A	Strong 3ATS	0.10				
Rpl41A	3AT^{R}	ND				
Rpl42B		0.07				
Rpl43A	Strong 3ATS	0.03				
				* paralogue		*paralogue

4.8 Relating findings to the current working model for Gcn2 activation and attempt to map Gcn1 and Gcn2 on the ribosome

The findings from attempting to assign Rpls causing $3AT^S$ to be due to possible loss of contact to either Gcn1 or Gcn2 in the previous sections can be considered with regards to their agreement with the current working model for how uncharged tRNA are transferred and lead to the activation of Gcn2 under starvation conditions (see Figure 1.9). This may help to give a clearer indication of a possible mapping of Gcn1 and Gcn2 on the ribosome.

In agreement to the working model is the suggestion that Rpl5 and Rpl11 are strong candidates for Gcn1 binding partners (see section 4.6). Rpl5 and Rpl11 and binding partners of eEF3, suggested to share binding sites with Gcn1. Rpl5 and Rpl11 have also found to interact with A-site associated charged t-RNAs. If Rpl5 and Rpl11 are true binding partners of Gcn1, then the binding of Gcn1 to the ribosome at this location that would position Gcn1 in a location within proximity of the A-site. This would be in agreement of the working model postulating a binding of Gcn1 near to the A-site where it has access to uncharged t-RNAs said to bind to the A-site in a codon specific manner under starvation conditions.

If Gcn1 truly is positioned in this location on the ribosome it would also give Gcn2, bound to Gcn1, access to P-stalk proteins, shown to bind Gcn2 under certain conditions (Inglis et al., 2019; Jiménez-Díaz et al., 2013). Binding of Gcn2 at this location, under amino acid starvation conditions, could occur as indicated by Rpl20 and Rpl40 inducing $3AT^S$ when overexpressed, which are located directly at the base of the P-stalk proteins.

The working model has been suggested to include mechanisms for placing Gcn2 in latent state under replete, or non-starvation conditions, which are removed during amino acid starvation conditions (see section 1.8) (Castilho et al., 2014; Visweswaraiah et al., 2011; Visweswaraiah et al., 2012)The translation elongation factors eEF1A and eEF3 are suggested to place Gcn2 into a latent state under non-starvation conditions in yeast (Visweswaraiah et al., 2011; Visweswaraiah et al., 2012). Rpl5 and Rpl11 as possible Gcn1 contacts would be in agreement of this hypothesis.

Under non-starvation conditions, eEF3 would be present on ribosomes making contact to Rpl5 and Rpl11. eEF3 would carry out its function with the release of uncharged tRNAs in the E-site of the ribosome. This would prevent Gcn1 making possible functionally important contacts to the

ribosome. Under amino acid starvation conditions, when eEF3 would have no functional purpose, it would be dissociated from the ribosome. This would expose Gcn1 to bind to the suggested similar contact points between Gcn1 and eEF3, possibly to Rpl5 and Rpl11. Gcn1 forming functionally important contacts in this position near to the A-site would, allowing transfer of uncharged t-RNAs to Gcn2 via Gcn1.

eEF1A is also suggested to place Gcn2 in a latent state during non-starvation conditions via direct contact to Gcn2 (Visweswaraiah et al., 2011). eEF1A is suggested to act as an inhibitor and possibly prevents contact or access to the substrate of Gcn2, eIF2α (Visweswaraiah et al., 2011). It would also be a possibility, under non-starvation conditions, that that eEF1A prevents Gcn2 contacting the P-stalk proteins which may be required for Gcn2 activation. As Gcn2 is shown to bind to eEF1A, and eEF1A also has been shown to interact with P-stalk proteins, this could mean eEF1A may interfere with a Gcn2-P-stalk contact. Under starvation conditions, uncharged t-RNAs would be delivered to Gcn2 via Gcn1, these uncharged tRNAs may be responsible of the dissociation of eEF1A that occurs under these conditions. This is suggested to occur as the uncharged tRNAs may prevent Gcn2 from contacting eEF1A. This could possibly lead to the association of Gcn2 to the P-stalk proteins. The binding of uncharged tRNAs to Gcn2 may work in unison with the contract of P-stalk proteins to allow for the full activation of Gcn2 under amino acid starvation conditions. The close location of Rpl20 and Rpl40 to the P-stalk proteins, causing $3AT^S$ when over expressed, would be in support of this possible mode of Gcn2 activation.

Given the above, and the findings from the previous chapters, a suggested mapping of Gcn1 and Gcn2 on the ribosome occurring under amino acid starvation conditions is presented below in Figure 4.6.

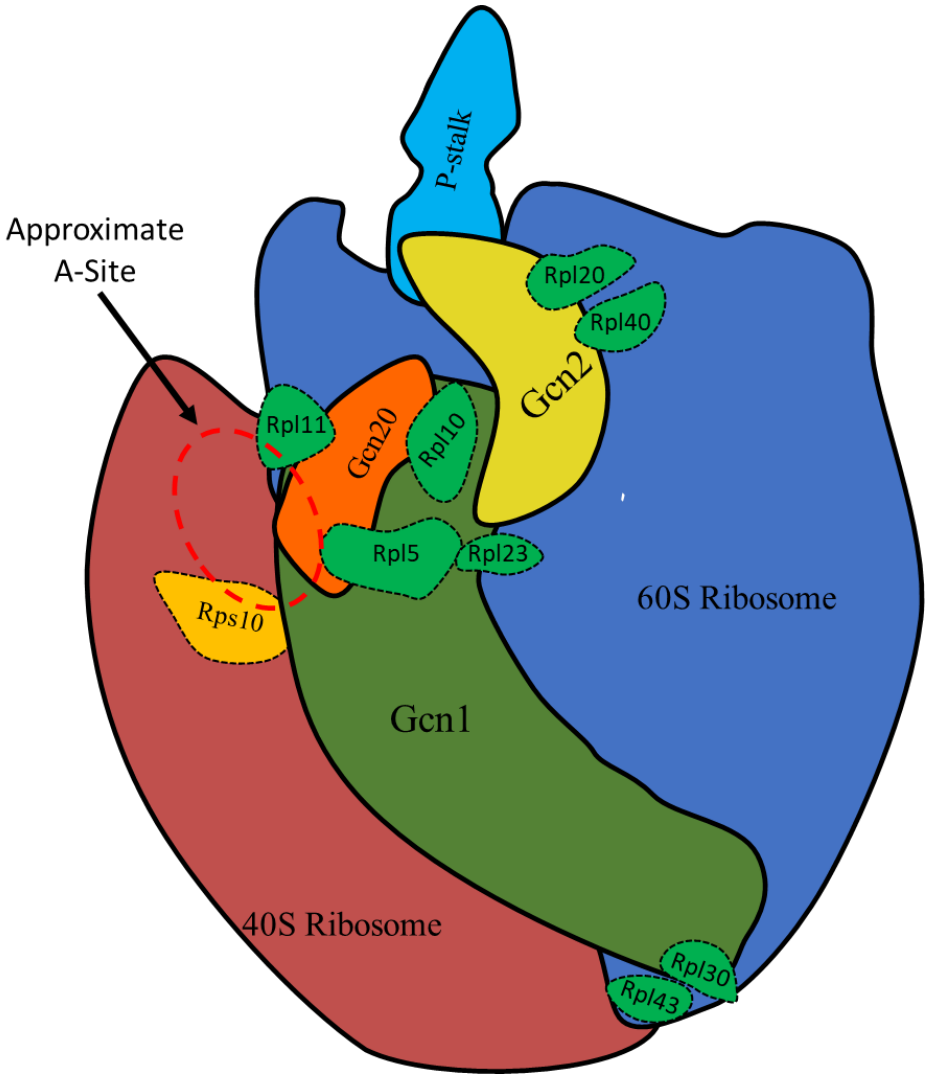

Figure 4.6 *Suggested mapping location of Gcn1 and Gcn2 on the ribosome under amino acid starvation conditions.*

Contact of Gcn1 is suggested to Rpl5 and Rpl11 as both proteins contact eEF3, which may share similar contacts to Gcn1.Proximity to Rps10, known to contact Gcn1 would support Gcn1 binding at this location. Contact at this location may be supported by Rpl10 and rpl11. Gcn1 may span across the large ribosomal subunit and also contact Rpl30 and Rpl43. Binding of Gcn2 occurs with P-stalk proteins. This contact may be supported by contacts to Rpl20 and Rpl40.

4.9 Conclusion and future perspectives

This study used a genetic approach to identify possible large ribosomal protein contact points with Gcn1 or Gcn2. Results indicated several large ribosomal proteins as possible Gcn1 or Gcn2 ribosomal contact points. The validity of the findings is supported by the fact the majority of the identified Rpls are found clustered in regions known or suggested to contact Gcn1 or Gcn2, with far fewer Rpls found some distance away from these regions.

Several Rpls were in proximity of the P-stalk proteins (part of the large ribosomal subunit), a confirmed binding partner of Gcn2 (Inglis et al., 2019). Rpl20 and Rpl40, which induced strong degrees of $3AT^S$, were found located close to the base of the P-stalk. The fact these two Rpls are in direct contact with each other would further support these as strong candidates for true Gcn2 ribosomal contact points. Studies suggest Gcn2 contact to P-stalk proteins is required for its activation (Inglis et al., 2019). The fact strong $3AT^S$ were induced when Rpls close to this region were overexpressed, indicating a strong degree of interference of the activation of Gcn2, would give support to the contact to this location being involved for Gcn2 activation.

Another region on the ribosome was recognised as a possible Gcn1 binding region. This region of the ribosome has been shown previously to bind eEF3, a protein with a large degree of homology to the complex of Gcn1-Gcn20 (Vazquez de Aldana et al., 1995). Given that evidence strongly suggest eEE3 and Gcn1 share some binding sites on the ribosome, Rpls identified in this current research located in this region were suggested as likely candidates for true Gcn1-ribosomal contact points (Visweswaraiah et al., 2012). These Rpls include Rpl5 and Rpl11, this is supported by the fact several other Rpls identified in this research are located within proximity, and some in direct contact to Rpl5 and Rpl11. Contact to this region would be in agreement also with the current working model, where Gcn1 would be placed on the ribosome in a location where it would have access to uncharged tRNAs to transfer to Gcn2.

Given several Rpls were identified in this current research as being strong candidates for contact to either Gcn1 or Gcn2 justifies future studies in to the exploration of the validity of these results. Several lines of research could be used to confirm and further the findings found in study.

For confirmation that the observed $3AT^S$ phenotypes seen for the identified possible Gcn1-Gcn2 large ribosomal contacts are due to inference of the amino acid starvation response and to support the claim that these large ribosomal proteins do indeed contact Gcn1 or Gcn2, the impairment of Gcn2 activity needs to be shown for those Rpl overexpressing strains giving $3AT^S$ phenotypes. This was attempted to be shown here with measurement of eIF2α-P levels, which increase under amino acid starvation conditions. However, the method of detecting eIF2α-P levels in this study was insufficient for the detection of eIF2α-P. It would be possible to overexpress large ribosomal proteins without the presence of the Protein A tag which interfered with eIF2α-P detection, or to investigate other sources of antibodies for eIF2α-P which may be more specific.

Several plasmids containing certain large ribosomal proteins were unavailable at the time this research was conducted; this includes the P-stalk proteins. These would need to be obtained for future research to confirm yeast Gcn2 directly contacts the P-stalk proteins as this has only been shown with mammalian ribosomes and Gcn2 so far. The same overexpression approach conducted here could be used to indicate whether Gcn2 contact to P-stalk proteins is required for the activation of Gcn2 and the response to amino acid starvation.

It would then be important to distinguish between either Gcn1 or Gcn2 binding to the identified Rpls which affect the activation of Gcn2, which could not be confirmed in this current study. To identify whether a physical interaction of a Rpl occurs with either Gcn1 or Gcn2 occurs, co-precipitation studies and Y2H system can be used. Both methods have been shown previously to successfully show a direct interaction between Gcn1 and the small ribosomal protein Rps10 (Lee et al., 2015).

A genetic approach could also be used to further give evidence for which Rpls bind to Gcn1 and which bind to Gcn2. Each Rpl could be co-overexpress with either Gcn1 or Gcn2, and their growth on starvation media, and resulting eIF2α-P measured. The hope would be that the cellular abundance of Gcn1 or Gcn2 overexpressed in Rpl overexpressing strains would titrate out the overexpressed Rpls by saturation of all exogenous Rpls present in the cell. This would lead to an overabundance of either Gcn1 or Gcn2 which can then bind to endogenous ribosomal contacts and carry out their function under starvation conditions. Resulting growth on starvation media and eIF2α-P levels could be compared to when only the Rpls are overexpressed alone, increased ability to grow when Gcn1 or Gcn2 is present may be indicative of true Gcn1 or Gcn2 contacts.

To identify which regions of Gcn1 and Gcn2 are involved in binding to large ribosomal proteins, fragments of either Gcn1 or Gcn2, encompassing different domains of either protein, could be used in co-precipitation studies. This would identify where on Gcn1 and Gcn2 large ribosomal proteins may contact. This would give insight on how Gcn1 and Gcn2 are placed on the ribosome and which regions are important with respect to function on the ribosome. This has been done in a similar manner previously for Gcn2-Pstalk contacts, where the domains required within Gcn2 for binding as well as its activation were revealed (Lee et al., 2015). This would reveal which regions or domains of Gcn1 or Gcn2 are important for their binding and function on the ribosome. This could lead to a better understanding for example of where uncharged tRNAs may interact with Gcn1 and how this leads to its possible transfer to Gcn2.

Which portions of each Rpl required for binding to Gcn1 or Gcn2 could also be investigated to identify which regions are required to bind to Gcn1 or Gcn2. Differing fragment sizes of each Rpl could be overexpressed and growth assays carried out to identify minimum fragments needed for impartment of Gcn1/Gcn2 ribosomal binding and Gcn2 activity.

Knowledge gained here and in future studies could also be vital in understanding the many other biological roles Gcn2 associated with besides amino acid starvation (see section 1.11). For example active Gcn2 is associated with Alzheimer's and the survival and proliferation of certain cancers (Bunpo et al., 2009; Ma et al., 2013; Wang et al., 2013). Revealing ribosomal contacts to Gcn1/Gcn2, and how they affect Gcn2 activation may lead to development of possible Alzheimer's and cancer treatment therapies which interfere with Gcn2 activation by prevention of ribosomal contacts between the ribosome Gcn1 and Gcn2. Potential drugs could be developed, which impair the activation of Gcn2. One possible means of this would be to develop a peptide that would interact with Gcn1 or Gcn2 and prevent its ribosomal association required for Gcn2 activation. This could be developed from future work investigating which minimum fragments of Rpls which are required for the binding to Gcn1 or Gcn2 with respect to preventing activation if Gcn2. This is an attractive means of cancer treatment considering Gcn2 is generally considered to only be required in cells not undergoing amino acid starvation.

Findings from this current research combined with the above-mentioned future work will help in furthering knowledge of how Gcn1 and Gcn2 interact with ribosomes during amino acid starvation. Knowledge of all functional contacts between the ribosome and Gcn1/Gcn2 will help

to formulate a more complete working model for how uncharged tRNAs, accumulating during amino acid starvation, are delivered to and activate Gcn2. This will help reveal a more complete understanding of the function of Gcn2 for responding to amino acid starvation and its involvement in other biological processes.

References

Andersen, C. B., Becker, T., Blau, M., Anand, M., Halic, M., Balar, B., et al. (2006). Structure of eEF3 and the mechanism of transfer RNA release from the E-site. *Nature, 443*(7112), 663-668. doi:10.1038/nature05126

Andrade, M. A., Petosa, C., O'Donoghue, S. I., Müller, C. W., & Bork, P. (2001). Comparison of ARM and HEAT protein repeats. *Journal of Molecular Biology, 309*(1), 1-18. doi:10.1006/jmbi.2001.4624

Armache, J.-P., Jarasch, A., Anger, A. M., Villa, E., Becker, T., Bhushan, S., et al. (2010). Localization of eukaryote-specific ribosomal proteins in a 5.5-Å cryo-EM map of the 80S eukaryotic ribosome. *Proceedings of the National Academy of Sciences, 107*(46), 19754-19759. doi:doi.org/10.1073/pnas.1010005107

Baba, K., Tumuraya, K., Tanaka, I., Yao, M., & Uchiumi, T. (2013). Molecular dissection of the silkworm ribosomal stalk complex: the role of multiple copies of the stalk proteins. *Nucleic Acids Research, 41*(6), 3635-3643. doi:10.1093/nar/gkt044

Baird, T. D., & Wek, R. C. (2012). Eukaryotic initiation factor 2 phosphorylation and translational control in metabolism. *Advances in Nutrition: An International Review Journal, 3*(3), 307-321. doi:doi.org/10.3945/an.112.002113

Ben-Shem, A., Garreau de Loubresse, N., S, M., Jenner, L., Yusupova, G., & Yusupov, M. (2011). The structure of the eukaryotic ribosome at 3.0 Å resolution. *Science, 6062*(334), 1524-1529. doi:10.1126/science.121264

Berlanga, J. J., Ventoso, I., Harding, H. P., Deng, J., Ron, D., Sonenberg, N., et al. (2006). Antiviral effect of the mammalian translation initiation factor 2α kinase GCN2 against RNA viruses. *The EMBO Journal, 25*(8), 1730-1740. doi:10.1038/sj.emboj.7601073

Boudeau, J., Miranda-Saavedra, D., Barton, G. J., & Alessi, D. R. (2006). Emerging roles of pseudokinases. *Trends in Cell Biology, 16*(9), 443-452. doi:10.1016/j.tcb.2006.07.003

Bunpo, P., Dudley, A., Cundiff, J. K., Cavener, D. R., Wek, R. C., & Anthony, T. G. (2009). GCN2 protein kinase is required to activate amino acid deprivation responses in mice treated with the anti-cancer agent L-asparaginase. *Journal of Biological Chemistry, 284*(47), 32742-32749. doi:10.1074/jbc.M109.047910

Castilho, B. A., Shanmugam, R., Silva, R. C., Ramesh, R., Himme, B. M., & Sattlegger, E. (2014). Keeping the eIF2 alpha kinase Gcn2 in check. *Biochimica et Biophysica Acta (BBA)-Molecular Cell Research, 1843*(9), 1948-1968. doi:10.1016/j.bbamcr.2014.04.006

Chaveroux, C., Lambert-Langlais, S., Cherasse, Y., Averous, J., Parry, L., Carraro, V., et al. (2010). Molecular mechanisms involved in the adaptation to amino acid limitation in mammals. *Biochimie, 92*(7), 736-745. doi:10.1016/j.biochi.2010.02.020

Chaveroux, C., Lambert-Langlais, S., Parry, L., Carraro, V., Jousse, C., Maurin, A.-C., et al. (2011). Identification of GCN2 as new redox regulator for oxidative stress prevention in vivo. *Biochemical and Biophysical Research Communications, 415*(1), 120-124. doi:10.1016/j.bbrc.2011.10.027

Cherry, J. M., Hong, E. L., Amundsen, C., Balakrishnan, R., Binkley, G., Chan, E. T., et al. (2011). Saccharomyces Genome Database: the genomics resource of budding yeast. *Nucleic Acids Research, 40*(D1), D700-D705. doi:10.1093/nar/gkr1029

Costa-Mattioli, M., Gobert, D., Harding, H., Herdy, B., Azzi, M., Bruno, M., et al. (2005). Translational control of hippocampal synaptic plasticity and memory by the eIF2α kinase GCN2. *Nature, 436*(7054), 1166. doi:10.1038/nature03897

del Pino, J., Jiménez, J. L., Ventoso, I., Castelló, A., Muñoz-Fernández, M. Á., de Haro, C., et al. (2012). GCN2 has inhibitory effect on human immunodeficiency virus-1 protein synthesis and is cleaved upon viral infection. *PloS One, 7*(10), e47272. doi:doi.org/10.1371/journal.pone.0047272

Deng, J., Harding, H. P., Raught, B., Gingras, A.-C., Berlanga, J. J., Scheuner, D., et al. (2002). Activation of GCN2 in UV-irradiated cells inhibits translation. *Current Biology, 12*(15), 1279-1286. doi:doi.org/10.1016/S0960-9822(02)01037-0

Deshmukh, M., Tsay, Y. F., Paulovich, A. G., & Woolford, J. L. (1993). Yeast ribosomal protein L1 is required for the stability of newly synthesized 5S rRNA and the assembly of 60S ribosomal subunits. *Molecular and Cellular Biology, 13*(5), 2835-2845. doi:10.1128/MCB.13.5.2835

Dharmacon. (2019). Yeast ORF Collection. Retrieved from https://dharmacon.horizondiscovery.com/cdnas-and-orfs/non-mammalian-cdnas-and-orfs/yeast/yeast-orf-collection/

Dong, J., Qiu, H., Garcia-Barrio, M., Anderson, J., & Hinnebusch, A. G. (2000). Uncharged tRNA activates GCN2 by displacing the protein kinase moiety from a bipartite tRNA-binding domain. *Molecular Cell, 6*(2), 269-279. doi:doi.org/10.1016/S1097-2765(00)00028-9

Foiani, M., Cigan, A. M., Paddon, C. J., Harashima, S., & Hinnebusch, A. G. (1991). GCD2, a translational repressor of the GCN4 gene, has a general function in the initiation of protein synthesis in Saccharomyces cerevisiae. *Molecular and Cellular Biology, 11*(6), 13. doi:10.1128/MCB.11.6.3203

Garcia-Barrio, M., Dong, J., Ufano, S., & Hinnebusch, A. G. (2000). Association of GCN1–GCN20 regulatory complex with the N-terminus of eIF2α kinase GCN2 is required for GCN2 activation. *The EMBO Journal, 19*(8), 1887-1899. doi:10.1093/emboj/19.8.1887

Gavin, A.-C., Aloy, P., Grandi, P., Krause, R., Boesche, M., Marzioch, M., et al. (2006). Proteome survey reveals modularity of the yeast cell machinery. *Nature, 440*(7084), 631. doi:10.1038/nature04532

Gontarek, R. R., Li, H., Nurse, K., & Prescott, C. D. (1998). The N terminus of eukaryotic translation elongation factor 3 interacts with 18 S rRNA and 80 S ribosomes. *Journal of Biological Chemistry, 273*(17), 10249-10252. doi:10.1074/jbc.273.17.10249

Hao, S., Sharp, J. W., Ross-Inta, C. M., McDaniel, B. J., Anthony, T. G., Wek, R. C., et al. (2005). Uncharged tRNA and Sensing of Amino Acid Deficiency in Mammalian Piriform Cortex. *Science, 307*(5716), 1776. doi:10.1126/science.1104882

Hinnebusch, A. G. (1997). Translational Regulation of Yeast GCN4 : A window on factors that control initiator-tRNA binding to the ribosome. *Journal of Biological Chemistry, 272*(35), 21661-21664. doi:10.1074/jbc.272.35.21661

Hinnebusch, A. G. (2005). Translational regulation of GCN4 and the general amino acid control of yeast. *Annual Review of Microbiology, 59*, 407-450. doi:10.1146/annurev.micro.59.031805.133833

Inglis, A. J., Masson, G. R., Shao, S., Perisic, O., McLaughlin, S. H., Hegde, R. S., et al. (2019). Activation of GCN2 by the ribosomal P-stalk. *Proceedings of the National Academy of Sciences,* 201813352. doi:doi.org/10.1073/pnas.1813352116

Ito, K., Honda, T., Suzuki, T., Miyoshi, T., Murakami, R., Yao, M., et al. (2014). Molecular insights into the interaction of the ribosomal stalk protein with elongation factor 1α. *Nucleic Acids Research, 42*(22), 14042-14052. doi:10.1093/nar/gku1248

Jiménez-Díaz, A., Remacha, M., Ballesta, J. P., & Berlanga, J. J. (2013). Phosphorylation of initiation factor eIF2 in response to stress conditions is mediated by acidic ribosomal P1/P2 proteins in Saccharomyces cerevisiae. *PloS One, 8*(12), e84219. doi:10.1371/journal.pone.0084219

Jochmann, V. A. (2014). *Identification of ribosomal proteins that are necessary for fully activating the protein kinase Gcn2: A thesis presented in partial fulfilment of the requirements for the degree of Master of Science in Biochemistry at Massey University, Albany, New Zealand.* Massey University.

Kiel, M. C., & Ganoza, M. C. (2001). Functional interactions of an Escherichia coli ribosomal ATPase. *European Journal of Biochemistry, 268*(2), 278-286. doi:10.1046/j.1432-1033.2001.01873.x

Kimball, S. R. (1999). Eukaryotic initiation factor eIF2. *The International Journal of Biochemistry & Cell Biology, 31*(1), 25-29. doi:10.1016/S1357-2725(98)00128-9

Koromilas, A. E. (2015). Roles of the translation initiation factor eIF2α serine 51 phosphorylation in cancer formation and treatment. *Biochimica et Biophysica Acta (BBA)-Gene Regulatory Mechanisms, 1849*(7), 871-880. doi:10.1016/j.bbagrm.2014.12.007

Kubota, H., Sakaki, Y., & Ito, T. (2000). GI domain-mediated association of the eukaryotic initiation factor 2α kinase GCN2 with its activator GCN1 is required for general amino acid control in budding yeast. *Journal of Biological Chemistry, 275*(27), 20243-20246. doi:10.1074/jbc.C000262200

Lageix, S., Rothenburg, S., Dever, T. E., & Hinnebusch, A. G. (2014). Enhanced interaction between pseudokinase and kinase domains in Gcn2 stimulates eIF2α phosphorylation in starved cells. *PLoS Genetics, 10*(5), e1004326. doi:10.1371/journal.pgen.1004326

Lee, S. J., Ramesh, R., de Boor, V., Gebler, J. M., Silva, R. C., & Sattlegger, E. (2017). Cost-effective and rapid lysis of Saccharomyces cerevisiae cells for quantitative western blot analysis of proteins, including phosphorylated eIF2α. *Yeast, 34*(9), 371-382. doi:10.1002/yea.3239

Lee, S. J., Swanson, M. J., & Sattlegger, E. (2015). Gcn1 contacts the small ribosomal protein Rps10, which is required for full activation of the protein kinase Gcn2. *Biochemical Journal, 466*(3), 547-559. doi:10.1042/BJ20140782

Ma, T., Trinh, M. A., Wexler, A. J., Bourbon, C., Gatti, E., Pierre, P., et al. (2013). Suppression of eIF2α kinases alleviates Alzheimer's disease–related plasticity and memory deficits. *Nature Neuroscience, 16,* 1299. doi:10.1038/nn.3486

Martín-Marcos, P., Hinnebusch, A. G., & Tamame, M. (2007). Ribosomal protein L33 is required for ribosome biogenesis, subunit joining, and repression of GCN4 translation. *Molecular and Cellular Biology, 27*(17), 5968-5985. doi:10.1128/MCB.00019-07

Marton, M., Crouch, D., & Hinnebusch, A. (1993). GCN1, a translational activator of GCN4 in Saccharomyces cerevisiae, is required for phosphorylation of eukaryotic translation initiation factor 2 by protein kinase GCN2. *Molecular and Cellular Biology, 13*(6), 3541-3556. doi:10.1128/MCB.13.6.3541

Marton, M. J., Vazquez de Aldana, C. R., Qiu, H., Chakraburtty, K., & Hinnebusch, A. G. (1997). Evidence that GCN1 and GCN20, translational regulators of GCN4, function on elongating ribosomes in activation of eIF2alpha kinase GCN2. *Molecular and Cellular Biology, 17*(8), 4474-4489. doi:10.1128/MCB.17.8.4474

Mateyak, M. K., & Kinzy, T. G. (2010). eEF1A: thinking outside the ribosome. *Journal of Biological Chemistry, 285*(28), 21209-21213. doi:10.1074/jbc.R110.113795

Mateyak, M. K., Pupek, J. K., Garino, A. E., Knapp, M. C., Colmer, S. F., Kinzy, T. G., et al. (2018). Demonstration of translation elongation factor 3 activity from a non-fungal species, Phytophthora infestans. *PloS One, 13*(1), e0190524. doi:doi.org/10.1371/journal.pone.0190524

Maurin, A.-C., Jousse, C., Averous, J., Parry, L., Bruhat, A., Cherasse, Y., et al. (2005). The GCN2 kinase biases feeding behavior to maintain amino acid homeostasis in omnivores. *Cell Metabolism, 1*(4), 273-277. doi:doi.org/10.1016/j.cmet.2005.03.004

Moritz, M., Pulaski, B., & Woolford, J. (1991). Assembly of 60S ribosomal subunits is perturbed in temperature-sensitive yeast mutants defective in ribosomal protein L16. *Molecular and Cellular Biology, 11*(11), 5681-5692. doi:10.1128/MCB.11.11.5681

Murakami, R., Singh, C. R., Morris, J., Tang, L., Harmon, I., Takasu, A., et al. (2018). The interaction between the ribosomal stalk proteins and translation initiation factor 5B

promotes translation initiation. *Molecular and Cellular Biology, 38*(16), e00067-00018. doi:10.1128/MCB.00067-18

Murchie, M.-J., & Leader, D. P. (1978). Codon-specific interaction of uncharged transfer-RNA with eukaryotic ribosomes. *Biochimica et Biophysica Acta (BBA) - Nucleic Acids and Protein Synthesis, 520*(1), 233-236. doi:dx.doi.org/10.1016/0005-2787(78)90024-2

National Center for Biotechnology Information. (2019). Amitrole, CID=1639. Retrieved from https://pubchem.ncbi.nlm.nih.gov/compound/1639

Padyana, A. K., Qiu, H., Roll-Mecak, A., Hinnebusch, A. G., & Burley, S. K. (2005). Structural basis for autoinhibition and mutational activation of eukaryotic initiation factor 2α protein kinase GCN2. *Journal of Biological Chemistry, 280*(32), 29289-29299. doi:10.1074/jbc.M504096200

Qiu, H., Garcia-Barrio, M. T., & Hinnebusch, A. G. (1998). Dimerization by translation initiation factor 2 kinase GCN2 is mediated by interactions in the C-terminal ribosome-binding region and the protein kinase domain. *Molecular and Cellular Biology, 18*(5), 2697-2711. doi:10.1128/MCB.18.5.2697

Qiu, H., Hu, C., Dong, J., & Hinnebusch, A. G. (2002). Mutations that bypass tRNA binding activate the intrinsically defective kinase domain in GCN2. *Genes & Development, 16*(10), 1271-1280. doi:10.1101/gad.979402

Rakesh, R., Krishnan, R., Sattlegger, E., & Srinivasan, N. (2017). Recognition of a structural domain (RWDBD) in Gcn1 proteins that interacts with the RWD domain containing proteins. *Biology Direct, 12*(1), 12. doi:doi.org/10.1186/s13062-017-0184-3

Ramirez, M., Wek, R. C., & Hinnebusch, A. G. (1991). Ribosome association of GCN2 protein kinase, a translational activator of the GCN4 gene of Saccharomyces cerevisiae. *Molecular and Cellular Biology, 11*(6), 3027-3036. doi:10.1128/mcb.11.6.3027

Remacha, M., Jimenez-Diaz, A., Santos, C., Briones, E., Zambrano, R., Gabriel, M. R., et al. (1995). Proteins P1, P2, and P0, components of the eukaryotic ribosome stalk. New structural and functional aspects. *Biochemistry and Cell Biology, 73*(11-12), 959-968. doi:doi.org/10.1139/o95-103

Saccharomyces Genome Database. (2019, March 17). The Saccharomyces Genome Database. Retrieved from https://www.yeastgenome.org/

Sattlegger, E., & Hinnebusch, A. G. (2000). Separate domains in GCN1 for binding protein kinase GCN2 and ribosomes are required for GCN2 activation in amino acid-starved cells. *The EMBO Journal, 19*(23), 6622-6633. doi:10.1093/emboj/19.23.6622
Sattlegger, E., & Hinnebusch, A. G. (2000). Separate domains in GCN1 for binding protein kinase GCN2 and ribosomes are required for GCN2 activation in amino acid-starved cells. *The EMBO Journal, 19*(23), 6622-6633. doi:10.1093/emboj/19.23.6622
Sattlegger, E., & Hinnebusch, A. G. (2005). Polyribosome binding by GCN1 is required for full activation of eukaryotic translation initiation factor 2α kinase GCN2 during amino acid starvation. *Journal of Biological Chemistry, 280*(16), 16514-16521. doi:10.1074/jbc.M414566200

Spahn, C. M., Beckmann, R., Eswar, N., Penczek, P. A., Sali, A., Blobel, G., et al. (2001). Structure of the 80S ribosome from Saccharomyces cerevisiae—tRNA-ribosome and subunit-subunit interactions. *Cell, 107*(3), 373-386. doi:doi.org/10.1016/S0092-8674(01)00539-6

Tanzawa, T., Kato, K., Girodat, D., Ose, T., Kumakura, Y., Wieden, H.-J., et al. (2018). The C-terminal helix of ribosomal P stalk recognizes a hydrophobic groove of elongation factor 2 in a novel fashion. *Nucleic Acids Research, 46*(6), 3232-3244. doi:10.1093/nar/gky115

Trinh, M. A., & Klann, E. (2013). Translational control by eIF2α kinases in long-lasting synaptic plasticity and long-term memory. *Neurobiology of Learning and Memory, 105*, 93-99. doi:doi.org/10.1016/j.nlm.2013.04.013

Underwood, M. R., & Fried, H. M. (1990). Characterization of nuclear localizing sequences derived from yeast ribosomal protein L29. *The EMBO Journal, 9*(1), 91-99. doi:https://doi.org/10.1002/j.1460-2075.1990.tb08084.x

van Beekvelt, C. A., de Graaff-Vincent, M., Faber, A. W., van't Riet, J., Venema, J., & Raué, H. A. (2001). All three functional domains of the large ribosomal subunit protein L25 are required for both early and late pre-rRNA processing steps in Saccharomyces cerevisiae. *Nucleic Acids Research, 29*(24), 5001-5008. doi:10.1093/nar/29.24.5001

Vazquez de Aldana, C. R., Marton, M. J., & Hinnebusch, A. G. (1995). GCN20, a novel ATP binding cassette protein, and GCN1 reside in a complex that mediates activation of the eIF-2 alpha kinase GCN2 in amino acid-starved cells. *The EMBO Journal, 14*(13), 3184. doi:doi.org/10.1002/j.1460-2075.1995.tb07321.x

Vilardell, J., & Warner, J. R. (1997). Ribosomal protein L32 of Saccharomyces cerevisiae influences both the splicing of its own transcript and the processing of rRNA. *Molecular and Cellular Biology, 17*(4), 1959-1965. doi:10.1128/MCB.17.4.1959

Visweswaraiah, J., Lageix, S., Castilho, B. A., Izotova, L., Kinzy, T. G., Hinnebusch, A. G., et al. (2011). Evidence that eukaryotic translation elongation factor 1A (eEF1A) binds the Gcn2 protein C terminus and inhibits Gcn2 activity. *Journal of Biological Chemistry, 286*(42), 36568-36579. doi:10.1074/jbc.M111.248898

Visweswaraiah, J., Lee, S. J., Hinnebusch, A. G., & Sattlegger, E. (2012). Overexpression of eukaryotic translation elongation factor 3 impairs Gcn2 protein activation. *Journal of Biological Chemistry, 287*(45), 37757-37768. doi:10.1038/protex. 2011.2122

Wang, Y., Ning, Y., Alam, G. N., Jankowski, B. M., Dong, Z., Nör, J. E., et al. (2013). Amino acid deprivation promotes tumor angiogenesis through the GCN2/ATF4 pathway. *Neoplasia, 15*(8), 989-997. doi:10.1593/neo.13262

Wek, R. C., Ramirez, M., Jackson, B. M., & Hinnebusch, A. G. (1990). Identification of positive-acting domains in GCN2 protein kinase required for translational activation of GCN4 expression. *Molecular and Cellular Biology, 10*(6), 2820-2831. doi:10.1128/MCB.10.6.2820

Wek, S. A., Zhu, S., & Wek, R. C. (1995). The histidyl-tRNA synthetase-related sequence in the eIF-2 alpha protein kinase GCN2 interacts with tRNA and is required for activation in response to starvation for different amino acids. *Molecular and Cellular Biology, 15*(8), 4497-4506. doi:10.1128/MCB.15.8.4497

Wendrich, T. M., Blaha, G., Wilson, D. N., Marahiel, M. A., & Nierhaus, K. H. (2002). Dissection of the mechanism for the stringent factor RelA. *Molecular Cell, 10*(4), 779-788. doi:10.1016/S1097-2765(02)00656-1

Won, S., Eidenschenk, C., Arnold, C. N., Siggs, O. M., Sun, L., Brandl, K., et al. (2012). Increased susceptibility to DNA virus infection in mice with a GCN2 mutation. *Journal of Virology, 86*(3), 1802-1808. doi:10.1128/JVI.05660-11

Yang, R., Wek, S. A., & Wek, R. C. (2000). Glucose limitation induces GCN4Translation by activation of Gcn2 protein kinase. *Molecular and Cellular Biology, 20*(8), 2706-2717. doi:10.1128/MCB.20.8.2706-2717.2000

Ye, J., Kumanova, M., Hart, L. S., Sloane, K., Zhang, H., De Panis, D. N., et al. (2010). The GCN2-ATF4 pathway is critical for tumour cell survival and proliferation in response to nutrient deprivation. *The EMBO Journal, 29*(12), 2082-2096. doi:10.1038/emboj.2010.81

Yusupov, M. M., Yusupova, G. Z., Baucom, A., Lieberman, K., Earnest, T. N., Cate, J., et al. (2001). Crystal structure of the ribosome at 5.5 Å resolution. *Science, 292*(5518), 883-896. doi:10.1126/science.1060089

Zhu, S., & Wek, R. C. (1998). Ribosome-binding domain of eukaryotic initiation factor-2 kinase GCN2 facilitates translation control. *Journal of Biological Chemistry, 273*(3), 1808-1814. doi:10.1074/jbc.273.3.1808

Chapter 5 Appendix

A)

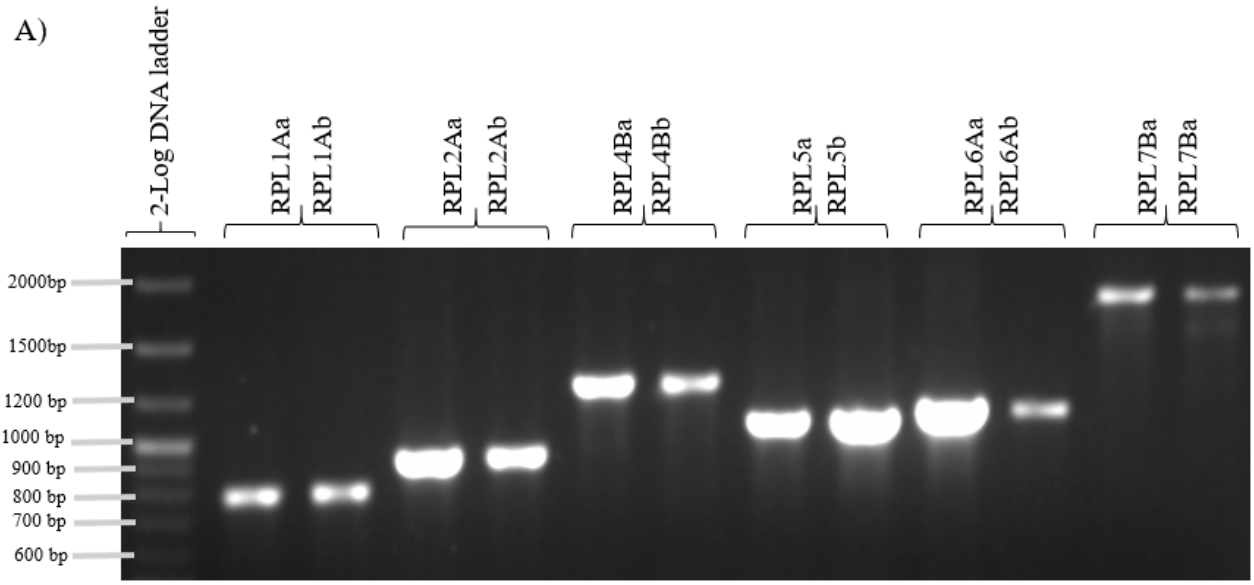

B)

yeast containing plasmid borne gene as indicated	Expected size (bp)	Found size (bp)
RPL1A	807	a) 789 b) 812
RPL2A	918	a) 932 b) 954
RPL4B	1242	a) 1287 b) 1302
RPL5	1047	a) 1102 b) 1088
RPL6A	684	a) 1129 b) 1171
RPL7B	888	a) 1898 b) 1923

Figure 5.1 *PCR analysis of RPL strains 1Aa to 7Bb, confirming the correct size for the respective RPL genes in the BG1805 vector*

A) shown is PCR analysis of RPL strains 1Aa to 7Bb loaded on a 1% agarose gel (lanes 2-11) compared against 2-log DNA ladder (lane 1) B) Table indicates the expected size in bp of each respective RPL gene and the found size obtained by molecular weight analysis using image lab software

A)

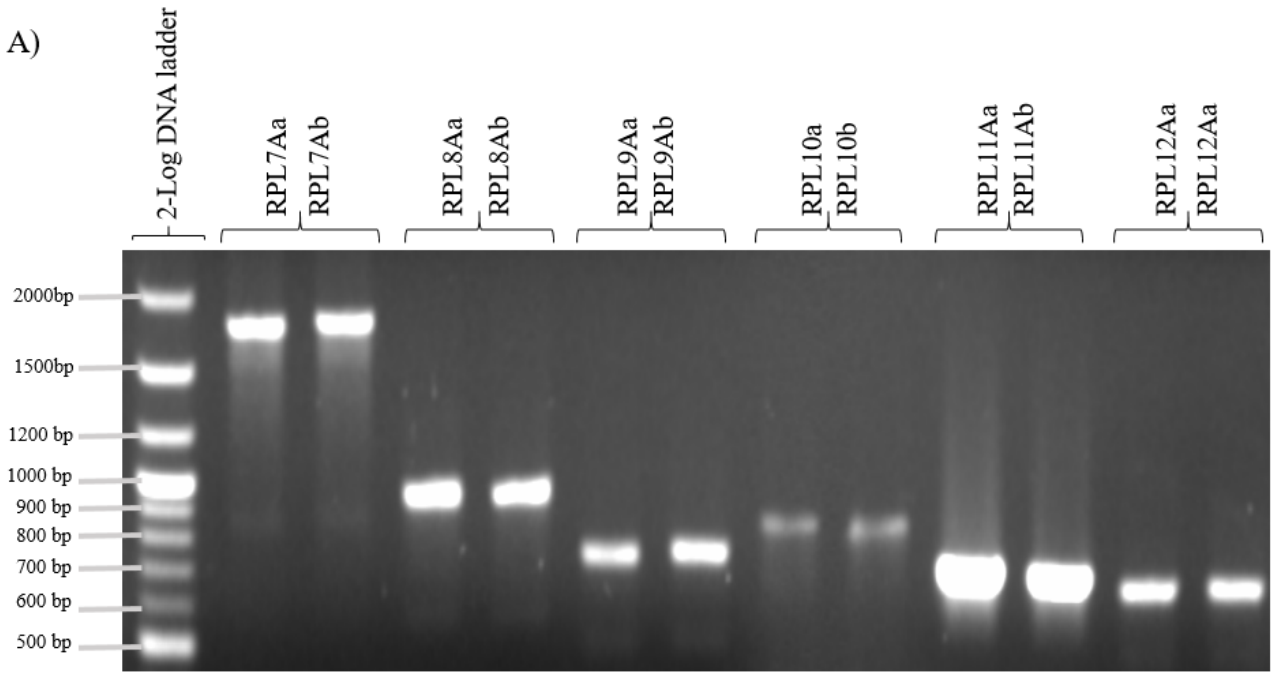

B)

yeast containing plasmid borne gene as indicated	Expected size (bp)	Found size (bp)
RPL7A	888	a) 1772 b) 1799
RPL8A	924	a) 941 b) 956
RPL9A	729	a) 736 b) 736
RPL10	819	a) 827 b) 814
RPL11A	678	a) 665 b) 643
RPL12A	651	a) 610 b) 610

Figure 5.2 *PCR analysis of RPL strains 7Aa to 12Ab, confirming the correct size for the respective RPL genes in the BG1805 vector*

A) shown is PCR analysis of RPL strains 7Aa to 12Ab loaded on a 1% agarose gel (lanes 2-11) compared against 2-log DNA ladder (lane 1) B) Table indicates the expected size in bp of each respective RPL gene and the found size obtained by molecular weight analysis using image lab software

A)

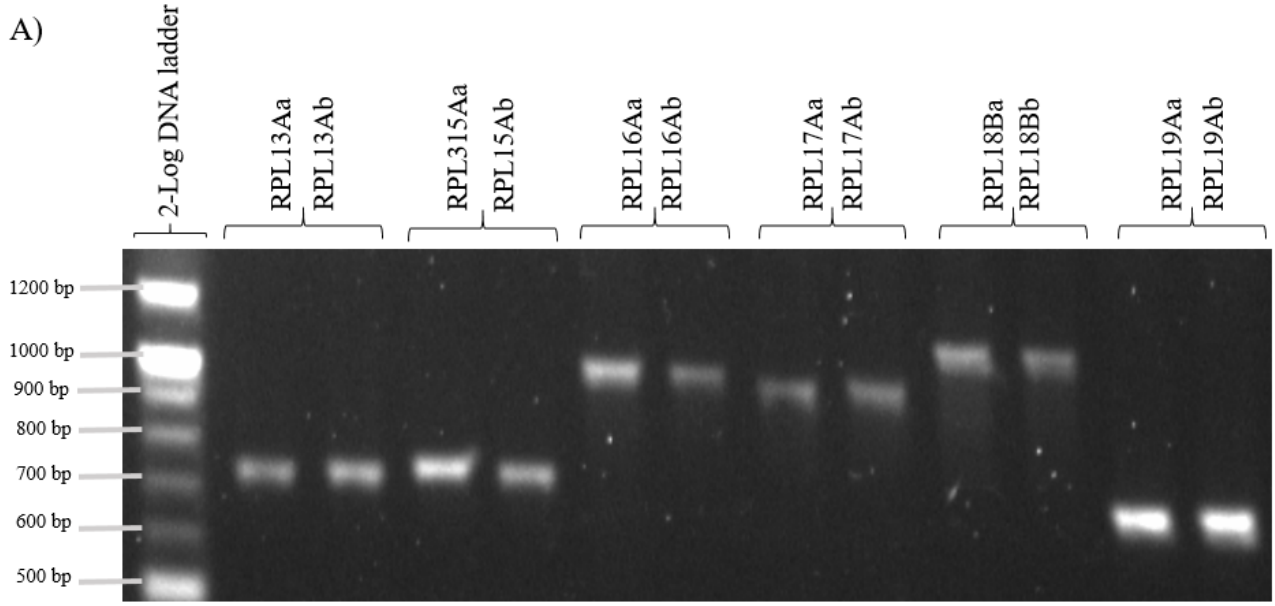

B)

yeast containing plasmid borne gene as indicated	Expected size (bp)	Found size (bp)
RPL13Aa and RPL13Ab	753	a) 725 b) 719
RPL15Aa and RPL15Ab	768	a) 725 b) 713
RPL16A and RPL16Ab	753	a) 971 b) 962
RPL17A and RPL17Ab	708	a) 917 b) 908
RPL18Ba and RPL18Bb	714	a) 1016 b) 1008
RPL19Aa and RPL19Ab	723	a) 618 b) 618

Figure 5.3 *PCR analysis of RPL strains 13Aa to 19Ab, confirming the correct size for the respective RPL genes in the BG1805 vector*

A) shown is PCR analysis of RPL strains 13Aa to 19Ab loaded on a 1% agarose gel (lanes 2-11) compared against 2-log DNA ladder (lane 1) B) Table indicates the expected size in bp of each respective RPL gene and the found size obtained by molecular weight analysis using image lab software.

A)

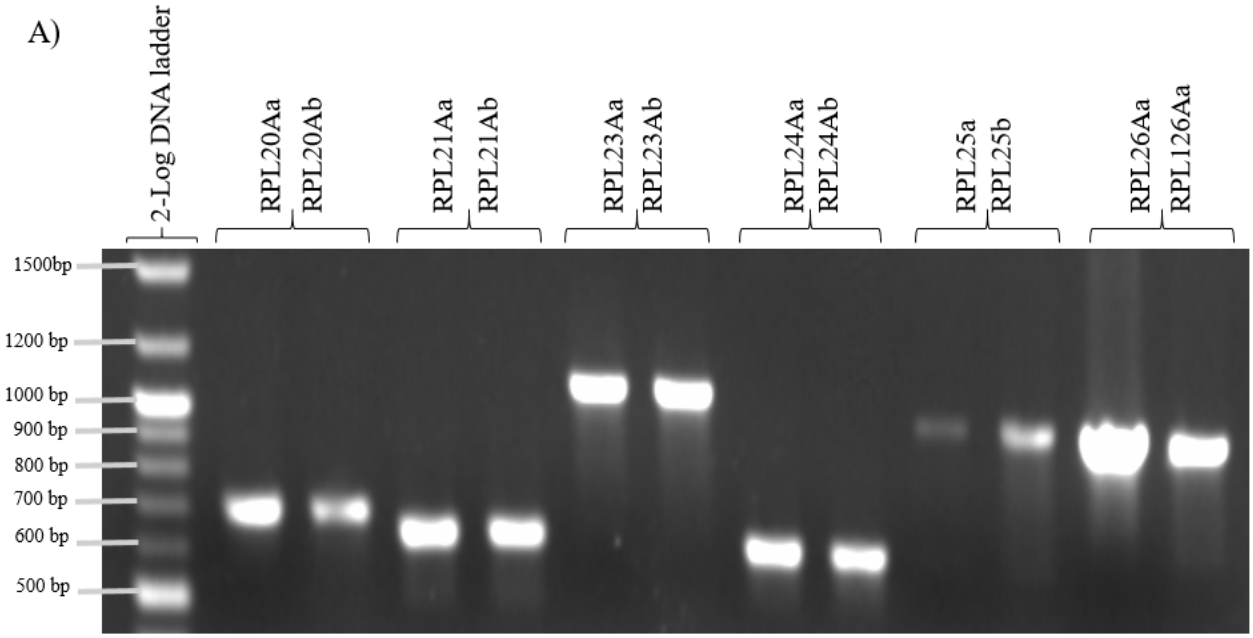

B)

Yeast containing plasmid borne gene as indicated	Expected size (bp)	Found size (bp)
RPL20A	672	a) 681 b) 681
RPL21A	636	a) 634 b) 634
RPL23A	567	a) 1049 b) 1024
RPL24A	621	a) 591 b) 573
RPL25	582	a) 924 b) 900
RPL26A	537	a) 861 b) 848

Figure 5.4 *PCR analysis of RPL strains 20Aa to 26Ab, confirming the correct size for the respective RPL genes in the BG1805 vector*

A) shown is PCR analysis of RPL strains 20Aa to 26Ab loaded on a 1% agarose gel (lanes 2-11) compared against 2-log DNA ladder (lane 1) B) Table indicates the expected size in bp of each respective RPL gene and the found size obtained by molecular weight analysis using image lab software

A)

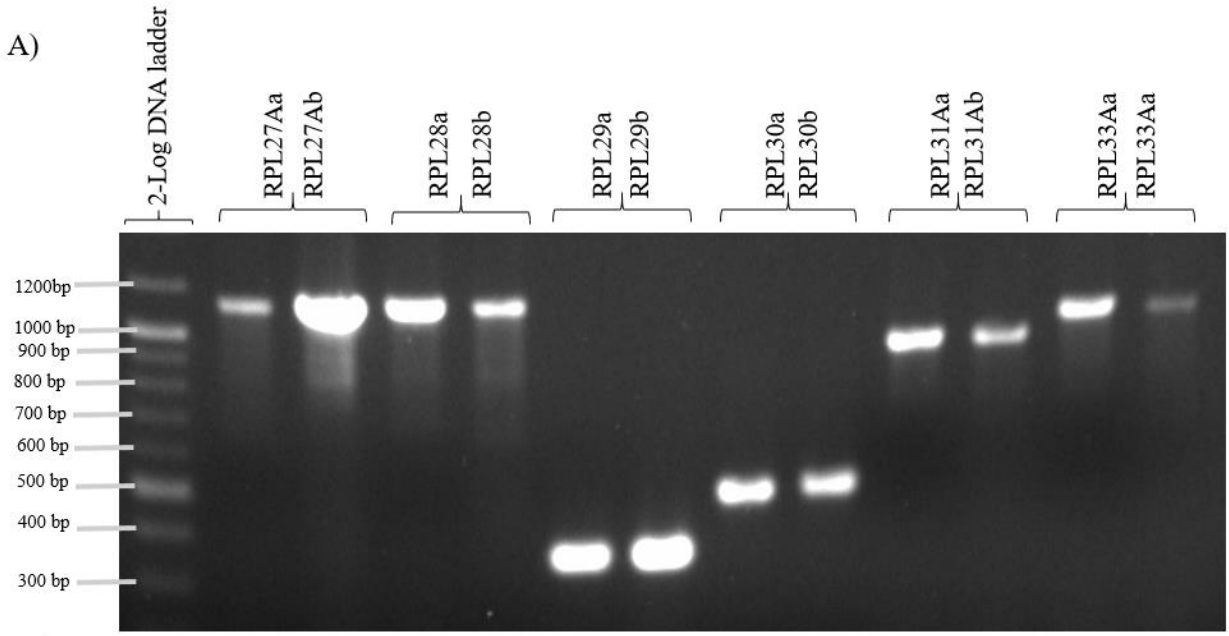

B)

yeast containing plasmid borne gene as indicated	Expected size (bp)	Found size (bp)
RPL27A	564	a) 1095 b) 1073
RPL28	603	a) 1073 b) 1073
RPL29	333	a) 334 b) 344
RPL30	471	a) 474 b) 487
RPL31A	595	a) 929 b) 938
RPL33A	477	a) 1041 b) 1062

Figure 5.5 *PCR analysis of RPL strains 27Aa to 33Ab, confirming the correct size for the respective RPL genes in the BG1805 vector*

A) shown is PCR analysis of RPL strains 27Aa to 33Ab loaded on a 1% agarose gel (lanes 2-11) compared against 2-log DNA ladder (lane 1) B) Table indicates the expected size in bp of each respective RPL gene and the found size obtained by molecular weight analysis using image lab software.

A)

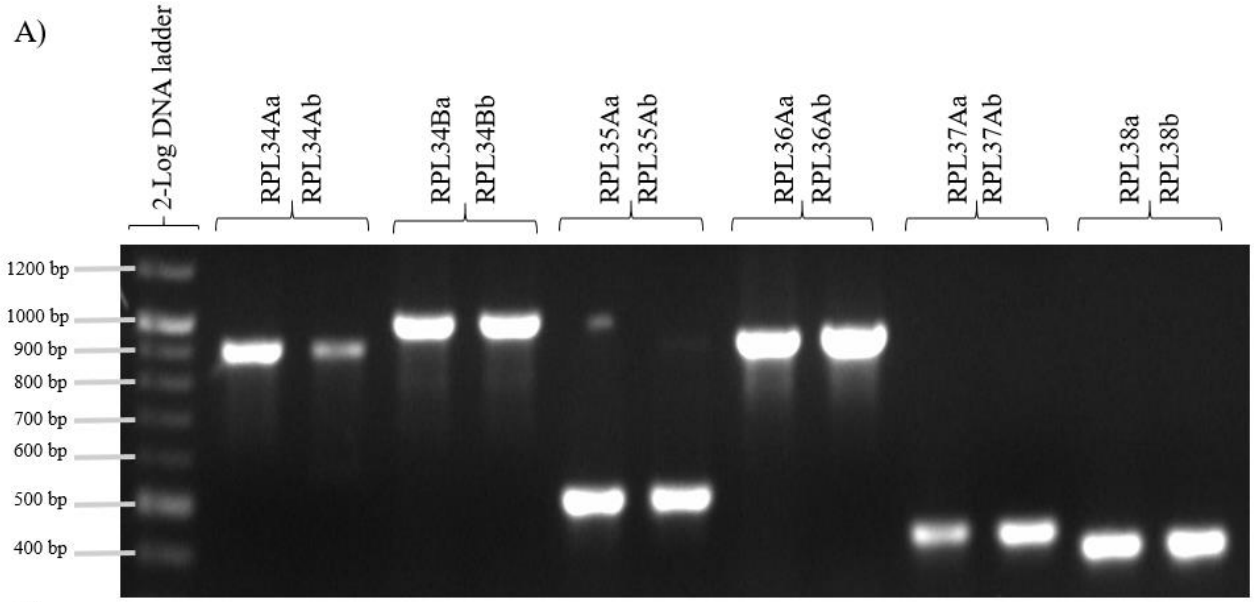

B)

yeast containing plasmid borne gene as indicated	Expected size (bp)	Found size (bp)
RPL34Aa and RPL34Ab	519	a) 900 b) 910
RPL34Ba and RPL34Bb	519	a) 976 b) 988
RPL35A and RPL35Ab	516	a) 506 b) 506
RPL36A and RPL36Ab	456	a) 921 b) 932
RPL37A and RPL37Ab	420	a) 441 b) 441
RPL38 and RPL38b	390	a) 417 b) 417

Figure 5.6 *PCR analysis of RPL strains 34Aa to 38b, confirming the correct size for the respective RPL genes in the BG1805 vector*

A) shown is PCR analysis of RPL strains 34Aa to 38b loaded on a 1% agarose gel (lanes 2-11) compared against 2-log DNA ladder (lane 1) B) Table indicates the expected size in bp of each respective RPL gene and the found size obtained by molecular weight analysis using image lab software.

A)

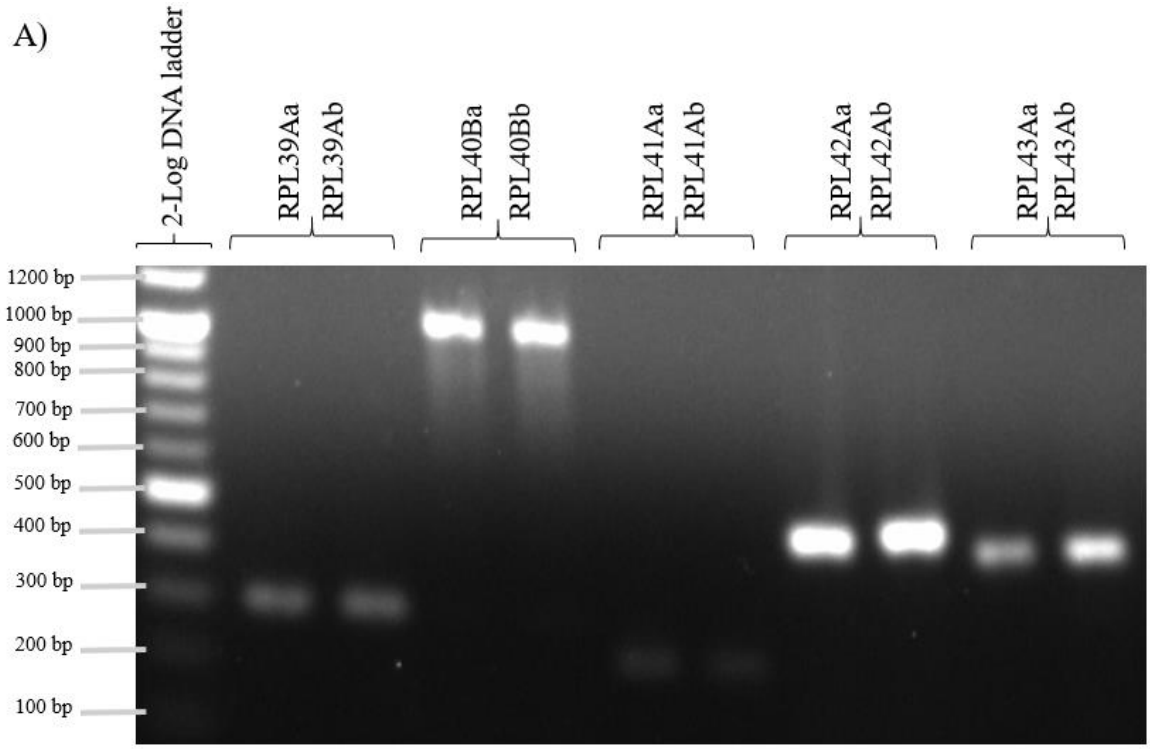

B)

yeast containing plasmid borne gene as indicated	Expected size (bp)	Found size (bp)
RPL39Aa and RPL39Ab	309	a) 283 b) 272
RPL40A and RPL40Ab	540	a) 1000 b) 968
RPL41A and RPL41Ab	231	a) 173 b) 168
RPL42A and RPL42Ab	474	a) 388 b) 400
RPL43A and RPL43Ab	432	a) 371 b) 371

Figure 5.7 *PCR analysis of RPL strains 39Aa to 43Ab, confirming the correct size for the respective RPL genes in the BG1805 vector*

A) shown is PCR analysis of RPL strains 39Aa to 43Ab loaded on a 1% agarose gel (lanes 2-11) compared against 2-log DNA ladder (lane 1) B) Table indicates the expected size in bp of each respective RPL gene and the found size obtained by molecular weight analysis using image lab software.

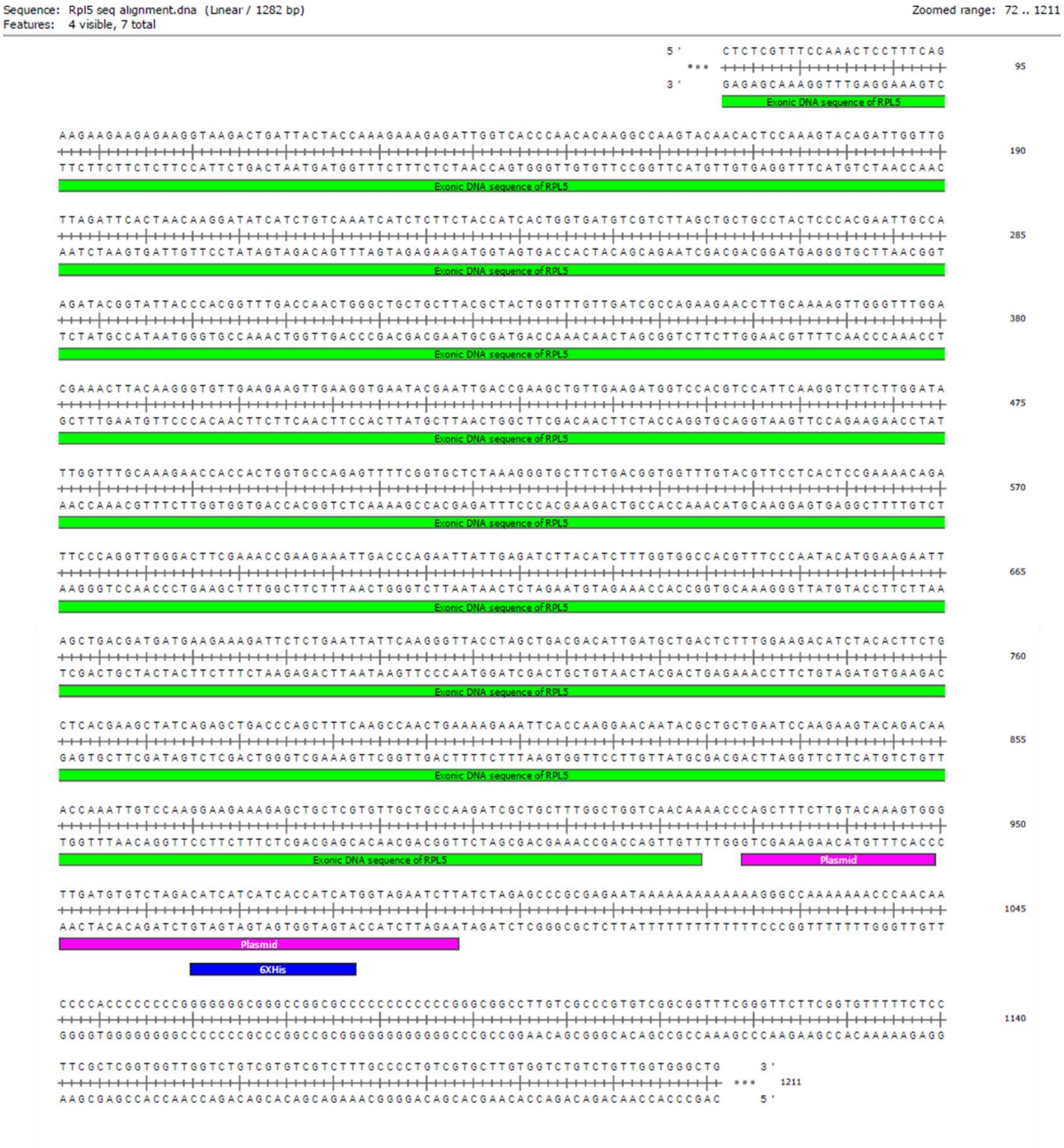

Figure 5.8 *Sequencing analysis of RPL5*

Analysis of sequencing obtained commercially of PCR product obtained from colony PCR of Rpl5 overexpressing yeast strain. Sequence shown is that obtained from commercial sequencing. Alignment with Green "Exonic DNA of RPL5" indicates matching of sequence to the sequence obtained from the yeast genome database. Other features sequenced including areas flanking the ORF from the BG1805 plasmid are also indicated.

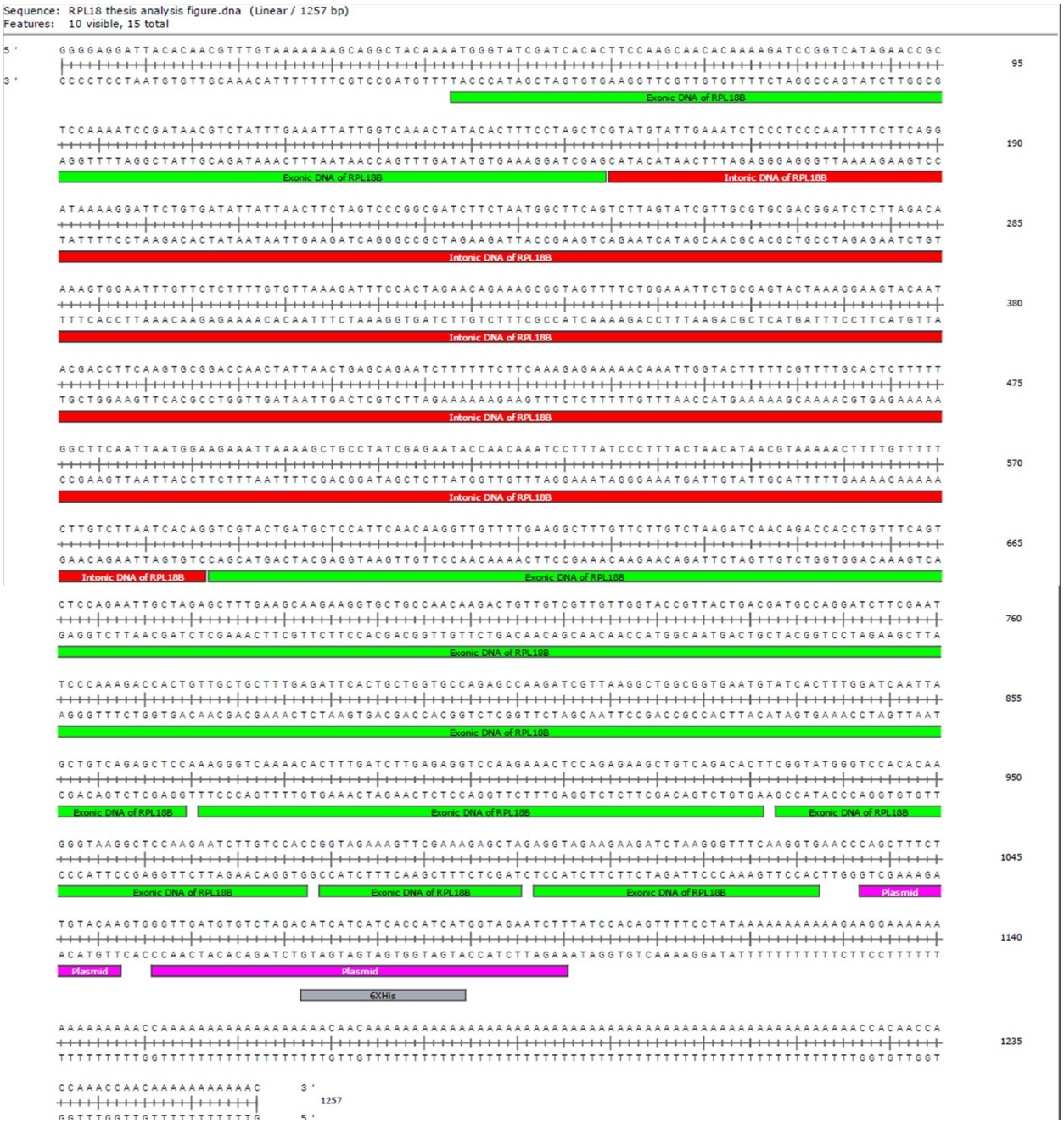

Figure 5.9 *Sequencing analysis of RPL18*

Analysis of sequencing obtained commercially of PCR product obtained from colony PCR of Rpl5 overexpressing yeast strain. Sequence shown is that obtained from commercial sequencing. Alignment with Green "Exonic DNA of RPL5" indicates matching of sequence to the sequence obtained from the yeast genome database. Note the matching to intronic DNA sequence also retrieved from the yeast genome database. Other features sequenced including areas flanking the ORF from the BG1805 plasmid are also indicated.

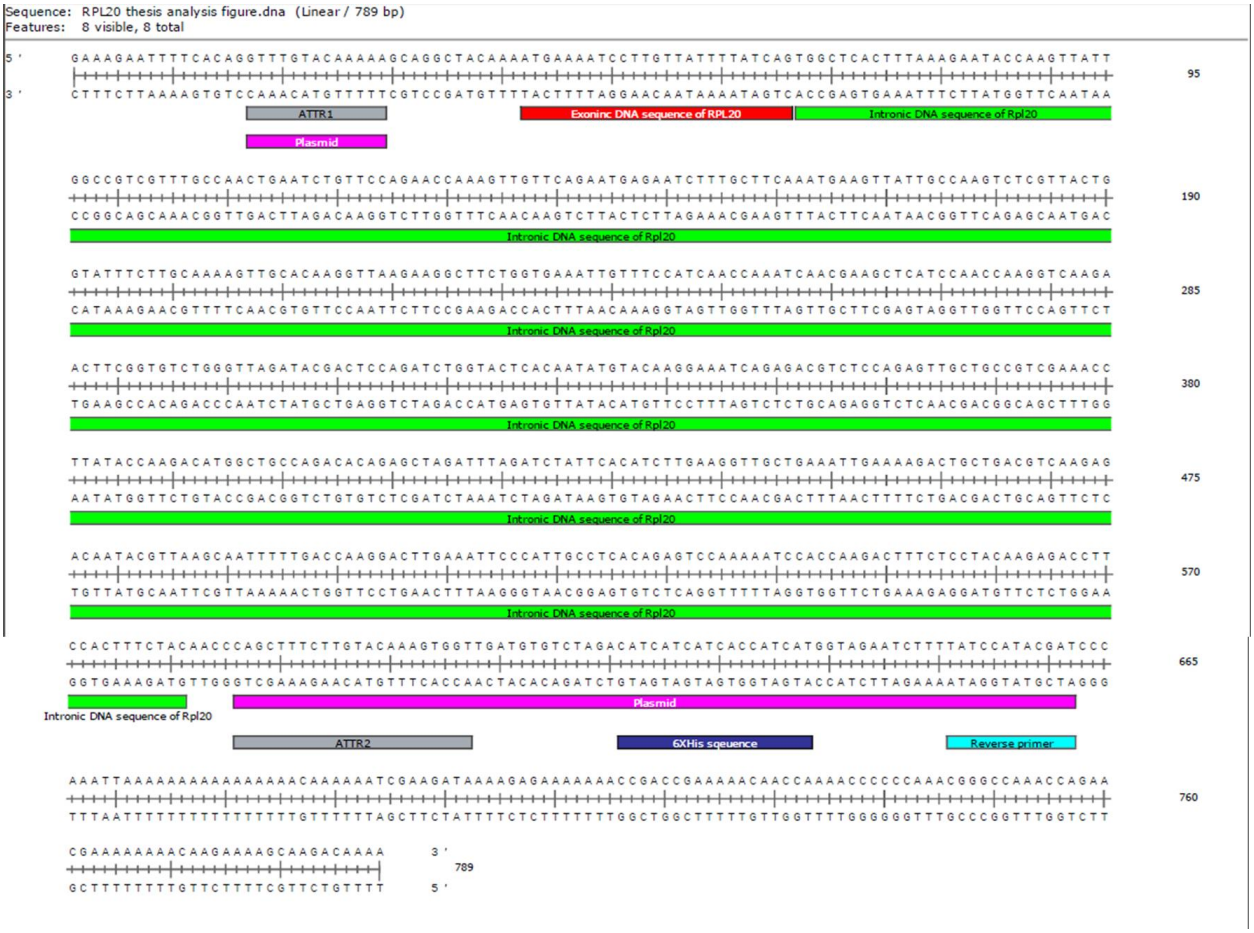

Figure 5.10 *Sequencing analysis of RPL20*

Analysis of sequencing obtained commercially of PCR product obtained from colony PCR of Rpl5 overexpressing yeast strain. Sequence shown is that obtained from commercial sequencing. Alignment with Green "Exonic DNA of RPL5" indicates matching of sequence to the sequence obtained from the yeast genome database. Note the matching to intronic DNA sequence also retrieved from the yeast genome database. Other features sequenced including areas flanking the ORF from the BG1805 plasmid are also indicated.

Figure 5.11 *Sequencing analysis of RPL30*

Analysis of sequencing obtained commercially of PCR product obtained from colony PCR of Rpl5 overexpressing yeast strain. Sequence shown is that obtained from commercial sequencing. Alignment with Green "Exonic DNA of RPL5" indicates matching of sequence to the sequence obtained from the yeast genome database. Other features sequenced including areas flanking the ORF from the BG1805 plasmid are also indicated.

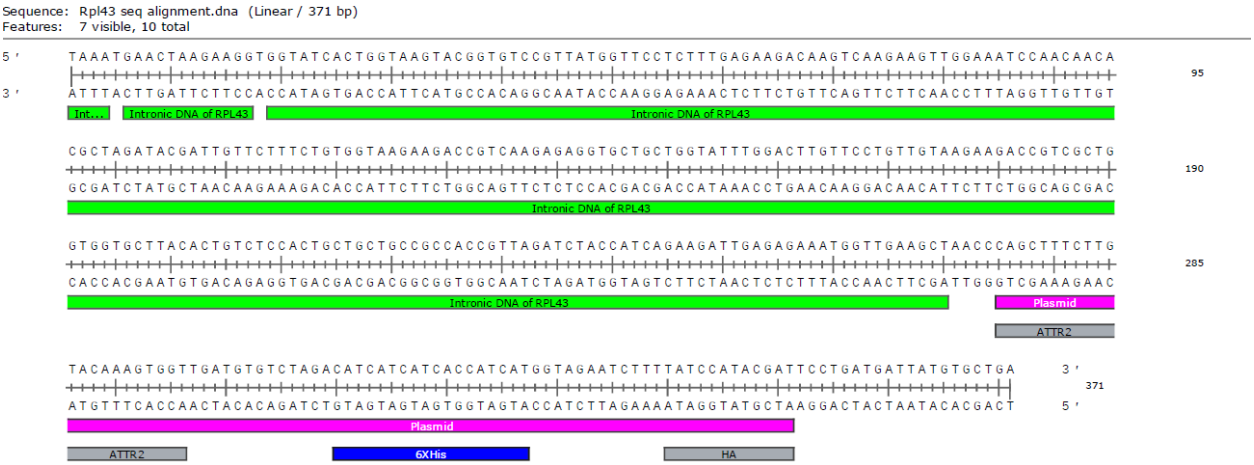

Figure 5.12 *Sequencing analysis of RPL43*

Analysis of sequencing obtained commercially of PCR product obtained from colony PCR of Rpl5 overexpressing yeast strain. Sequence shown is that obtained from commercial sequencing. Alignment with Green "Exonic DNA of RPL5" indicates matching of sequence to the sequence obtained from the yeast genome database. Other features sequenced including areas flanking the ORF from the BG1805 plasmid are also indicated.

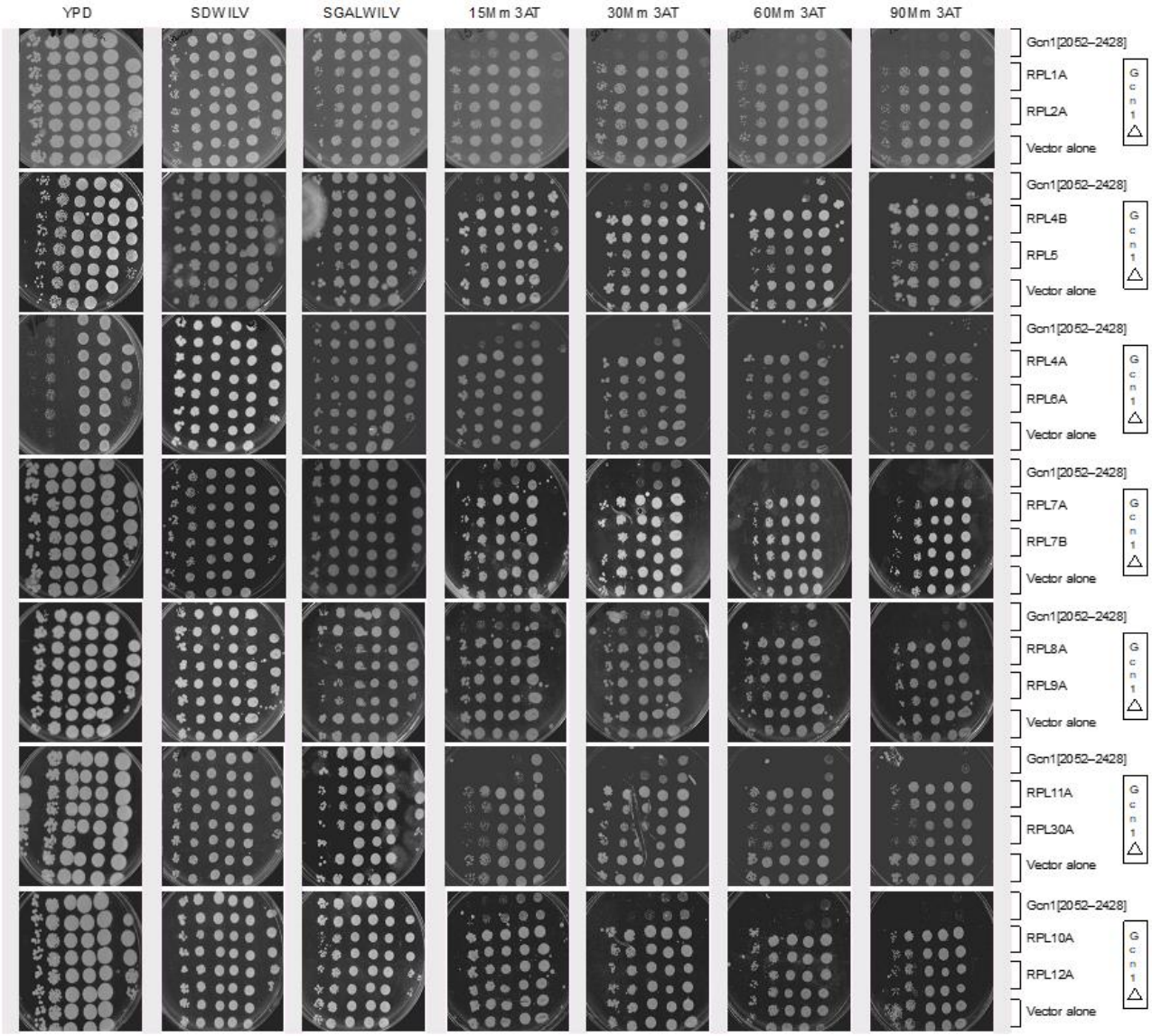

Figure 5.13 *Semi quantitative growth assays for yeast strains overexpressing large ribosomal proteins 1a to 12a*

Semi-quantitative growth assays were performed with the yeast strains as indicated to the right of the images. Plates used included YPD, SD (SDWILV) with glucose, SGal (SGALWILV) and SD with galactose containing four different concentrations of 3AT (15 mM, 30 mM, 60 mM, 90 mM). Strains assessed for growth on starvation media are indicated to the right of the figure. Stains displaying sensitivity to amino acid starvation when a Rpl is overexpressed are indicated by bold red text to the right of the Figure.

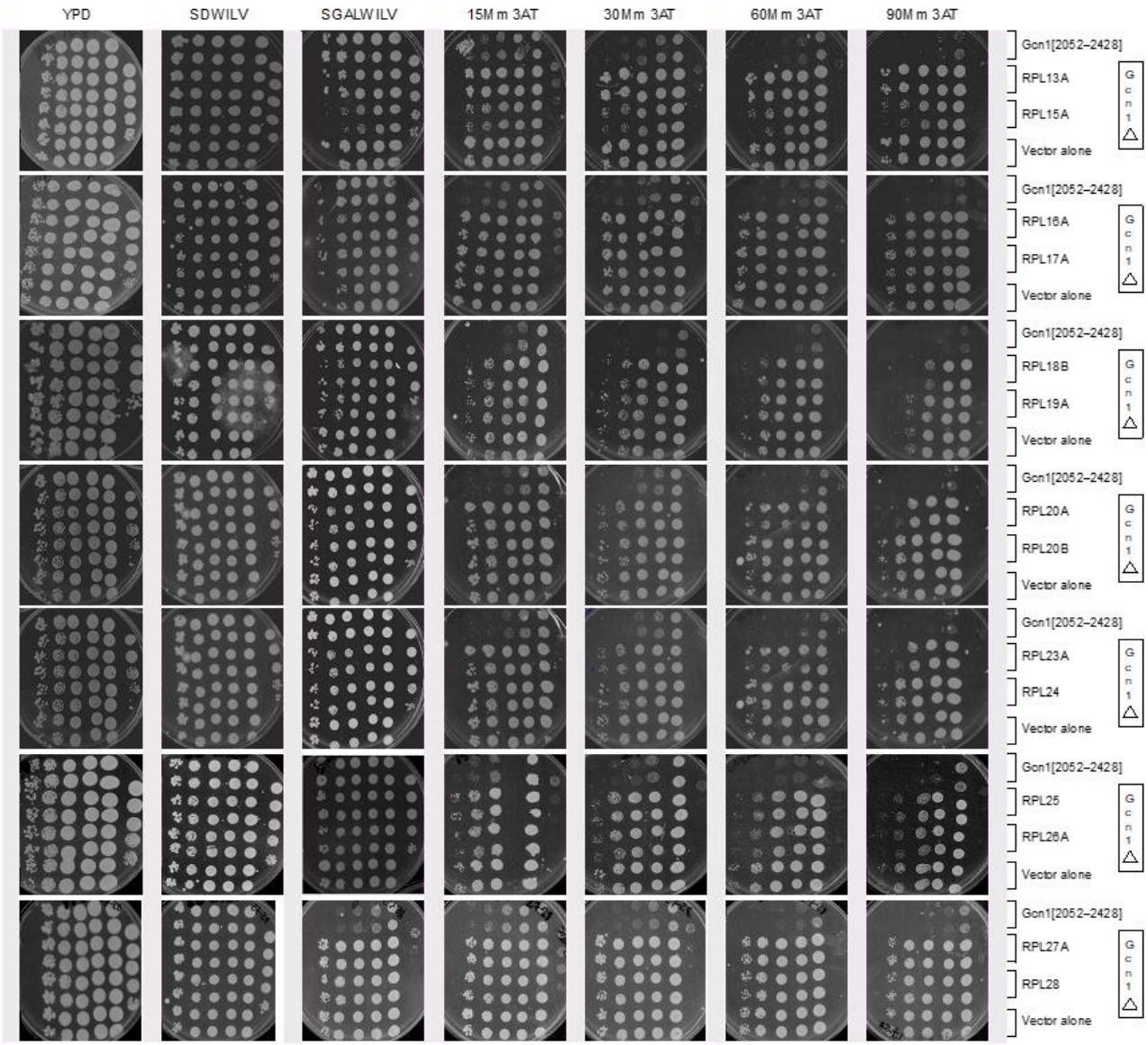

Figure 5.14 *Semi quantitative growth assays for yeast strains overexpressing large ribosomal proteins 13a to 28*

Semi-quantitative growth assays were performed with the yeast strains as indicated to the right of the images. Plates used included YPD, SD (SDWILV) with glucose, SGal (SGALWILV) and SD with galactose containing four different concentrations of 3AT (15 mM, 30 mM, 60 mM, 90 mM). Strains assessed for growth on starvation media are indicated to the right of the figure. Stains displaying sensitivity to amino acid starvation when a Rpl is overexpressed are indicated by bold red text to the right of the Figure.

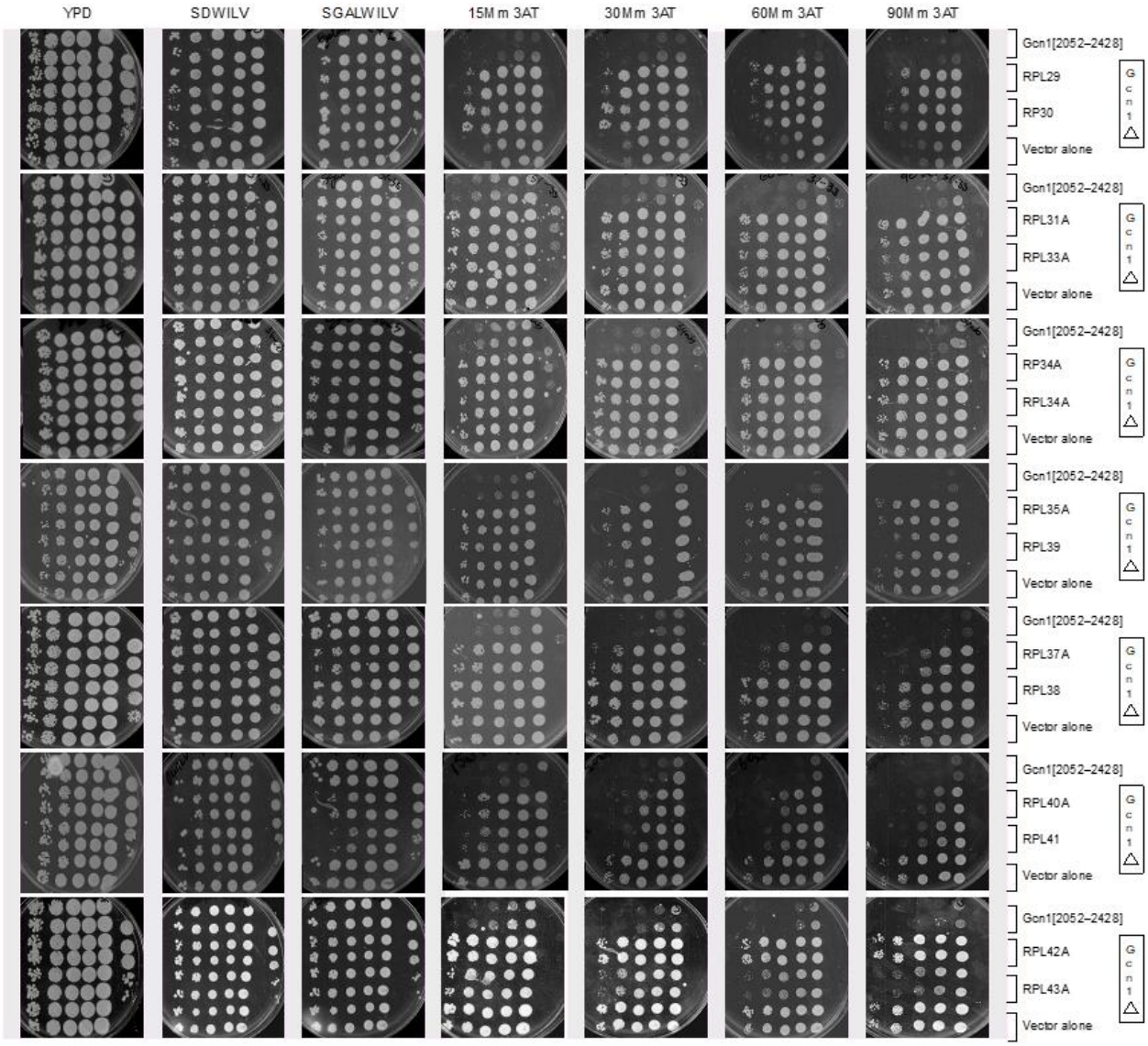

Figure 5.15 *Semi quantitative growth assays for yeast strains overexpressing large ribosomal proteins 29 to 43a*

Semi-quantitative growth assays were performed with the yeast strains as indicated to the right of the images. Plates used included YPD, SD (SDWILV) with glucose, SGal (SGALWILV) and SD with galactose containing four different concentrations of 3AT (15 mM, 30 mM, 60 mM, 90 mM). Strains assessed for growth on starvation media are indicated to the right of the figure. Stains displaying sensitivity to amino acid starvation when a Rpl is overexpressed are indicated by bold red text to the right of the Figure.

Table 5.1 *Scoring of growth from semi quantitative growth assays from figures 5.13-5.15*

Set	Strain	SGalWILV	15mM 3AT	30mM 3AT	60mM 3AT	90mM 3AT
1	Rpl1A	42.5	42.5	40	40	37.5
	Rpl2A	42.5	42.5	40	40	37.5
	gcn1[2052–2428]	42.5	20	12.5	10.5	7.5
	Vector	45	45	42.5	42.5	40
2	Rpl4A	45	45	45	45	45
	Rpl5	40	40	37.5	37.7	37.5
	gcn1[2052–2428]	45	25	17.5	12.5	2.5
	Vector	45	45	45	45	45
3	Rpl4B	45	50	45	45	45
	Rpl6A	45	45	45	45	45
	gcn1[2052–2428]	45	5	5	0	0
	Vector	45	45	45	45	45
4	Rpl7A	45	42.5	42.5	37.5	37.5
	Rpl7B	45	42.5	42.5	37.5	37.5
	gcn1[2052–2428]	45	10	7.5	5	2.5
	Vector	45	42.5	42.5	37.5	37.5
5	Rpl8A	47.5	45	45	45	45
	Rpl9A	47.5	45	45	45	45
	gcn1[2052–2428]	47.5	25	25	7.5	0.5
	Vector	47.5	45	42.5	42.5	42.5
6	Rpl11A	45	45	45	45	42.5
	Rpl30	45	45	45	40	30
	gcn1[2052–2428]	45	10	20	7.5	0
	Vector	45	45	45	45	45
7	Rpl10A	45	45	45	42.5	40
	Rpl12A	45	45	45	42.5	40
	gcn1[2052–2428]	45	15	15	2.5	0
	Vector	45	45	45	42.5	40
8	Rpl13A	45	45	45	45	45
	Rpl15A	37.5	37.5	37.5	35	35
	gcn1[2052–2428]	45	25	12.5	5	2.5
	Vector	45	45	45	45	45
9	Rpl16A	42.5	45	45	45	45
	Rpl17A	42.5	45	45	45	45
	gcn1[2052–2428]	42.5	25	15	12.5	2.5
	Vector	42.5	45	45	45	45
10	Rpl18A	42.5	40	37.5	35	25
	Rpl19A	42.5	40	37.5	37.5	35
	gcn1[2052–2428]	45	7.5	5	5	0
	Vector	45	40	37.5	37.5	35

11	Rpl20A	45	45	42.5	42.5	30
	Rpl21A	45	45	42.5	42.5	42.5
	gcn1[2052–2428]	45	10	7.5	5	0
	Vector	47.5	45	42.5	42.5	42.5
12	Rpl23A	45	45	45	42.5	42.5
	Rpl24A	47.5	47.5	47.5	47.7	47.5
	gcn1[2052–2428]	40	22.5	7.5	5	5
	Vector	47.5	47.5	47.5	47.5	47.5
13	Rpl25A	45	45	45	45	42.5
	Rpl26A	45	45	45	45	42.5
	gcn1[2052–2428]	45	22.5	7.5	5	5
	Vector	45	45	45	45	42.5
14	Rpl27A	47.5	47.5	47.5	45	42.5
	Rpl28A	47.5	47.5	47.5	45	42.5
	gcn1[2052–2428]	47.5	22.5	7.5	5	2.5
	Vector	47.5	47.5	47.5	45	42.5
15	Rpl29A	42.5	42.5	42.5	40	37.5
	Rpl30A	42.5	40	35	30	22.5
	gcn1[2052–2428]	42.5	20	2.5	0	0
	Vector	42.5	42.5	42.5	42.5	40
16	Rpl31A	45	45	45	45	42.5
	Rpl33A	45	45	45	45	42.5
	gcn1[2052–2428]	40	22	7.5	5	2.5
	Vector	45	45	45	45	42.5
17	Rpl34A	45	45	45	45	42.5
	Rpl34B	45	45	45	45	42.5
	gcn1[2052–2428]	40	22	7.5	5	2.5
	Vector	45	45	45	45	42.5
18	Rpl35A	45	45	42.5	42.5	42.5
	Rpl39	42.5	45	40	37.5	30
	gcn1[2052–2428]	45	7.5	7.5	2.5	0
	Vector	45	45	42.5	42.5	42.5
19	Rpl37A	40	40	37.5	30	27.5
	Rpl38A	50	47.5	45	40	35
	gcn1[2052–2428]	50	20	5	5	2.5
	Vector	50	47.5	45	40	35
20	Rpl40A	35	42.5	32.5	30	22.5
	Rpl41A	30	40	35	32.5	27.5
	gcn1[2052–2428]	45	10	7.5	5	2.5
	Vector	42.5	50	45	42.5	40
21	Rpl42B	45	45	45	45	37.5
	Rpl43A	45	42.5	35	30	25
	gcn1[2052–2428]	45	10	7.5	5	2.5
	Vector	45	45	45	45	37.7

Table 5.2 *Growth scores for 3AT plates in Table 5.1, adjusted by dividing the original growth score by that of the control plate and then diving that ratio by the ratio of the WT control plate*

Strain	15mM 3AT	30mM 3AT	60mM 3AT	90mM 3AT
Rpl1A	1.0000	0.9965	0.9965	0.9926
Rpl2A	1.0000	0.9965	0.9965	0.9926
Rpl4A	1.0000	1.0000	1.0000	1.0000
Rpl5	1.0000	0.9375	0.9425	0.9375
Rpl4B	1.1111	1.0000	1.0000	1.0000
Rpl6A	1.0000	1.0000	1.0000	1.0000
Rpl7A	1.0000	1.0000	1.0000	1.0000
Rpl7B	1.0000	1.0000	1.0000	1.0000
Rpl8A	1.0000	1.0588	1.0588	1.0588
Rpl9A	1.0000	1.0588	1.0588	1.0588
Rpl11A	1.0000	1.0000	1.0000	0.9444
Rpl10A	1.0000	1.0000	1.0000	1.0000
Rpl12A	1.0000	1.0000	1.0000	1.0000
Rpl13A	1.0000	1.0000	1.0000	1.0000
Rpl15A	1.0000	1.0000	0.9333	0.9333
Rpl16A	1.0000	1.0000	1.0000	1.0000
Rpl17A	1.0000	1.0000	1.0000	1.0000
Rpl18A	1.0588	1.0588	0.9882	0.7563
Rpl19A	1.0588	1.0588	1.0588	1.0588
Rpl20A	1.0556	1.0556	1.0556	0.7451
Rpl21A	1.0556	1.0556	1.0556	1.0556
Rpl23A	1.0000	1.0000	0.9444	0.9444
Rpl24A	1.0000	1.0000	1.0042	1.0000
Rpl25a	1.0000	1.0000	1.0000	1.0000
Rpl26a	1.0000	1.0000	1.0000	1.0000
Rpl27A	1.0000	1.0000	1.0000	1.0000
Rpl28A	1.0000	1.0000	1.0000	1.0000
Rpl29A	1.0588	1.0588	0.9412	0.9375
Rpl30	1.0000	1.0000	0.8889	0.6667
Rpl30A	0.9412	0.8235	0.7059	0.5625
Rpl31A	1.0000	1.0000	1.0000	1.0000
Rpl33A	1.0000	1.0000	1.0000	1.0000
Rpl34A	1.0000	1.0000	1.0000	1.0000
Rpl34B	1.0000	1.0000	1.0000	1.0000
Rpl35A	1.0000	1.0000	1.0000	1.0000
Rpl37A	1.0526	1.0417	0.9375	0.9821
Rpl38A	1.0000	1.0000	1.0000	1.0000
Rpl39	1.0588	0.9965	0.9343	0.7474
Rpl40A	1.0321	0.8770	0.8571	0.6830
Rpl41A	1.1333	1.1019	1.0833	0.9740
Rpl42B	1.0000	1.0000	1.0000	0.9947
Rpl43A	0.9444	0.7778	0.6667	0.6631

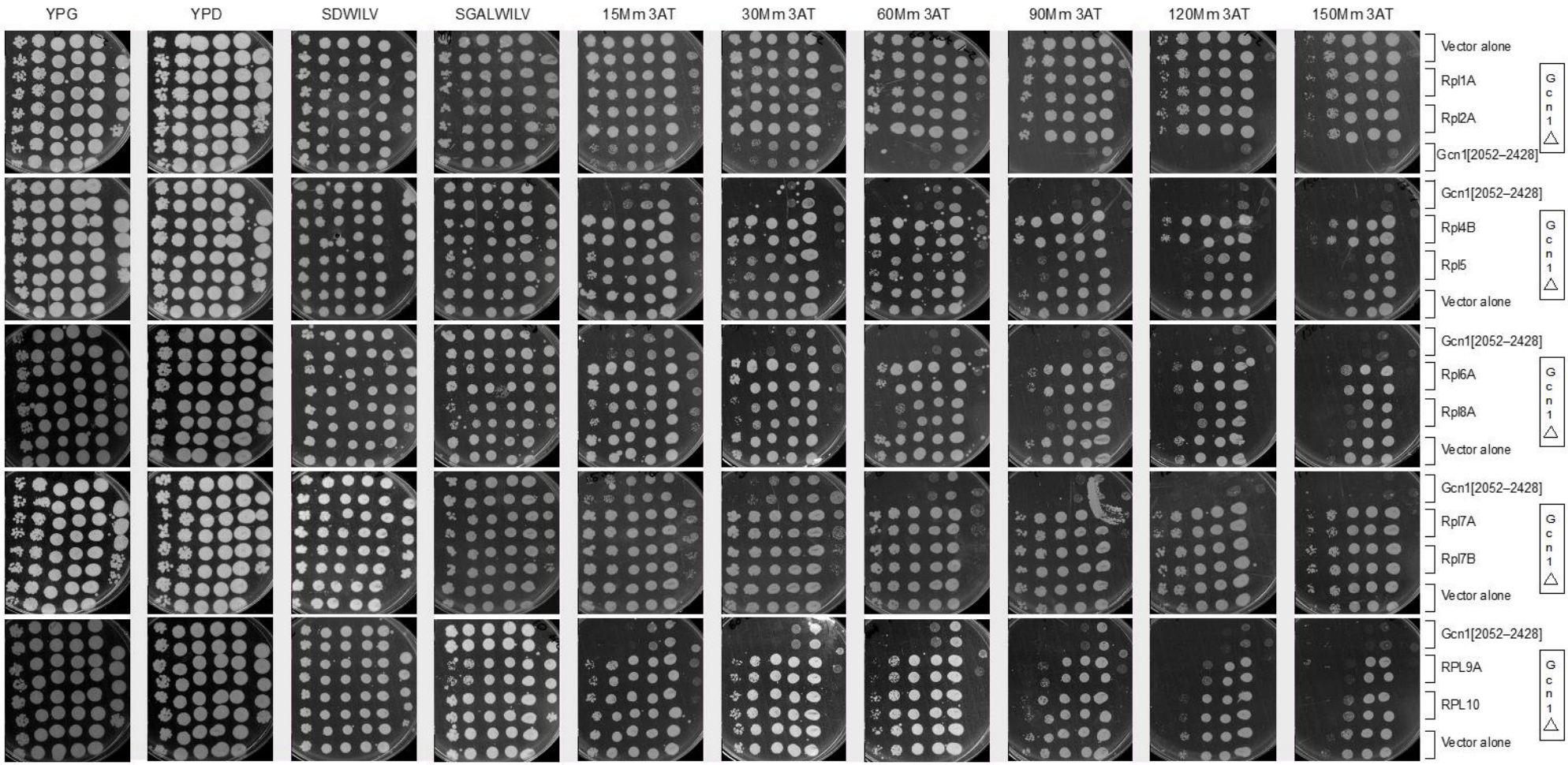

Figure 5.16 *Semi quantitative growth assays for yeast strains overexpressing Rpl1A to Rpl10*

Semi-quantitative growth assays were performed with the yeast strains as indicated to the right of the images. Plates used included YPD, SD (SDWILV) with glucose, SGal (SGALWILV) and SD with galactose containing six different concentrations of 3AT (15 mM, 30 mM, 60 mM, 90 mM, 120 mM and 150 mM 3AT). Strains assessed for growth on starvation media are indicated to the right of the figure. Stains displaying sensitivity to amino acid starvation when a Rpl is overexpressed are indicated by bold red text to the right of the Figure.

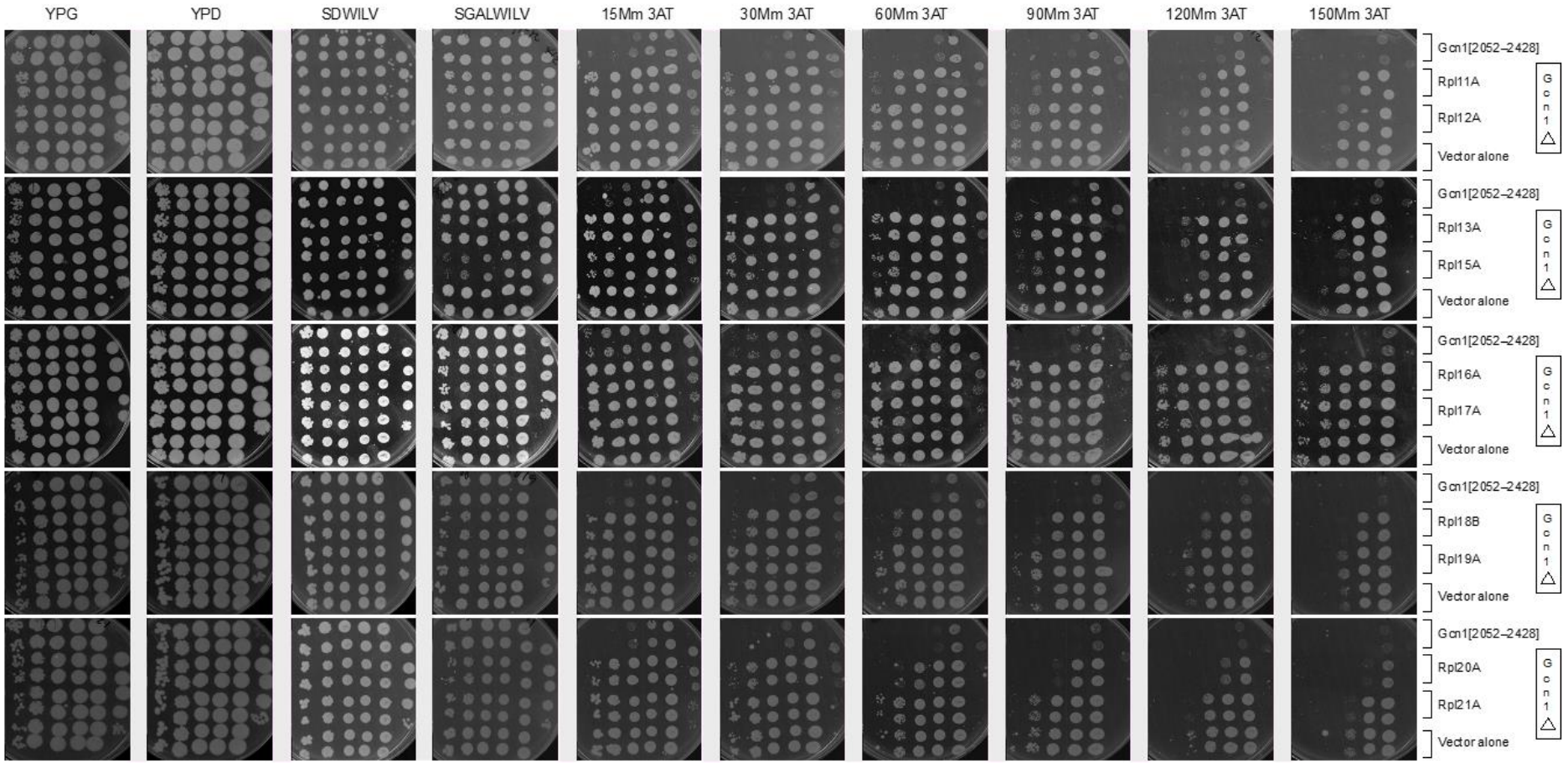

Figure 5.17 *Semi quantitative growth assays for yeast strains overexpressing Rpl11A to Rpl21A*

Semi-quantitative growth assays were performed with the yeast strains as indicated to the right of the images. Plates used included YPD, SD (SDWILV) with glucose, SGal (SGALWILV) and SD with galactose containing six different concentrations of 3AT (15 mM, 30 mM, 60 mM, 90 mM, 120 mM and 150 mM 3AT). Strains assessed for growth on starvation media are indicated to the right of the figure. Stains displaying sensitivity to amino acid starvation when a Rpl is overexpressed are indicated by bold red text to the right of the Figure.

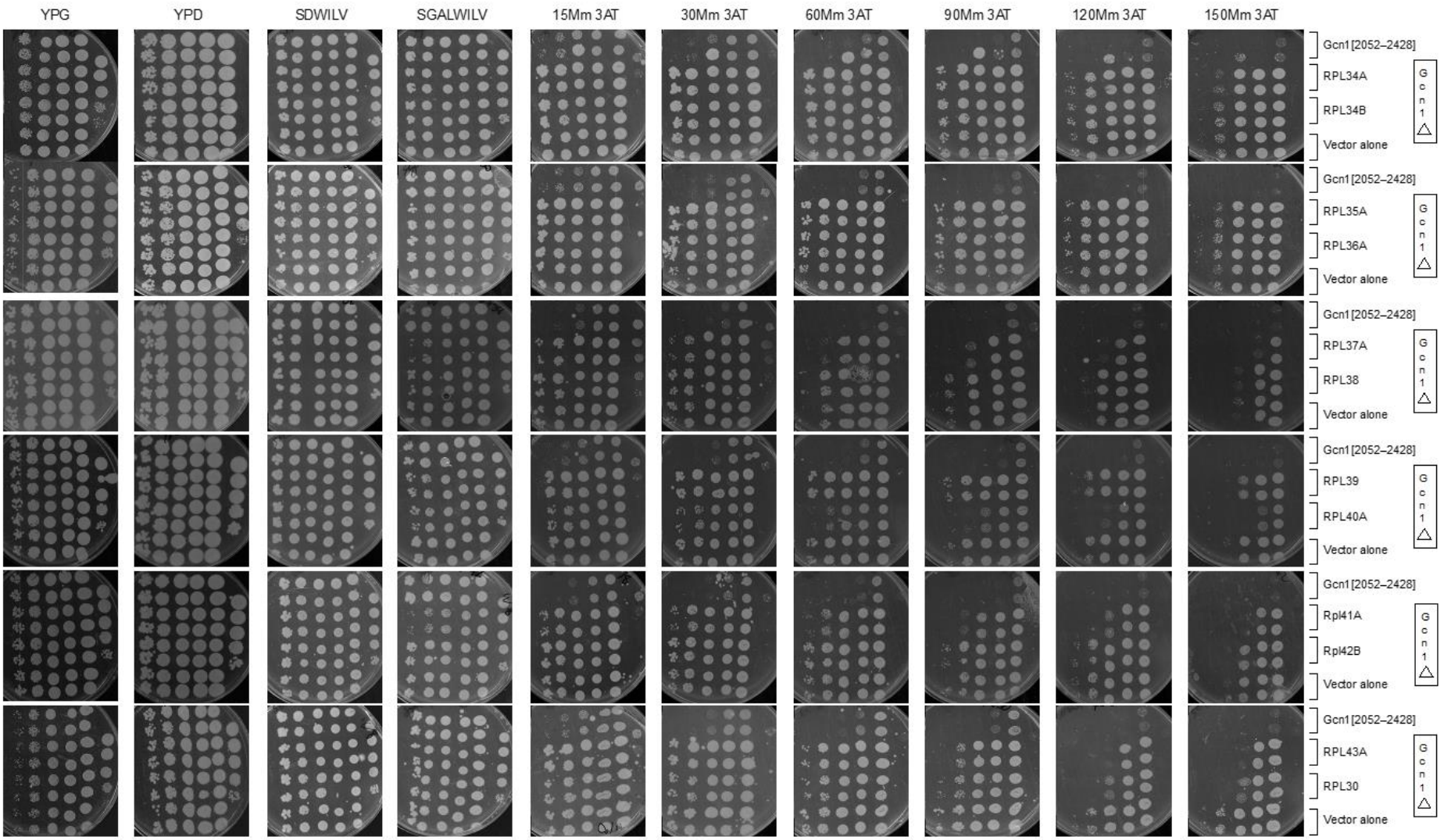

Figure 5.18 *Semi quantitative growth assays for yeast strains overexpressing Rpl34A to Rpl30*

Semi-quantitative growth assays were performed with the yeast strains as indicated to the right of the images. Plates used included YPD, SD (SDWILV) with glucose, SGal (SGALWILV) and SD with galactose containing six different concentrations of 3AT (15 mM, 30 mM, 60 mM, 90 mM, 120 mM and 150 mM 3AT). Strains assessed for growth on starvation media are indicated to the right of the figure. Stains displaying sensitivity to amino acid starvation when a Rpl is overexpressed are indicated by bold red text to the right of the Figure.

Table 5.3 *Scoring of growth from semi quantitative growth assays from figures 5.16-5.18*

Set	Strain	SGalWILV	15mM 3AT	30mM 3AT	60mM 3AT	90mM 3AT	120mM 3AT	150mM 3AT
1	Rpl1A	45	50	50	47.5	45	40	37.5
	Rpl2A	45	50	50	47.5	45	40	37.5
	gcn1[2052–2428]	50	35	30	12.5	10	5	12.5
	Vector	50	50	50	47.5	45	40	37.5
2	Rpl4B	49	50	50	48	47.5	45	38
	Rpl5	47	45	40	37.5	32	29	20
	gcn1[2052–2428]	50	22.5	17.5	15	10	5	1
	Vector	50	50	50	47.5	45	35	30
3	Rpl6A	50	50	48	45	42	32	28
	Rpl8A	43	44	40	35	31	25	21
	gcn1[2052–2428]	50	20	20	11	11	2	1
	Vector	50	50	48	45	42	34	30
4	Rpl7A	44	50	49	46	42	40	36
	Rpl7B	45	50	49	46	45	42	38
	gcn1[2052–2428]	5	37	27	11	10	2	2
	Vector	50	50	50	48	46	45	40
5	Rpl9A	39	40	39	37	32	23	21
	Rpl10	47	44	43	41	40	30.5	24
	gcn1[2052–2428]	50	18	15	13	12	2	1
	Vector	49	49	44	42	41	31	30
6	Rpl11A	47	47	42	40	31	29	21
	Rpl12A	48	49	49	47	40	34	28
	gcn1[2052–2428]	50	22	12	11	8	6	2
	Vector	50	49	49	48	42	38	30
7	Rpl13A	50	49	48	44	39	32	29
	Rpl15A	36	42	42	39	34	28	21
	gcn1[2052–2428]	50	23	15	11	10	5	2
	Vector	50	50	50	46	42	37	31
8	Rpl16A	46	50	50	48	46	44	39
	Rpl17A	47	50	48	49	46	44	39
	gcn1[2052–2428]	48	30	30	18	8	5	3
	Vector	48	50	50	49	48	44	39
9	Rpl18A	41	42	37	32	30	24	20
	Rpl19A	45	49	48	44	39	34	24
	gcn1[2052–2428]	48	22	19	14	10	2	1
	Vector	45	47	46	43	35	33	22
10	Rpl20A	41	42	38	30	21	15	10
	Rpl21A	46	46	42	40	35	31	21
	gcn1[2052–2428]	50	23	14	11	4	2	1

	Vector	50	49	42	40	35	32	24
11	Rpl23A	43	47	45	41	38	31	28
	Rpl24A	50	49	48	45	45	40	36
	gcn1[2052–2428]	50	34	22	12	11	8	2
	Vector	50	50	49	44	44	39	35
12	Rpl25	50	50	46	45	41	33	31
	Rpl26A	48	48	44	42	40	33	31
	gcn1[2052–2428]	50	33	10	10	10	1	1
	Vector	50	50	46	45	41	34	32
13	Rpl27A	48	50	50	50	50	45	43
	Rpl28	49	50	50	50	50	45	43
	gcn1[2052–2428]	50	40	37	15	12	8	2
	Vector	50	50	50	50	50	45	43
14	Rpl29	48	50	50	48	44	40	32
	Rpl30	48	45	43	37	34	28	22
	gcn1[2052–2428]	50	26	24	15	12	1	1
	Vector	49	50	50	49	45	42	36
15	Rpl31A	46	50	50	50	42	37	30
	Rpl33A	46	50	50	48	40	36	29
	gcn1[2052–2428]	50	30	20	12	3	2	1
	Vector	48	50	50	48	40	37	29
16	Rpl34A	50	50	50	48	45	40	32
	Rpl34B	50	50	49	48	45	40	32
	gcn1[2052–2428]	50	33	20	12	10	1	1
	Vector	50	50	49	48	45	40	32
17	Rpl35A	49	50	46	45	42	39	31
	Rpl36A	49	50	45	45	42	39	31
	gcn1[2052–2428]	50	30	20	12	1	1	0
	Vector	50	47	44	44	41	38	31
18	Rpl37A	37	38	36	31	34	20	11
	Rpl38	44	45	44	39	32	30	21
	gcn1[2052–2428]	48	24	12	10	5	2	21
	Vector	45	45	44	36	32	30	1
19	Rpl39	49	50	49	46	41	36	29
	Rpl40A	45	44	35	31	25	21	16
	gcn1[2052–2428]	44	30	21	16	10	4	1
	Vector	49	50	49	45	40	36	30
20	Rpl41A	34	41	40	35	30.5	24	20
	Rpl42B	49	49	48	46	41	37	29
	gcn1[2052–2428]	49	21	15	11	3	2	1
	Vector	49	49	48	45	40	37	29
21	Rpl43	45	48	45	41	34	20	20
	Rpl30	45	45	40	36	35	22	22
	gcn1[2052–2428]	50	26	21	13	11	1	0.5
	Vector	45	45	46	43	41	35	35

Table 5.4 *Growth scores for 3AT plates from Table 5.3 adjusted by dividing the original growth score by that of the control plate and then diving that ratio by the ratio of the WT control plate*

Strain	15 mM 3AT	30 mM 3AT	60 mM 3AT	90 mM 3AT	120 mM 3AT	150 mM 3AT
Rpl1A	1.0000	0.9965	0.9965	0.9926	1.0000	1.0000
Rpl2A	1.0000	0.9965	0.9965	0.9926	1.0000	1.0000
Rpl4B	1.0204	1.0204	1.0311	1.0771	1.3120	1.2925
Rpl5	0.9574	0.8511	0.8399	0.7565	0.8815	0.7092
Rpl6A	1.0000	1.0000	1.0000	1.0000	0.9412	0.9333
Rpl8A	1.0233	0.9690	0.9044	0.8583	0.8550	0.8140
Rpl7A	1.1364	1.1136	1.0890	1.0375	1.0101	1.0227
Rpl7B	1.1111	1.0889	1.0648	1.0870	1.0370	1.0556
Rpl9A	1.0256	1.1136	1.1068	0.9806	0.9322	0.8795
Rpl10	0.9362	1.0189	1.0177	1.0171	1.0257	0.8340
Rpl11A	1.0204	0.9119	0.8865	0.7852	0.8119	0.7447
Rpl12A	1.0417	1.0417	1.0200	0.9921	0.9320	0.9722
Rpl13A	0.9800	0.9600	0.9565	0.9286	0.8649	0.9355
Rpl15A	1.1667	1.1667	1.1775	1.1243	1.0511	0.9409
Rpl16A	1.0435	1.0435	1.0222	1.0000	1.0435	1.0435
Rpl17A	1.0213	0.9804	1.0213	0.9787	1.0213	1.0213
Rpl18A	0.9808	0.8828	0.8168	0.9408	0.7982	0.9978
Rpl19A	1.0426	1.0435	1.0233	1.1143	1.0303	1.0909
Rpl20A	1.0453	1.1034	0.9146	0.7317	0.5716	0.5081
Rpl21A	1.0204	1.0870	1.0870	1.0870	1.0530	0.9511
Rpl23A	1.0930	1.0679	1.0835	1.0042	0.9243	0.9302
Rpl24A	0.9800	0.9796	1.0227	1.0227	1.0256	1.0286
Rpl25	1.0000	1.0000	1.0000	1.0000	0.9706	0.9688
Rpl26A	1.0000	0.9964	0.9722	1.0163	1.0110	1.0091
Rpl27A	1.0417	1.0417	1.0417	1.0417	1.0417	1.0417
Rpl28	1.0204	1.0204	1.0204	1.0204	1.0204	1.0204
Rpl29	1.0208	1.0208	1.0000	0.9981	0.9722	0.9074
Rpl30	0.9188	0.8779	0.7708	0.7713	0.6806	0.6238
Rpl31A	1.0435	1.0435	1.0870	1.0957	1.0435	1.0795
Rpl33A	1.0435	1.0435	1.0435	1.0435	1.0153	1.0435
Rpl34A	1.0000	1.0204	1.0000	1.0000	1.0000	1.0000
Rpl34B	1.0000	1.0000	1.0000	1.0000	1.0000	1.0000
Rpl35A	1.0855	1.0668	1.0436	1.0453	1.0473	1.0204
Rpl36A	1.0855	1.0436	1.0436	1.0453	1.0473	1.0204
Rpl37A	0.9722	1.0227	1.0764	0.9274	0.9052	0.6875
Rpl38	1.0227	1.0227	1.1080	1.0557	1.0580	1.0227
Rpl39	1.0000	1.0000	1.0222	1.0250	1.0000	0.9667
Rpl40A	0.9582	0.7778	0.7501	0.6806	0.6352	0.5807
Rpl41A	1.2059	1.2010	1.1209	1.0989	0.9348	0.9939
Rpl42B	1.0000	1.0000	1.0222	1.0250	1.0000	1.0000
Rpl43	1.0667	0.9783	0.9535	0.8293	0.5714	0.5714
Rpl30	1.0000	0.8696	0.8372	0.8537	0.6286	0.6286

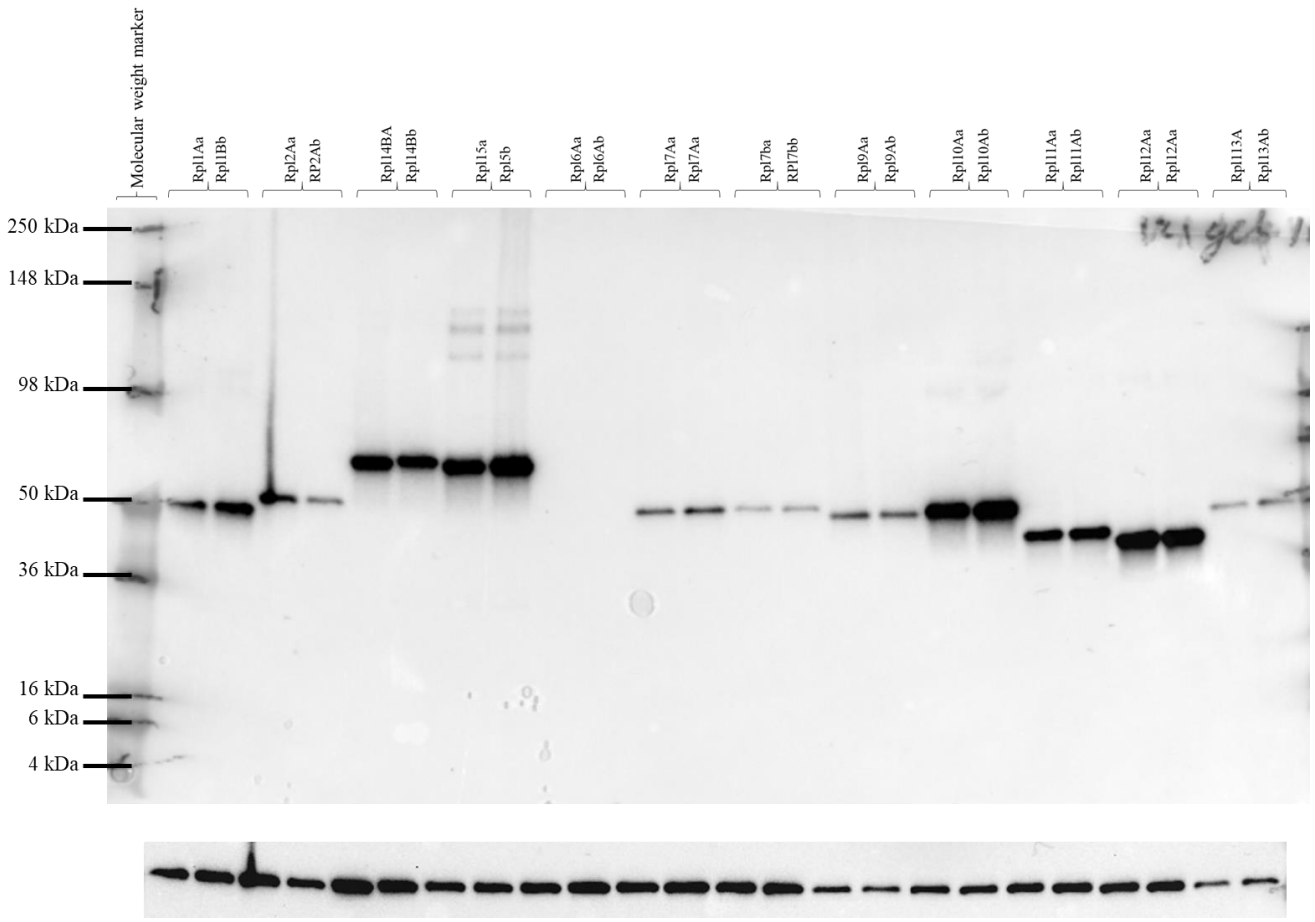

Figure 5.19 *Western blot confirming protein expression of Rpl overexpressing strains Rpl1Aa to Rpl13Ab and expression levels.*

Shown in A) each Rpl overexpressing sample as indicated above the Figure was probed for eIF2αP to detect presence of fusion tagged Rpl overexpressed proteins (fusion tag 19kDa). Molecular weight ladder was loaded in the first lane for determination of molecular weights of corresponding tagged Rpls, molecular weights of ladder are indicated to the left of the Figure. B) The same blot in A) was re-probed for housekeeping gene of Pgk1 for determination of equal loading.

Table 5.5 *Normalisation of expression levels from Figure 5.14*

Values are normalised to Pgk1 signal intensities. Normalisation was carried out using image lab analysis software.

Strain	Volume (Intensity)	Normalisation Factor	Normalised Volume (Intensity)
Rpl1Aa	3938076	1.719529	6771634
Rpl1Ab	8285724	1	8285724
Rpl2Aa	5644116	0.642359	3625551
Rpl2Ab	1496736	1.875796	2807571
Rpl4Ba	14142024	0.621561	8790132
Rpl4Bb	11758140	0.944371	11104041
Rpl5a	15332688	1.78984	27443053
Rpl5b	20995200	1.48176	31109852
Rpl6Aa	ND	ND	ND
Rpl6Ab	ND	ND	ND
Rpl7Aa	2163924	1.268818	2745625
Rpl7Ab	2563704	0.947196	2428331
Rpl7Ba	765864	1.131153	866309
Rpl7Bb	944280	1.092802	1031910
Rpl9Aa	2447928	3.355791	8214734
Rpl9Ab	2650176	4.513464	11961474
Rpl10Ab	16575156	2.533447	41992286
Rpl10Ab	21295944	2.266204	48260946
Rpl11Aa	6933744	1.597514	11076750
Rpl11Ab	9564804	1.377755	13177958
Rpl12Aa	16919424	1.519103	25702341
Rpl12Ab	17836236	1.301902	23221034
Rpl13Aa	968004	5.698776	5516438
Rpl13Ab	1270548	4.623361	5874202

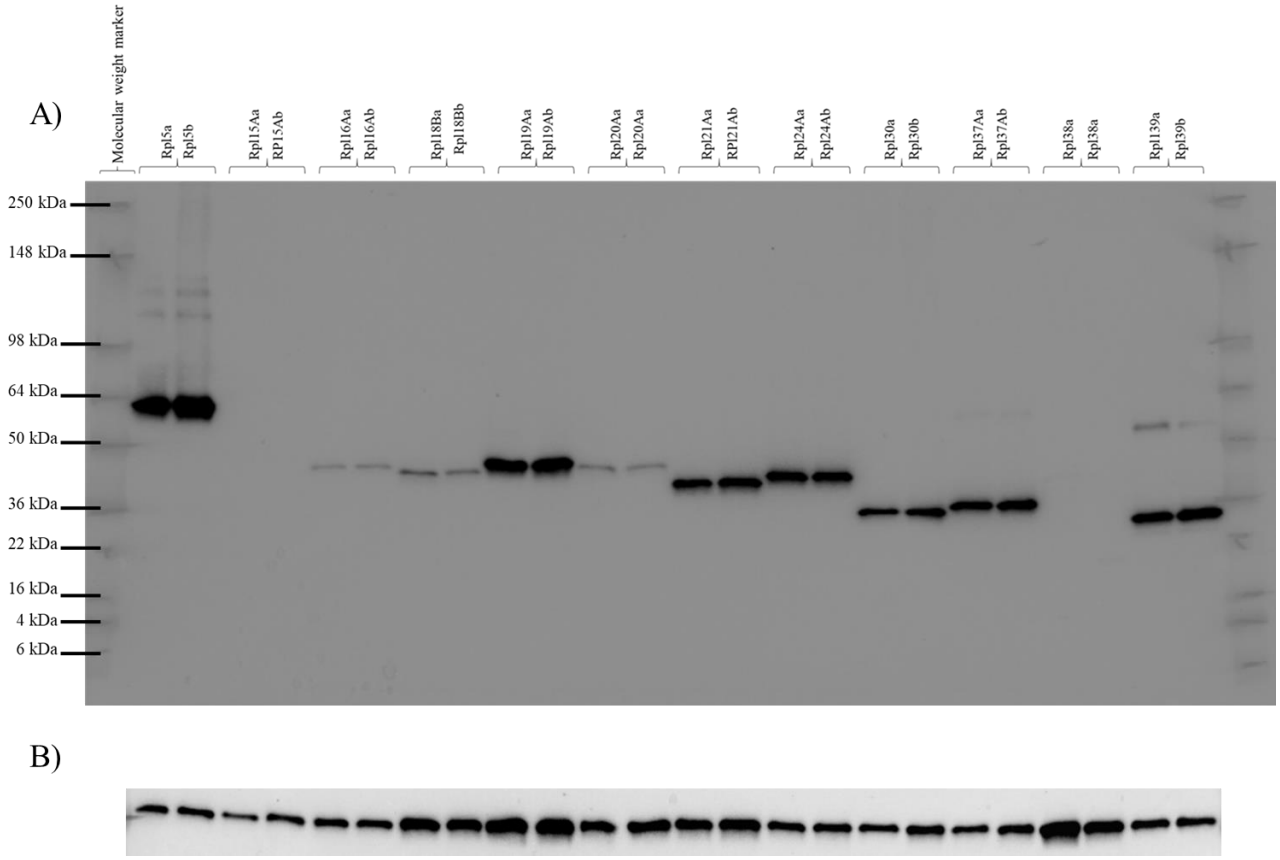

Figure 5.20 *Western blot confirming protein expression of Rpl overexpressing strains Rpl1Aa to Rpl13Ab and expression levels*

Shown in A) each Rpl overexpressing sample as indicated above the Figure was probed for eIF2αP to detect presence of fusion tagged Rpl overexpressed proteins (fusion tag 19kDa). Molecular weight ladder was loaded in the first lane for determination of molecular weights of corresponding tagged Rpls, molecular weights of ladder are indicated to the left of the Figure. B) The same blot in A) was re-probed for housekeeping gene of Pgk1 for determination of equal loading.

Table 5.6 *Normalisation of expression levels from Figure 5.15*

Values are normalised to Pgk1 signal intensities. Normalisation was carried out using image lab analysis software.

Strain	Volume (Intensity)	Normalisation Factor	Normalised Volume (Intensity)
Rpl5a	14032980	1.424055	19983735
Rpl5b	10928196	1	10928196
Rpl15Aa	ND	ND	ND
Rpl15Ab	ND	ND	ND
Rpl16Aa	629748	1.004883	632823
Rpl16Ab	721656	1.013032	731060
Rpl18Ba	2073852	0.414894	860427
Rpl18Bb	1158048	0.53962	624905
Rpl19Aa	10792332	0.322998	3485903
Rpl19Ab	12360096	0.3044	3762416
Rpl20Aa	1117836	0.688747	769906
Rpl20Ab	890064	0.501049	445965
Rpl21Aa	7076088	0.583486	4128800
Rpl21Ab	9315684	0.461479	4298990
Rpl24Aa	9974196	0.820555	8184374
Rpl24Ab	9626508	0.813159	7827884
Rpl30a	5617620	1.072225	6023350
Rpl30b	8073648	0.71481	5771124
Rpl37Aa	8366724	1.233435	10319806
Rpl37Ab	10168236	0.819196	8329774
Rpl38a	ND	ND	ND
Rpl38b	ND	ND	ND
Rpl39Aa	7543224	0.898264	6775803
Rpl39Ab	10770840	1.038175	11182014

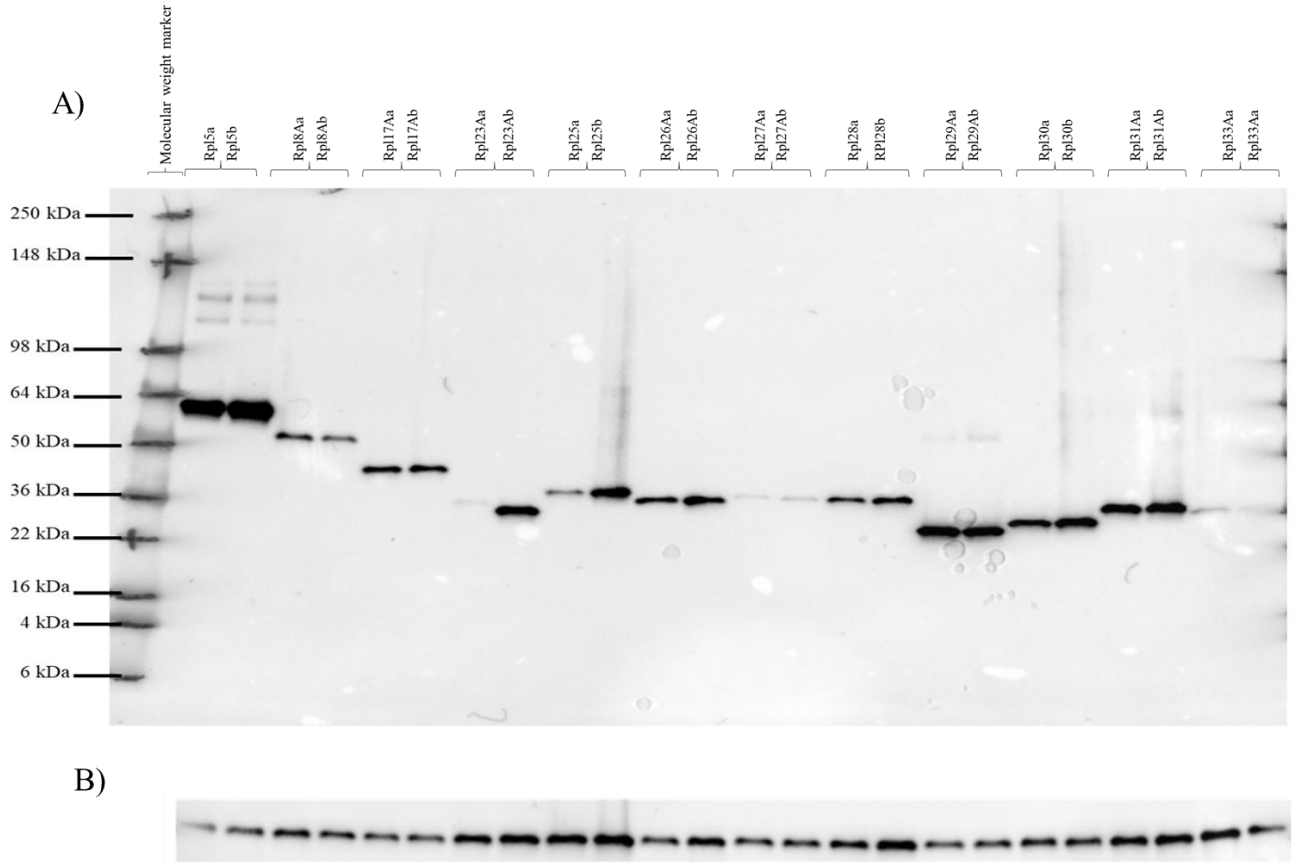

Figure 5.21 *Western blot confirming protein expression of Rpl overexpressing strains Rpl5a to Rpl133Ab and expression levels*

Shown in A) each Rpl overexpressing sample as indicated above the Figure was probed for eIF2αP to detect presence of fusion tagged Rpl overexpressed proteins (fusion tag 19kDa). Molecular weight ladder was loaded in the first lane for determination of molecular weights of corresponding tagged Rpls, molecular weights of ladder are indicated to the left of the Figure. B) The same blot in A) was re-probed for housekeeping gene of Pgk1 for determination of equal loading.

Table 5.7 *Normalisation of expression levels from Figure 5.16*

Values are normalised to Pgk1 signal intensities. Normalisation was carried out using image lab analysis software.

Strain	Volume (Intensity)	Normalisation Factor	Normalised Volume (Intensity)
Rpl5a	7669984	1.529053	11727814
Rpl5b	10364150	1	10364150
Rpl8Aa	1159950	0.619835	718978
Rpl8Ab	750550	0.745017	559172
Rpl17Aa	1701025	0.949359	1614883
Rpl17Ab	1597975	0.950122	1518271
Rpl23Aa	40850	1.358828	55508
Rpl23Aa	3333600	0.884466	2948455
Rpl25a	660275	1.880276	1241499
Rpl25b	3435625	0.546347	1877044
Rpl26Aa	1494125	1.309694	1956846
Rpl26Ab	2593950	0.835267	2166641
Rpl27Aa	78150	2.071656	161899
Rpl27Aa	192175	1.645589	316241
Rpl28a	1223625	1.315121	1609214
Rpl28b	1907000	1.441238	2748441
Rpl29a	4218025	3.009084	12692393
Rpl29b	3869775	2.658095	10286228
Rpl30a	2627532	1.761959	4629602
Rpl30b	3564525	1.119276	3989688
Rpl31Aa	3314175	1.666352	5522583
Rpl31Ab	3696400	1.233376	4559051
Rpl33Aa	295700	0.930894	275265
Rpl33Ab	25125	1.546885	38865

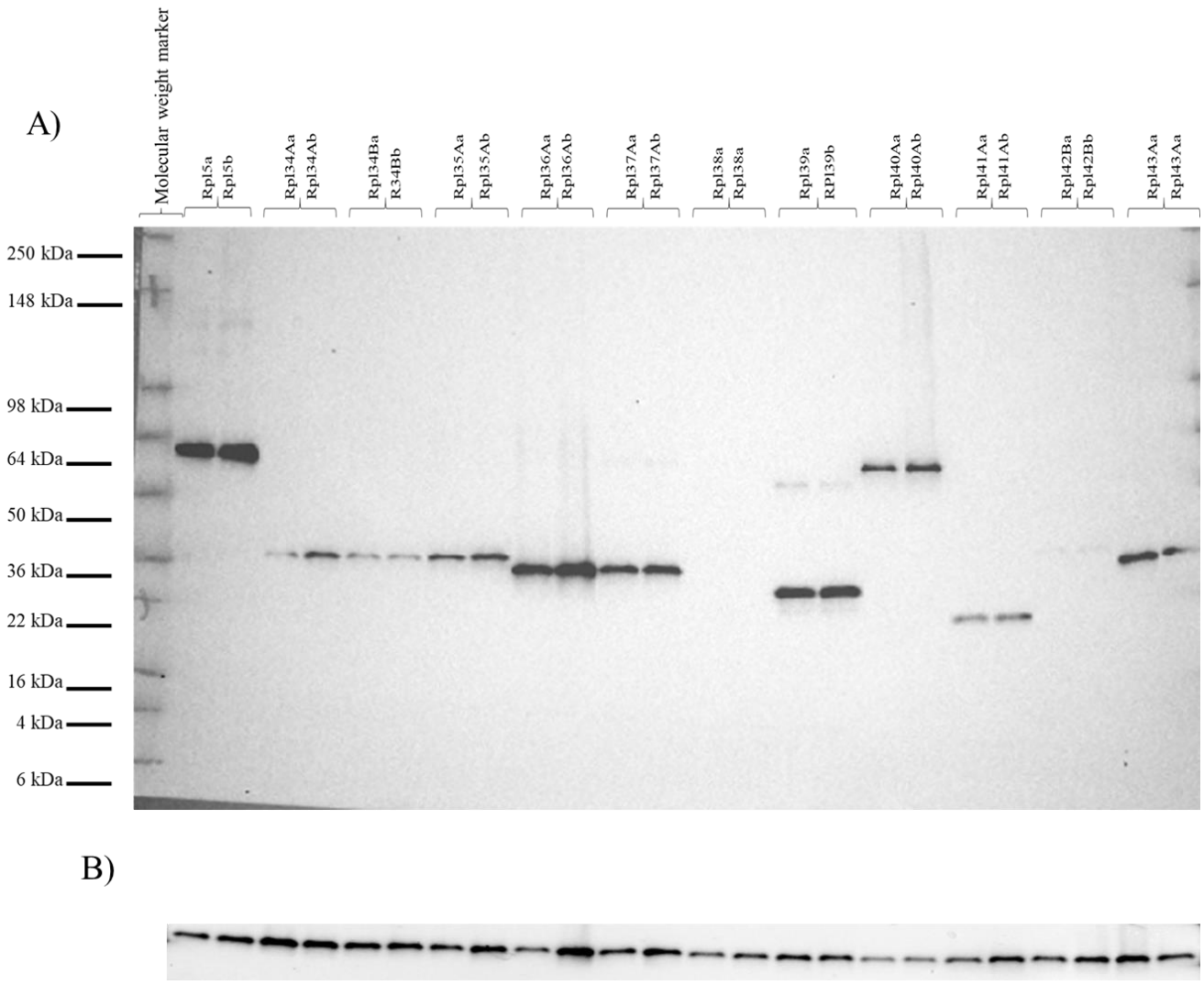

Figure 5.22 *Western blot confirming protein expression of Rpl overexpressing strains Rpl5a to Rpl143Ab and expression levels*

Shown in A) each Rpl overexpressing sample as indicated above the Figure was probed for eIF2αP to detect presence of fusion tagged Rpl overexpressed proteins (fusion tag 19kDa). Molecular weight ladder was loaded in the first lane for determination of molecular weights of corresponding tagged Rpls, molecular weights of ladder are indicated to the left of the Figure. B) The same blot in A) was re-probed for housekeeping gene of Pgk1 for determination of equal loading.

Table 5.8 *Normalisation of expression levels from Figure 5.17*

Values are normalised to Pgk1 signal intensities. Normalisation was carried out using image lab analysis software.

Strain	Volume (Intensity)	Normalisation Factor	Normalised Volume (Intensity)
Rpl5a	3898704	3.229918	12592492
Rpl5b	5714604	1.426282	8150636
Rpl34Aa	238488	1	238488
Rpl34Ab	1036272	1.132579	1173660
Rpl34Ba	379080	1.353202	512971
Rpl34Bb	319944	1.417724	453592
Rpl35Aa	802447	0.809854	649864
Rpl35Ab	1704672	0.624871	1065200
RPl36Aa	3289296	0.593307	1951563
Rpl36Ab	4808688	0.465136	2236692
Rpl37Aa	2107776	1.306965	2754790
Rpl37Ab	2296848	0.829262	1904689
Rpl38a	ND	ND	ND
Rpl38b	ND	ND	ND
Rpl39a	2436936	0.84447	2057918
Rpl39b	2551728	0.550645	1405096
Rpl40Aa	1199520	1.333531	1599597
Rpl40Ab	1654200	1.271362	2103086
Rpl41Aa	448704	1.029396	461893
Rpl41Ab	62D9064	0.957108	602082
Rpl42Ba	ND	ND	ND
Rpl42Bb	ND	ND	ND
Rpl43Aa	1850976	0.646049	1195820
Rpl43Ab	610416	1.277628	779884

Table 5.9 *Determined expression levels relative to Rpl5a*

Highlighted in red are Rpls which gave no detectable level of expression.

Strain	Expression level (relative to Rpl5a)
Rpl1Aa	0.2468
Rpl1Ab	0.3019
Rpl2Aa	0.1321
Rpl2Ab	0.1023
Rpl4Ba	0.3203
Rpl4Bb	0.4046
Rpl5a	1.0000
Rpl5b	0.8030
Rpl6Aa	0.0000
Rpl6Ab	0.0000
Rpl7Aa	0.1000
Rpl7Ab	0.0885
Rpl7Ba	0.0316
Rpl7Bb	0.0376
Rpl8Aa	0.0613
Rpl8Ab	0.0477
Rpl9Aa	0.2993
Rpl9Ab	0.4359
Rpl10Ab	1.5302
Rpl10Ab	1.7586
Rpl11Aa	0.4036
Rpl11Ab	0.4802
Rpl12Aa	0.9366
Rpl12Ab	0.8462
Rpl13Aa	0.2010
Rpl13Ab	0.2141
Rpl15Aa	0.0000
Rpl15Ab	0.0000
Rpl16Aa	0.0317
Rpl16Ab	0.0366
Rpl17Aa	0.1377
Rpl17Ab	0.1295
Rpl18Bb	0.0313
Rpl19Aa	0.1744
Rpl19Ab	0.1883
Rpl20Aa	0.0385
Rpl20Ab	0.0223
Rpl21Aa	0.2066
Rpl21Ab	0.2151
Rpl23Aa	0.0047
Rpl23Aa	0.2514

Strain	Expression level (relative to Rpl5a)
Rpl24Aa	0.4096
Rpl24Ab	0.3917
Rpl25a	0.1059
Rpl25b	0.1601
Rpl26Aa	0.1669
Rpl26Ab	0.1847
Rpl27Aa	0.0138
Rpl27Aa	0.0270
Rpl28a	0.1372
Rpl28b	0.2344
Rpl29a	1.0822
Rpl29b	0.8771
Rpl30a	0.3948
Rpl30b	0.3402
Rpl31Aa	0.4709
Rpl31Ab	0.3887
Rpl33Aa	0.0235
Rpl33Ab	0.0033
Rpl34Aa	0.0189
Rpl34Ab	0.0932
Rpl34Ba	0.0407
Rpl34Bb	0.0360
Rpl35Aa	0.0516
Rpl35Ab	0.0846
RPl36Aa	0.1550
Rpl36Ab	0.1776
Rpl37Aa	0.2188
Rpl37Ab	0.1513
Rpl38Aa	0.0010
Rpl38Ab	0.0000
Rpl39a	0.1634
Rpl39b	0.1116
Rpl40Aa	0.1270
Rpl40Ab	0.1670
Rpl41Aa	0.0367
Rpl41Ab	0.0478
Rpl42Ba	0.0000
Rpl42Bb	0.0000
Rpl43Aa	0.0950
Rpl43Ab	0.0619

Table 5.10 *Determined expression levels relative to Rpl5a (averages of a and b from Table 5.9)*

Highlighted in red are Rpls which gave no detectable level of expression.

Strain	Expression level
Rpl1Aa	0.27434
Rpl2Aa	0.11721
Rpl4Ba	0.36246
Rpl5a	0.90150
Rpl6Aa	0.00000
Rpl7Aa	0.09427
Rpl7Ba	0.03458
Rpl8Aa	0.05449
Rpl9Aa	0.36760
Rpl10Ab	1.64437
Rpl11Aa	0.44191
Rpl12Aa	0.89136
Rpl13Aa	0.20753
Rpl15Aa	0.00000
Rpl16Aa	0.03412
Rpl17Aa	0.13358
Rpl18Ba	0.03716
Rpl19Aa	0.18136
Rpl20Aa	0.03042
Rpl21Aa	0.21087
Rpl23Aa	0.12807
Rpl24Aa	0.40063
Rpl25a	0.13295
Rpl26Aa	0.17580
Rpl27Aa	0.02038
Rpl28a	0.18578
Rpl29a	0.97966
Rpl30a	0.33100
Rpl31Aa	0.42982
Rpl33Aa	0.01339
Rpl34Aa	0.05607
Rpl34Ba	0.03838
Rpl35Aa	0.06810
RPl36Aa	0.16630
Rpl37Aa	0.32600
Rpl38a	0.00099
Rpl39a	0.29350
Rpl40Aa	0.14702
Rpl41Aa	0.04225
Rpl42Ba	0.00000
Rpl43Aa	0.07845